Activation of NF-κB nuclear transcription factor by flow and tumour necrosis factor alpha in cultured endothelial cells: role of microtubules.

Victoria Cameron

A thesis submitted in partial fulfilment of the requirements for the degree of Doctor of Philosophy at the University of St Andrews

School of Biology

May 2005

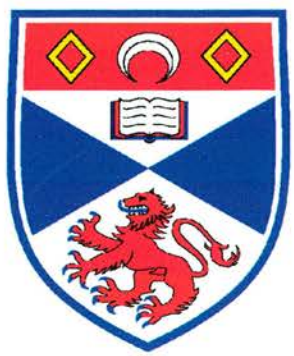

(i) I, Victoria Cameron, hereby certify that this thesis, which is approximately 29,000 words in length, has been written by me, that it is the record of work carried out by me and that it has not been submitted in any previous application for a higher degree.

Date..20/5/05....Signature of Candidate..

(ii) I was admitted as a research student in September 1999 and as a candidate for the degree of Doctor of Philosophy in Biology: the higher study for which this is a record was carried out in the University of St Andrews between 1999 and 2005.

Date..20/5/05..... Signature of Candidate..

(iii) I hereby certify that the candidate has fulfilled the conditions of the Resolution and Regulations appropriate for the degree of Doctor of Philosophy in the University of St Andrews and that the candidate is qualified to submit this thesis in application for that degree.

Date....20/5/05...Signature of Supervisor.

In submitting this thesis to the University of St Andrews I understand that I am giving permission for it to be made available for use in accordance with the regulations of the University Library for the time being in force, subject to any copyright vested in the work not being affected thereby. I also understand that the title and abstract will be published, and that a copy of the work may be made and supplied to any bona fide library of research worker.

Date.....20/5/05.....Signature of Candidate...

ACKNOWLEDGEMENTS

I would like to express my gratitude to the following people who have helped and supported me throughout this time;

Dr Eric Flitney and Dr John Sommerville, thank-you for your guidance over the course of this work.

Many thanks to all those in the Bute Medical Building who provided help and technical advice.

Dr Dave Hay and Dr Lesley Thomson, thank-you for carrying out cell transfections, luciferase assays and IKK assays – your technical help and knowledge is appreciated enormously.

Dr Jeff Graves for advice on statistical tests and Miss Sarah Spring for tutelage in the Minitab programme.

To my family and friends, who have stuck with me through everything, especially Mum and Dad.

ABSTRACT

Endothelial cells are uniquely responsive to the shear stress associated with blood flow. A parallel plate flow chamber was used to study the effects of fluid shear stress (FSS) on: (A) the activation of NF-κB, an inducible nuclear transcription factor in cultured human endothelial cells (HUVEC) and (B) the effect of the microtubule cytoskeleton on this activation.

(A) Using electrophoretic mobility shift assay (EMSA), it was shown that FSS causes increased binding of p50/p65 (an NF-κB heterodimer) to a known shear stress response element (SSRE) in nuclear cell extracts. A luciferase assay showed upregulation of a NF-κB reporter in response to FSS and immunofluorescent observations showed that FSS caused nuclear translocation of the NF-κB subunit, p65. These results indicate that FSS activates NF-κB in HUVEC.
Inhibitory κB's (IκBα and IκBβ$_1$), which hold NF-κB in a complex in the nucleus were shown, using western blotting, to be degraded in response to FSS and also to tumour necrosis factor alpha (TNFα), an agonist stimulant of NF-κB. p105, a precursor of the p50 subunit, was not degraded in response to FSS or TNFα. Furthermore, inhibitory κB kinases (IKK1 and IKK) were shown, using a kinase assay, to be activated by both FSS and TNFα. Immunofluorescence studies confirmed that inactive mutants of these kinases blocked p65 nuclear translocation in response to FSS. Using an inactive mutant of NF-κB inducing kinase (NIK), HUVEC were seen, using immunofluorescence, to have p65 nuclear translocation blocked in response to FSS. This was not seen with use of an inactive mutant to tumour progression locus 2 (TPL2), which is involved in post-translational modification of p105. Use of an agonist which blocks protein kinase C (PKC) did not inhibit FSS-induced p65 nuclear translocation.
Together, these results confirm that FSS can cause NF-κB activation and IκBα and IκBβ$_1$ degradation. This process is dependent on IKK1, IKK2 and NIK, but not on TPL2 or PKC.

(B) Colchicine, which depolymerises microtubules (MT), was used to investigate any role of this cytoskeletal element might have in FSS and TNFα-stimulated activation of NF-κB. Immunostaining showed that MT are depolymerised by colchicine in a concentration-dependent manner. This depolymerisation did not prevent FSS or TNFα-induced p65 nuclear translocation, indicating that an intact MT network is not essential for this. The effect of leptomycin B (LMB), which blocks nuclear export of p65 (an auto-regulatory phenomenon seen after 120 min. FSS) is not affected by MT depolymerisation, confirming that an intact MT network is not necessary for auto-regulation of NF-κB. Immunofluorescence revealed a high level of co-localisation of p65 and tubulin (MT subunits) both in areas surrounding the nucleus and in regions of membrane ruffling at the cell periphery.

CONTENTS

Declarations		i
Acknowledgements		iii
Abstract		iv
Contents		v
Figure Index		xii
Abbreviations		xv
Chapter 1	**Introduction**	1
1.1	The endothelium	2
1.2	The endothelium and haemodynamics	3
1.3	Fluid shear stress	5
1.4	Atherosclerosis	6
1.5	Scope of the present study	7
Chapter 2	**NF-κB Introduction**	9
2.1	Introduction	10
2.2	NF-κB Proteins	10
2.3	Structural aspects of DNA binding	12
2.4	Inhibitory κB proteins (IκBs)	13
2.5	Structure of IκBs	14
2.6	NF-κB activation	16
2.7	IκB phosphorylation	17
2.8	Ubiquitination of phosphorylated IκB	17
2.9	IκB degradation and NF-κB activation	19
2.10	IκB kinases (IKK)	20

2.11	IKK regulation	23
2.12	Fluid shear stress mediated activation of NF-κB	25
2.13	Scope of the present study	26
Chapter 3	**NF-κB Materials and Methods**	**27**
3.1	Cell culture	28
3.1.1	Maintenance of HUVEC	28
3.1.2	Trypsinisation and seeding of HUVEC	28
3.1.3	DNA plasmid and transient transfection	29
3.2	Drug treatment of HUVEC	30
3.3	Flow apparatus	30
3.4	Immunofluorescence and fluorescence microscopy	31
3.4.1	Paraformaldehyde fixation method and immunofluorescence	31
3.4.2	Microscopy	32
3.5	Western blotting	33
3.5.1	Cell extract preparation	33
3.5.2	Protein estimation	33
3.5.3	Gel electrophoresis and western blotting	34
3.6	Electrophoretic mobility shift assay (EMSA)	35
3.7	Luciferase Assay	36
3.8	IKK immunocomplex kinase activity assay	36

Chapter 4	**NF-κB Results**	**38**
4.1	NF-κB dependent gene transcription is stimulated by FSS	39
4.2	IκBα and IκBβ degradation, but not p105, is stimulated by FSS and TNFα	40
4.3	Endogenous IKK is activated by FSS and TNFα	42
4.4	Single cell observations of NF-κB activation by FSS	43
4.5	Nuclear translocation of p65 is blocked by catalytically inactive mutants of IKK1 and IKK2	45
4.6	Nuclear translocation of p65 is blocked by a catalytically inactive mutant of NIK, but not TPL-2	46
4.7	FSS activation of NF-κB is not dependent on protein kinase C	47
Chapter 5	**NF-κB Discussion**	49
Chapter 6	**Microtubule Introduction**	55
6.1	The role of microtubules in the cell	56
6.2	Structure of microtubules	56
6.3	Dynamic properties of microtubules	57
6.4	Tubulin-drug interactions	60
6.5	Cell responses to microtubule binding agents	61
6.6	Effect of microtubule disruption on flow-induced responses of endothelial cells	65
6.7	Effect of microtubule depolymerising agents on the activation of NF-κB nuclear transcription factor	66

6.8	Immunofluorescent studies linking MT to other cellular components	67
6.9	Scope of the present study	69
Chapter 7	**Microtubule Materials and Methods**	71
7.1	Cell culture	72
7.1.1	Maintenance of HUVEC	72
7.1.2	Trypsinisation and seeding of HUVEC	72
7.2	Drug treatment of HUVEC	72
7.3	FSS apparatus	72
7.4	Immunofluorescence and microscopy	72
7.4.1	Glutaraldehyde fixation and immunofluorescence	72
7.4.2	Deconvolution microscopy	73
7.5	Quantitative analysis	74
Chapter 8	**Microtubule Results**	75
8.1.1 8.1.2	Colchicine depolymerises MT in a concentration dependent manner without affecting p65 distribution	76
8.2	Colchicine treatment does not prevent TNFα induced nuclear translocation of p65 from observations of immunofluorescent images	77
8.3	Quantitative analysis reveals that increasing colchicine concentration does not significantly affect nuclear p65 translocation in the presence of TNFα	78
8.4	Colchicine does not prevent flow-induced nuclear translocation of p65	80

8.5	Colchicine does not interfere with autoregulation of NF-κB gene transcription	81
Chapter 9	**Microtubule Discussion**	83
9.1	MT depolymerisation does not cause NF-κB activation	84
9.2	Nuclear translocation of NF-κB in response to TNFα is unaffected by colchicine	86
9.3	Intact MT are not required for flow-induced activation of NF-κB	87
9.4	Intact MT are not required for flow-induced autoregulation of NF-κB	88
9.5	Summary	88
Chapter 10	**Overall Discussion and Scope for Further Study**	90
10.1	Physiological relevance of the present study	91
10.2	Signalling pathway intermediates involved in FSS-induced NF-κB gene transcription	92
10.3	Involvement of the cytoskeleton in the mechanotransduction of FSS	93
10.4	Role of MT in FSS-induced NF-κB activation	94
10.5	Further experiments	96
10.6	Scope for extended study	97
References		99
Appendix 1	**NF-κB**	122
1.1	Cell culture techniques	123

1.1.1	Maintenance of HUVEC	123
1.1.2	Trypsinisation and seeding of HUVEC	123
1.1.3	DNA plasmid and transient transfection of NIK, IKK1 and IKK2	124
1.2	Drug treatment of HUVEC	124
1.3	Flow apparatus	125
1.4	Immunofluorescence	126
1.4.1	Paraformaldehyde fixation method	126
1.5	Fluorescence and confocal microscopy	127
1.6	Western blotting	128
1.6.1	Cell extract preparation	128
1.6.2	Protein estimation	128
1.6.3	Gel electrophoresis and western blotting	129
1.7	Electrophoretic mobility shift assay (EMSA)	132
1.8	Data for response of IκBα, IκBβ, p105, p50 to flow and TNFα	133
1.9	Luciferase assay	136
2.0	IKK immunocomplex kinase activity assay	136
2.0.1	Solutions and equipment	136
2.0.2	Data tables	138
Appendix 2	**Microtubules**	140
2.1	Cell culture techniques	141
2.1.1	Maintenance, trypsinisation and seeding of HUVEC	141

2.2	Drug treatment of HUVEC	141
2.3	Flow experiments	141
2.4	Immunofluorescence	141
2.4.1	Glutaraldehyde fixation method	141
2.5	Deconvolution microscopy	143
2.6	Quantitative analysis	143

FIGURES

Chapter 1 **Introduction**

1.1 Scanning electron micrograph of an arteriole in transverse section.

1.2 Schematic representation of blood pressure and fluid shear stress on the endothelium.

Chapter 2 **NF-κB Introduction**

2.1 Schematic diagram of the mammalian NF-κB protein family

2.2 Schematic diagram of the IκB protein family.

2.3 Table of selected genes which are activated by NF-κB in the immune response.

2.4 Schematic diagram of the ubiquitination of IκB

2.5 Schematic diagram of IKKα and IKKβ

Chapter 3 **NFκB Materials and Methods**

3.1 Illustration of side-on and aerial views of a flow chamber.

3.2 Schematic diagram of closed loop perfusion chamber for fluid shear stress experiments.

Chapter 4 **NF-κB Results**

4.1 Flow causes an increase in binding of p50/p65 to an SSRE and upregulates an NF-κB luciferase reporter.

4.2.1 Examples of immunoblots used to determine if expression of IκBα, IκBβ, p105 or p50 proteins is altered by exposure to FSS or TNFα.

4.2.2 Degradation of IκBα and $IκBβ_1$, but not p105/p50, is induced by flow and TNFα treatment.

4.3 Endogenous IKKs are activated by flow.

4.4 Nuclear translocation of p65 is stimulated by flow.

4.5 IKK1 and IKK2 catalytically inactive mutants block p65 nuclear translocation.

4.6 NIK catalytically inactive mutant, but not that of TPL-2 kinase, blocks p65 nuclear translocation.

4.7 Bisindolymaleimide 1 (Bisin) blocks agonist, but not flow-induced p65 nuclear translocation.

Chapter 6 **Microtubule Introduction**

6.1 Schematic diagram of the assembly of tubulin dimers, lattices and microtubules.

6.2 Schematic diagram of the tubulin dimer and its sites of drug interaction.

6.3 Table of action of MT depolymerising agents on p65 in different cell types.

Chapter 8 Microtubule Results

8.1.1 & 8.1.2 Effect of increasing concentrations of colchicine on MT and p65.

8.2 Effect of TNFα and colchicine on p65 nuclear translocation.

8.3 Quantitative analysis of the effect of colchicine on p65 nuclear translocation in TNFα-stimulated cells.

8.4 Effect of FSS and colchicine on p65 nuclear translocation.

8.5 Effect of LMB, colchicine and FSS on p65 nuclear translocation.

ABBREVIATIONS

ρ	Medium density ($g.cm^{-3}$)
τ	Experimental shear stress
τ^*	Theoretical shear stress
β-TRCP	β-transducin repeat containing protein
2B4	T cell hybridoma
a	Flow chamber half height (cm)
ANOVA	Analysis of variance
AP-1	Activator protein-1
APS	Ammonium persulphate
ARD	Ankyrin repeat domain
ATP	Adenosine triphosphate
BAEC	Bovine aortic endothelial cells
Bcl-3	B cell leukaemia/lymphoma 3
Bisin	Bisindolylmaleimide
BP	Blood pressure
BSA	Bovine serum albumin
C	Colchicine binding site
cDNA	Complementary deoxyribonucleic acid
CHO-K1	Chinese hamster ovary cells
CK II	Casein kinase II
Con A Luc	Con A luciferase reporter
COS-1	Monkey kidney cells

CRM-1	Chromosome region maintenance-1
DH_2O	Distilled water
Dlc-1	Dynein light chain 1
DNA	Deoxyribonucleic acid
DTT	Diothiothreitol
E1	Ubiquitin activating enzyme
E2	Ubiquitin conjugating enzyme
E3	Ubiquitin protein ligase
EBM-2	Endothelial cell basal medium-2
EC	Endothelial cells
ECL	Enhanced chemiluminescence
EDTA	Ethylene diamine tetra acetic acid
EGM-2	Endothelial cell growth medium-2
EGTA	Ethylene glycol bis(b-aminoethylether) tetraacetic acid
EMSA	Electrophoretic mobility shift assay
E-Site	Exchangeable site
ET-1	Endothelin-1
FA	Focal adhesion
FBS	Foetal bovine serum
FCS	Foetal calf serum
FITC	Fluorescein isothiocyanate
FSS	Fluid shear stress
G2-M	Gap2 - Mitosis
g	Acceleration due to gravity ($cm.s^{-2}$)

G	Glycine rich region
GAMF	Goat anti mouse fluorescein isothiocyanate
GART	Goat anti rabbit texas red
G-CSF	Granulocyte colony stimulating factor
GDP	Guanosine diphosphate
GFP	Green fluorescent protein
GM-CSF	Granulocyte macrophage colony stimulating factor
GST	Glutathione-S-transferase
GTP	Guanosine triphosphate
h	Difference in pressure along flow chamber (cm water)
HT29-D4	Human colon adenocarcinoma cells
HBL100	Human epithelial mammary cells
HBSS	Hepes buffered saline solution
hEGF	Human epidermal growth factor
HeLa	Human cervical adenocarcinoma cells
hFGF	Human fibroblast growth factor
HIV	Human immune deficiency virus
HLH	Helix loop helix
hnRNP A1	Heterogenous nuclear ribonuclear protein
HRP	Horseradish peroxidase
HUVEC	Human umbilical vein endothelial cells
IκB	Inhibitory κB
ICAM-1	Intracellular adhesion molecule-1
IF	Intermediate filaments

IFN-β	Interferon β
Igκ	Immunoglobulin κ light chain
IKAP	Inhibitory κB kinase complex associated protein
IKK	Inhibitory κB kinase
IL-1	Interleukin 1
IL-1R	Interleukin-1 receptor
IONO	Ionomycin
kDa	KiloDalton
l	Distance between pressure measuring points
LMB	Leptomycin B
LPS	Lipopolysaccharide
LZ	Leucine zipper
MAP 30	Microtubule associated protein 30
MAP3K	Mitogen activated protein kinase-kinase kinase
MAPKKK	See MAP3K
MC3T3-E1	Murine preosteoblastic cells
M-CSF	Macrophage colony stimulating factor
MEKK	See MAP3K
MF	Microfilaments
MG132	MG132 protease inhibitor
MHC	Major histocompatibility complex
MI	Myocardial infarction
mRNA	Messenger ribonucleic acid
MT	Microtubule(s)

MTOC	Microtubule organising centre
N:C	Nuclear:cytoplasmic ratio
NEMO	Nuclear factor κB essential modulating factor
NES	Nuclear export sequence
NF-κB	Nuclear factor κB
NIH3T3	Mouse fibroblast cells
NIK	NF-κB inducing kinase
NLS	Nuclear localising signal
NO	Nitric oxide
NP-40	Nonidet P-40
N-Site	Non-exchangeable site
p50	50 kiloDalton NF-κB1 subunit
p52	53 kiloDalton RelA subunit
p65	65 kiloDalton RelA subunit
p100	100 kiloDalton NF-κB2 subunit
p105	105 kiloDalton NF-κB1 subunit
PBS	Phosphate buffered saline
PBSc	Phosphate buffered saline - calcium
PBS-T	Phoshate buffered saline –Tween
pcDNA	Recombinant plasma deoxyribonucleic acid
PDGF-B	Platelet derived growth factor B
PEST	Proline (P), glutamic acid (E), serine (S), threonine (T)
PIPES	Piperazine –1,4-bis(1 –ethanesulfonic acid)
PIS	Pre-immune serum

PKA	Protein kinase A
PKC	Protein kinase C
PKR	Double stranded ribonucleic acid –dependent kinase
PMA	Phorbol 12-myristyl 13-acetate
PMSF	Phenylmethylsulfonyl fluoride
PSL	Photo-stimulated luminescence
Q	Volume flow rate ($ml.s^{-1}$)
R3-IGF-1	Long R3-insulin-like growth factor 1
RHD	Rel homology domain
RISC	Ribonucleic acid induced silencing complex
RLU	Relative light unit
RNA	Ribonucleic acid
RPM	Revolutions per minute
S	Phosphorylated serine residue
SDS	Sodium dodecyl sulphate
SDS-PAGE	Sodium dodecyl sulphate polyacrylamide gel
S.E.	Standard error
siRNA	Small interfering ribonucleic acid
SRD	Signal response domain
SSRE	Shear stress response element
T	Taxol binding site
TCR	T cell receptor
TD	Transactivation domain
TEMED	N'N'N'N' –tetramethylethylenediamine

TNFα	Tumour necrosis factor α
TNFR	Tumour necrosis factor receptor
TPL-2	Tumour progression locus-2
TRAF	Tumour necrosis factor associated factor
Ub	Ubiquitin
UV	Ultraviolet
v	Medium viscosity (poise)
V	Vinca binding site
VCAM-1	Vascular adhesion molecule-1
VEGF	Vascular endothelial growth factor
VMA	Vimentin-associated matrix adhesion
W	Channel width (cm)
WT	Wild type

CHAPTER 1

INTRODUCTION

1.1 The Endothelium

The endothelium comprises a single layer of cells which lines the entire cardiovascular system and forms an interface between the blood and the vessel wall (Fig. 1.1). It is highly dynamic and has many functions. Due to its location, it is exposed to both chemical and mechanical stimuli, both of which can lead to activation of the cells. Chemical stimuli which activate endothelial cells include cytokines and bacteria and the mechanical stimuli are the haemodynamic forces associated with blood flow (Gimbrone et al, 1997). The endothelium controls such things as vascular tone and permeability, inflammatory responses, regulation of cell growth and repair and angiogenesis (Davies, 1995; Kirkpatrick et al, 1997).

Vessel tone is controlled by the endothelium in response to altered blood flow by the production and release of vasoconstrictors such as endothelin-1 (ET-1) (Kirkpatrick et al, 1997) and vasodilators such as nitric oxide (NO) (Palmer and Moncada, 1987). Impaired NO release from the endothelium often leads to endothelial dysfunction and disease states.

The endothelium is vital for tissue growth and also for repair following injury. Embryonic vasculature arises initially from purely endothelial vessels in a process known as vasculogenesis. This is followed by angiogenesis where new blood vessels are formed from pre-existing

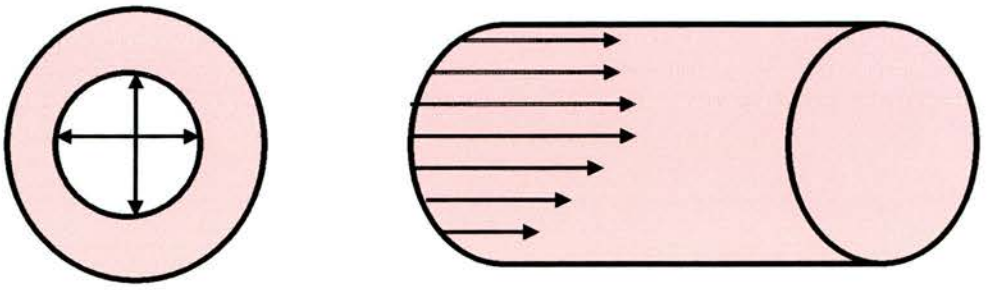

Figure 1.2 Schematic representation of the effect of blood pressure and fluid shear stress upon the endothelial lining of the blood vessel wall.

vessels in a process involving the sprouting of endothelial cells (Patan, 2000). Angiogenesis also takes place in adults, where endothelial cells proliferate and migrate to damaged sites to form new vessels.

1.2 The endothelium and haemodynamics

Endothelial cells have been shown to alter their gene expression, cytoskeletal arrangement and metabolism in response to changes in blood flow (Girard & Nerem, 1995; Davies, 1995; Topper & Gimbrone, 1999). There are complex fluid dynamics associated with blood flow. Blood vessels are compliant tubes with changing cross-sectional area and they experience pulsatile flow. There has been extensive research in this area using *in vitro* models and it is now believed that an accurate description of blood flow characteristics has been reached (Davies, 1995).

Blood flow is associated with fluid forces exerted on the wall of the vessel. Stress is a force per unit area of which there are two main types; blood pressure (BP) and fluid shear stress (FSS). BP causes tension and compression and FSS exerts a frictional force (Fig. 1.2). Blood pressure acts perpendicularly to the vessel wall. Pulsatile blood flow means that BP oscillates and causes cyclical 'stretch' on the endothelium and the vessel wall. FSS is a frictional force which exerts its effects parallel to the direction of flow and is responsible for initiating many cellular responses (Davies, 1995). FSS is a much smaller force

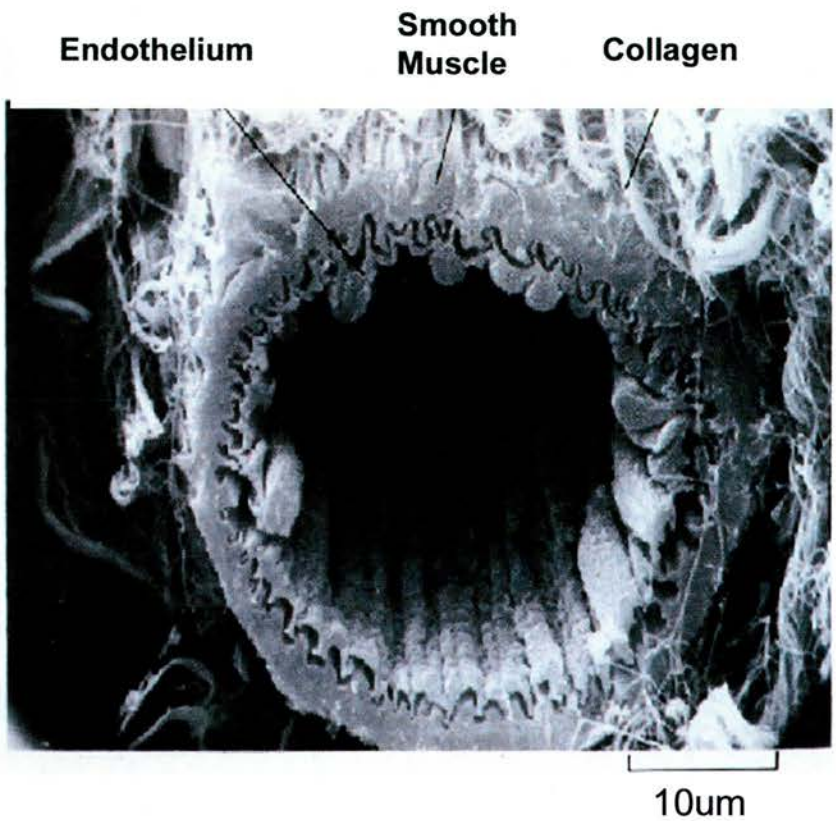

Figure 1.1 Scanning electron micrograph of an arteriole in transverse section. A single layer of endothelial cells is seen on the luminal surface of the vessel.
Taken from http:/cats.med.uvm.edu/cats_teachingmod/histology/lectures_online/ems/cv/cm.html

than BP but is very important in the regulation of structure and function of endothelial cells. Shear stress, rather than the shear rate, is responsible for stimulating the endothelium. Both the direction and magnitude of the force can be sensed by endothelial cells (Masuda & Fujiwara, 1993).

Vascular blood flow is laminar and unidirectional in straight sections of vessel, but turbulent flow can occur in curved or bifurcated areas. Turbulent flow results in a decrease of the magnitude of shear stress acting on the endothelium and loss of directionality of flow (Davies, 1989). The cyclical effects of BP are largely absorbed by smooth muscle in the vessel wall whereas FSS acts directly on the endothelium (Davies, 1989). Shear responses exert a great influence over vascular biology (Dewey et al, 1981; Levesque & Nerem, 1985). Significant cellular differences can be observed in regions of the vasculature where flow conditions vary, demonstrating the effect and influence of FSS on individual endothelial cells (Nerem et al, 1998).

Endothelial cells are able to sense and respond to blood flow. Extensive research has revealed that FSS-induced endothelial responses occur in a time-dependent manner (Davies, 1995). Within seconds 'acute' responses are elicited. These include potassium channel activation, increased intracellular calcium, cell membrane hyperpolarisation and release of agents that regulate vascular tone, such as prostacyclin and

NO. Within a minutes-hours timescale, FSS causes stimulation of signal transduction pathways, leading to nuclear transcription factor activation and regulation of gene expression. 'Chronic' responses in endothelial cells are seen after hours-days. These include cytoskeletal remodelling, cells becoming elongated and realigned in the direction of flow, flattening of cells to decrease the effects of FSS, alterations in mRNA for protein synthesis and inhibition of growth and division of cells (Levesque & Nerem, 1985; Davies, 1995).

1.3 Fluid shear stress

Normal physiological shear stress in the arterial system ranges between 2-40 dynes.cm^{-2}, but can reach up to 200 dynes.cm^{-2} in aortic bifurcations (Dewey et al, 1981). Major arteries normally experience shear stress gradients between 2-20 dynes.cm^{-2} with increases from 30-100 dynes.cm^{-2} at bifurcations (White et al, 1983). Pulsatile flow in the arterial system results in varying gradients of shear and hence varying levels of FSS. Artery bifurcations can cause disrupted laminar flow leading to turbulent flow and even blood vortices. *In vivo* observations of atherosclerotic vessels showed that lesions are confined largely to bifurcated and curved parts of the vessel (Topper & Gimbrone, 1999) suggesting that areas of disturbed flow are potential sites for dysfunction of endothelial cells. This led to *in vitro* studies where monolayers of cultured endothelail cells were subjected to defined haemodynamic conditions. Davies et al (1986) showed that there was an increase in the

turnover of endothelial cells at sites of turbulent FSS, suggesting a disturbance in the integrity of the endothelium. Traub & Berk (1998) showed that endothelial integrity and wound healing was favoured by exposure to steady, uniform FSS and that atherogenesis may be modulated by alterations in coagulation, smooth muscle growth, leukocyte and monocyte migration and lipoprotein uptake and metabolism, all of which are endothelial-mediated. These findings suggest that FSS has a function in maintaining the normal function of the endothelium and that laminar flow may even protect against atherogenesis.

1.4 Atherosclerosis

Atherosclerosis is a vascular disease characterised by a number of changes in the vessel wall and reflects a chronic 'response to injury' process. Vessel walls become partly or totally occluded, resulting in ischaemia of the tissue downstream from the atherosclerotic lesion (Davies, 1995). At worst this can lead to myocardial infarction (MI) or stroke. In Europe, Japan and the USA, atherosclerosis is responsible for over half of all mortalities (Ross, 1993).

Endothelial injury is believed to be the trigger for the growth of atherosclerotic lesions, and this occurs especially in areas where blood flow patterns are disturbed. These include bifurcations and tight curves. It has been shown that atherosclerotic lesions form more readily in areas

where FSS is low and flow is disturbed, rather than in areas where disturbed flow causes particularly elevated FSS (Davies, 1995). It was suggested by Traub & Berk (1998) that laminar flow stimulates atheroprotective responses in the endothelium. Laminar flow was also shown to protect endothelial cells from apoptosis by Dimmeler (1998). It would appear that flow reponses can be either helpful or harmful to endothelial cells, depending on the type of FSS experienced. Kirkpatrick (1997) suggested that the endothelium exists in dynamic equilibrium where under normal physiological conditions, opposing effects are balanced and controlled but any upset of this balance can result in pathological changes.

1.5 Scope of the present study

FSS changes cause regulation and/or reorganisation of cellular structure. Stress activates signalling cascades and results in transcription factor activation and de-novo protein synthesis which ultimately regulates gene expression and structural responses. Davies (1995) reviews the dozens of cellular responses elicited via the effect of FSS on the endothelium.

This study focuses on some of the effects of FSS on human umbilical vein endothelial cells (HUVEC). Identification of the pathway intermediates involved in the activation of the transcription factor NF-κB by FSS is studied and compared with those involved in TNF-α-mediated

activation of NF-κB to determine whether the pathways are identical or even similar. This study also attempts to discover how endothelial cells detect and respond to FSS; specifically, whether microtubules (MT), an important cytoskeletal element, are involved in the process and in what capacity.

CHAPTER 2

NF-κB INTRODUCTION

2.1 Introduction

Nuclear factor kappa B (NF-κB) is a nuclear transcription factor which is present in most eukaryotic cell types (May and Ghosh, 1997).

It was first identified by Sen and Baltimore in 1986 who showed it to be a protein which binds to a specific DNA sequence (5'-GGGACTTTCC-3') within the intronic enhancer of the immunoglobulin kappa light chain and initiates transcription in a manner independent of protein synthesis.

NF-κB is now known to be a critical regulator of gene expression following its activation. It is essential to many immune and inflammatory responses and it regulates gene expression in a large number of cell responses, such as apoptosis, cell adhesion, differentiation and immune stimulation (de Martin et al, 2000). NF-κB is associated with the initiation and/or progression of a number of disease states including rheumatoid arthritis, septic shock, oncogenesis, HIV and atherosclerosis (Baldwin, 1996; Brand et al, 1996). Inducers of NF-κB are numerous and include UV radiation, cytokines (e.g. tumour necrosis factor (TNFα)), interleukin-1 (IL-1), bacterial products (e.g. lipopolysaccharide (LPS)), hypoxia (Baldwin, 1996; Papadaki & Eskin, 1997) and fluid shear stress (FSS) (Lan et al, 1994).

2.2 NFκB Proteins

In quiescent cells, NF-κB resides in the cytoplasm as a homo- or heterodimer of a group of structurally related proteins known as the NF-

κB proteins (May & Ghosh, 1997). There are 5 members of this family which have been identified and cloned, namely NF-κB_1 (p50/p105), NF-κB_2 (p52/p100), Rel A (p65), Rel B and c-Rel (Fig 2.1; (Mercurio & Manning, 1999)). Each protein contains a highly conserved 300 amino acid N-terminal region called the Rel homology domain (RHD). The RHD contains regions for dimerisation, allowing NFκB homo- or heterodimers to form. These dimers are pre-requisites for DNA binding, the domain for which is also contained within the RHD. The RHD also contains a binding site for inhibitory proteins of NF-κB (IκBs) (Baldwin, 1996; May & Ghosh, 1998). The c-terminal end of the RHD contains a nuclear localising signal (NLS) necessary for the transport of NF-κB from the cytoplasm to the nucleus (May & Ghosh, 1998).

The classical NF-κB dimer exists as a Rel A (p65) and NF-κB_1 (p50) heterodimer (Mercurio & Manning, 1999). Other dimers which have been identified include p50/p50, p52/p52, RelA/RelA homodimers and p50/p52, p52/c-Rel, p65/c-Rel heterodimers. Rel-B only forms heterodimers with either p50 or p52 and these are found in lymphoid cell nuclei where they are constitutively active (May & Ghosh, 1997).

Rel A (p65), Rel B and c-Rel contain transactivation domains, the importance of which can be demonstrated via amino acid mutations which cause a decrease or even complete abolition of NF-κB-dependent gene transcription (May & Ghosh, 1997). p50 and p52 are synthesised as larger precursor molecules, respectively p105 and p100, which

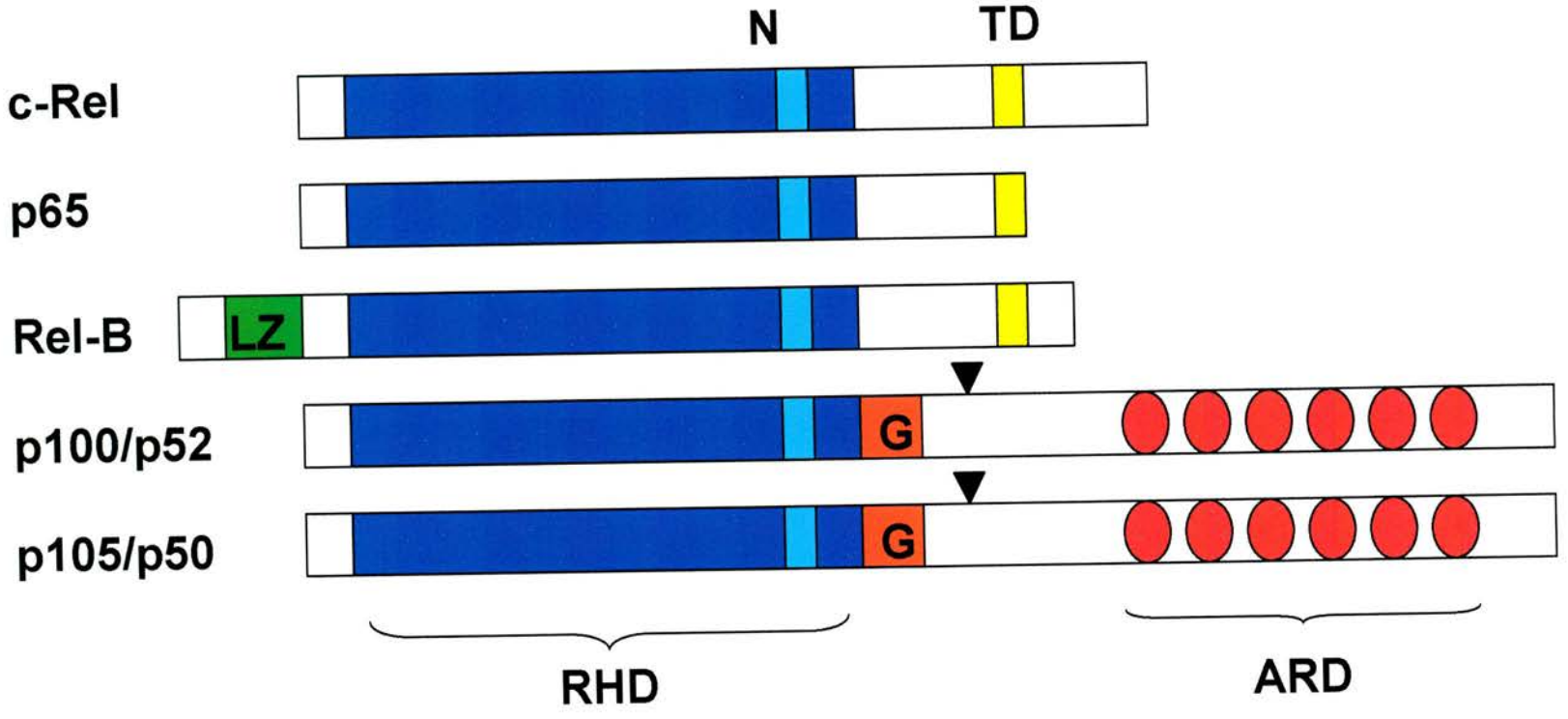

Figure 2.1. – Schematic diagram of the mammalian NFκB protein family.

RHD - Rel homology domain
TD – Transactivation domain
N - Nuclear localisation sequence
LZ – Leucine zipper
G – Glycine rich region
ARD – Ankyrin repeat domain

The arrowheads indicate the endoproteolytic cleavage sites which cleave p100 and p105 to produce p52 and p50 respectively.

undergo further processing to produce these smaller forms (Mercurio & Manning, 1999). P50 and p52 do not contain transactivation domains and can only activate transcription when part of a heterodimer with Rel A (p65) or Rel B. p50/p52 heterodimers inhibit transcription due to the lack of transactivation domains. This may be due to competition with other active dimers for DNA binding sites (May & Ghosh, 1997).

P105 and p100 do not bind DNA. The C-terminus of these proteins is phosphorylated, ubiquitinated and degraded, leaving the N-terminal region containing the RHD domains of p50 and p52 respectively. The process involves cleavage by a Mg^{2+} and ATP-dependent protease. A similar mechanism is involved in signal induced dissociation of NF-κB dimers from their IκB inhibitory proteins. The RHD in p105 and p100 is followed by a glycine rich region and then by the C-terminus which contains ankyrin repeat sequences (Fig 2.1). These ankyrin repeats are also found in IκB proteins and are important in masking the NLS of NF-κB dimers, which prevents their activation. p105 and p100 can likewise mask the NLS, as a result of their ankyrin repeats (May & Ghosh, 1997).

2.3 Structural aspects of NFκB – DNA binding

After activation, NF-κB is translocated to the nucleus where it binds to κB sites on the helix of DNA. X-Ray crystallography provides an insight into the binding arrangement and therefore into the interaction between the NF-κB p50 homodimer and DNA (Ghosh et al, 1995; Muller et al,

1995). The NF-κB binding site involves almost all of the RHD. The RHD consists of two anti-parallel β-sheets in a sandwich structure. The overall structure resembles that of the immunoglobulin fold (May & Ghosh, 1997). Binding of the two p50 subunits produces a structure which resembles a butterfly with the DNA cylinder trapped within its wings. Interaction with DNA involves ten loops at the end of each β strand on p50, resulting in very high affinity between NF-κB and DNA (Muller et al, 1995). These loops provide increased flexibility which means that there are a greater variety of DNA sites to which binding of an NF-κB dimer is possible.

2.4 Inhibitory κB proteins (IκBs)

In unstimulated cells, NF-κB is held in the cytoplasm via binding to inhibitory κB proteins termed IκBs. IκBs bind to the RHD on NFκB dimers, masking the NLS and preventing import into the nucleus (May & Ghosh, 1998; Mercurio & Manning, 1999). There are currently five mammalian IκB proteins which have been identified. These are IκBα, IκBβ, IκBγ, IκBε and Bcl-3 (Fig. 2.2).

The most extensively studied IκBs are IκBα and β which have molecular weights of 37 and 43kDa respectively. IκBα specifically and reversibly inhibits NF-κB binding to DNA (Baeuerle & Baltimore, 1988). Zabel &

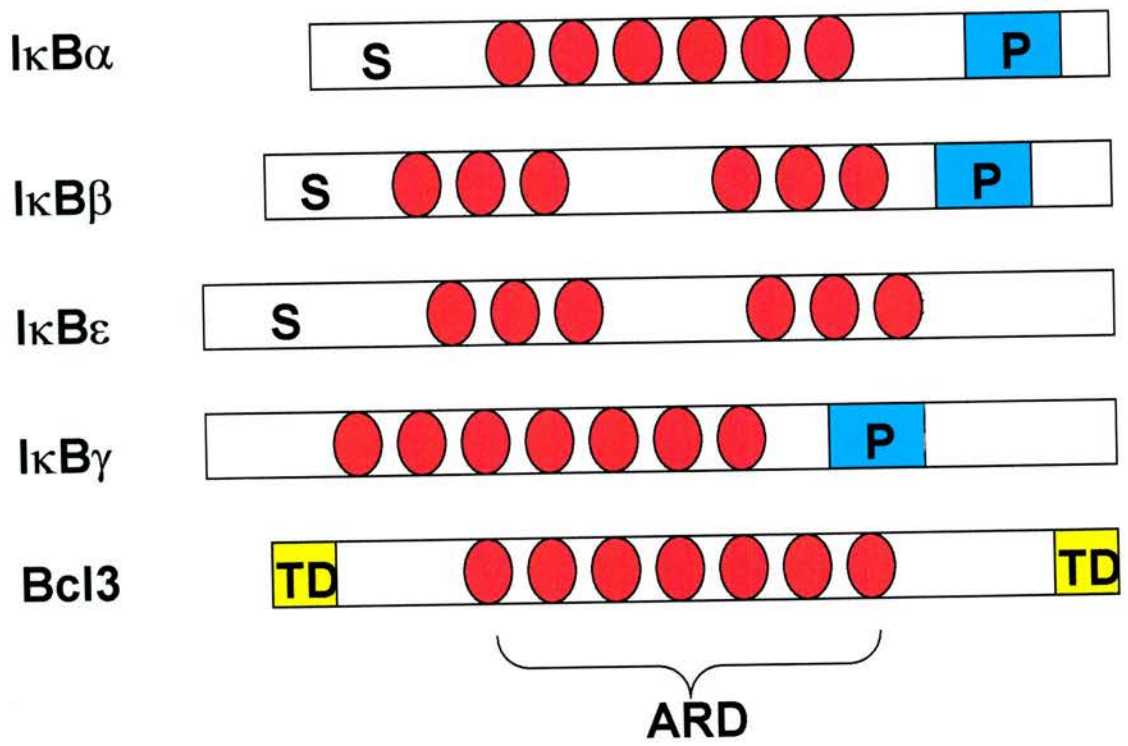

Figure 2.2. Schematic diagram of the IκB protein family.

S – Serine residues which are phosphorylated
P – PEST region
TD – Transactivation domain
ARD – Ankyrin repeat domain

Baeuerle (1990) also showed that IκBα could cause dissociation of NF-κB already bound to DNA.

IκB isoforms exhibit preferential inhibition of certain NF-κB dimers in the cytoplasm. IκBα and β inhibit c-Rel and Rel A containing dimers. Bcl-3 inhibits only p50 or p52 homodimers. IκBγ inhibits c-Rel, p50 and p65 heterodimers and IκBε binds only c-Rel, Rel A or their homodimers (Mercurio et al, 1993). IκBα is targeted by Il-1, LPS, TNFα and phorbol 12-myristyl 13-acetate (PMA) pathways, but IκBβ is only targeted by IL-1 and LPS in some cells (e.g. Jurkat T and 70Z/3 pre-B cell lines; Baldwin, 1996).

IκBα is rapidly produced during the post-induction repression of NF-κB, but IκBβ does not re-accumulate following NF-κB activation, resulting in persistent activity. p100 and p105, the precursors of p52 and p50 respectively, have been shown via cloning experiments to have a similar structure to the IκB family and can thus be technically classed as IκB proteins (Baldwin, 1996). They show little specificity and only fail to form complexes with Rel B (Mercurio et al, 1993).

2.5 Structure of IκBs

IκBα has a tripartite structure with a central domain which contains five ankyrin repeats, a small, highly acidic C-terminal domain and an

unstructured N-terminal signal response domain (SRD; Rodriguez et al, 1999). The SRD contains the phosphorylation and ubiquitination sites which are involved in activation of the NF-κB-IκB complex.

The central domain in all IκBs contains a structural motif known as the ankyrin repeat domain (ARD). This contains between five and seven ankyrin repeats which range from 30-35 amino acids in length (Jaffray et al, 1995). These ankyrin repeats are so called as they were first discovered in the erythrocyte protein ankyrin. Ankyrin repeats are thought to mask the NLS in NFκB dimers, preventing nuclear translocation of NF-κB dimers (Phelps et al, 2000).

The C-terminus in most IκBs contains a region of around 42 amino acids called the PEST domain because it contains a high proportion of proline (P), glutamic acid (E), serine (S) and threonine (T) residues. PEST regions are found in a range of proteins which undergo rapid degradation within the cell (Jaffray et al, 1995). This PEST region is thought to be involved in stabilisation of molecules (Beauparlant et al, 1996) and prevention of NF-κB-DNA binding (Ernst et al, 1995). Ernst et al (1995) also showed that the C-terminus is required to inhibit DNA binding but is not involved in protein-protein binding and does not mask the NLS. The C-terminus is thought, therefore, to inhibit NF-κB binding to DNA either by direct interaction of the PEST region with one subunit of the NF-κB dimer or with the NFκB binding site on DNA. Beauparlant

et al (1996) showed that presence of the whole PEST region is not necessary for inhibition of the NF-κB-DNA complex. Deletion of amino acids 269-287 prevented TNFα mediated breakdown of IκB. Deletion of amino acids 288-317, which includes a large part of the PEST region, did not prevent IκB breakdown, leading these residues to be deemed dispensable.

Mutation of IκBα showed that both the ARD and the C-terminal acidic domains are necessary for interaction of Iκβα with NFκB proteins (Roff et al, 1996). Deletion of either domain does not affect IκB-NF-κB binding. Loss of the C-terminus (including the PEST region) alone prevents IκB from inhibiting NF-κB binding to DNA. Loss of the N-terminus (including ARD) results in IκBα still being able to interact with NF-κB and hence inhibit its binding to DNA. Removal of both terminals causes IκB to lose its inhibitory effect on NF-κB-DNA binding, revealing the importance of the C-terminus (Jaffray et al, 1995; Ernst et al, 1995).

2.6 NFκB Activation

There are many inducers of NF-κB and numerous signal transduction pathways which all converge on the cytosolic NF-κB-IκB complex. These pathways cause IκB to be degraded and the NF-κB-IκB complex to dissociate, leaving NF-κB dimers free to translocate to the nucleus, bind DNA and induce gene expression (Fig. 2.3). IκB dissociation and

Class of Gene	NFκB-Dependent Gene
Cytokines/Growth Factors	IL-1 α and β TNFα IFN-β G-CSF M-CSF GM-CSF
Leukocyte Adhesion Molecules	ICAM-1 VCAM-1 E-selectin
Immunoregulatory Molecules	Igκ MHC class I & II TCR α and β β2-microglobulin

Figure 2.3. Table of selected genes which are activated by NFκB in the immune response.

IL-1 - Interleukin-1
TNFα - Tumour necrosis factor α
IFN-β - Interferon β
G-CSF – Granulocyte colony stimulating factor
M-CSF – Macrophage colony stimulating factor
GM-CSF – Granulocyte macrophage colony stimulating factor
ICAM-1 – Intracellular adhesion molecule-1
VCAM-1 – Vascular adhesion molecule-1
Igκ - Immunoglobulin κ light chain
MHC – Major histocompatibility complex
TCR – T-Cell receptor

degradation is a multi-step process. IκB must be phosphorylated, ubiquitinated and degraded by the proteasome before NF-κB can translocate to the nucleus.

2.7 IκB Phosphorylation

IκB phosphorylation occurs on serine residues 32 and 36. DiDonato et al (1996) replaced these serine residues on IκBα with threonine and found that IκBα phosphorylation was blocked. This suggested that phosphorylation is the rate limiting step in IκB breakdown. DiDonato et al suggested that IκBα and IκBβ (phosphorylated on serine residues 19 and 23) were phospohorylated by the same kinase or members of a family of similar kinases.

The kinase responsible in the majority for phosphorylation of IκB is the so called IκB kinase (IKK) complex (DiDonato et al, 1997). However, many NF-κB inducing stimuli cause IκB to be targeted for phosphorylation via casein kinase II (CKII). CKII can also phosphorylate p65, which increases the transactivation potential of the NF-κB dimer (Wang et al, 2000).

2.8 Ubiquitination of phosphorylated IκB

Phosphorylated IκBα and IκBβ undergo rapid modification by the addition of several ubiquitin (Ub) molecules (Scherer et al, 1995).

Ubiquitination of IκBα happens at lysine residues 21 and 22, which are situated next to the phosphorylation sites of serine 32 and 36. It is postulated that phosphorylation of serine 32 and 36 causes a conformational change exposing lysines 21 and 22, allowing ubiquitination to take place (Scherer et al, 1995).

Beauparlant et al (1996) treated NIH3T3 cells with a proteasome inhibitor and found that IκBα degradation was inhibited but phosphorylation was not. These results suggest that these events are not dependent on each other. Phosphorylation seems to serve almost as a tag which identifies the protein for ubiquitination.

There are several enzymatic processes involved in the ubiquitination of IκB (Fig. 2.4). The first step is ATP dependent and requires Ub to form a thioester bond with the Ub-activating enzyme known as E1 (Adams et al, 1992). This Ub-E1 complex, referred to as "activated Ub", is then acted upon by a second enzyme, E2, a Ub-conjugating enzyme (Pickart & Rose, 1985). E2 can directly conjugate Ub to IκB but in some cases a third enzyme, E3, which is a Ub protein ligase, is required. More than one form of E3 ligase exists. In the case of IκBα, a specific part of the Iκβα-Ub ligase complex is a protein known as β-transducin repeat containing protein (β-TRCP). Spencer et al (1999) showed that β–TRCP exhibits specificity for signal-induced IκBα ubiquitination.

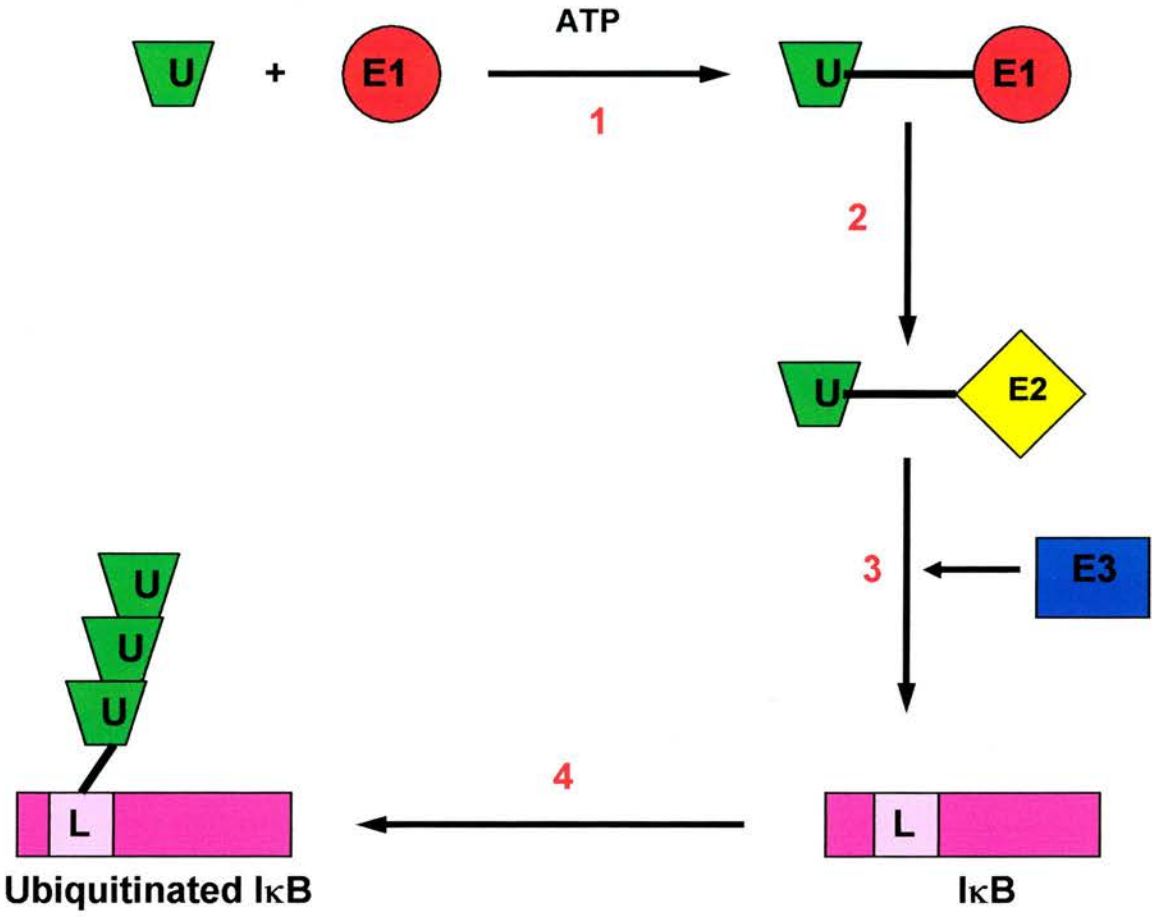

Figure 2.4. Schematic diagram of the ubiquitination of IκB.

1. Ubiquitin forms a thioester bond with ubiquitin activating enzyme (E1) in the presence of ATP.
2. Activated ubiquitin is presented to the ubiquitin carrier enzyme (E2).
3. Ubiquitin protein ligase (E3) transfers ubiquitin from E2 to lysine residues on IκB.
4. A ubiquitin chain is formed on IκB by repeating the pathway.

U – Ubiquitin
E1 – Ubiquitin activating enzyme
E2 – Ubiquitin carrier enzyme
E3 – Ubiquitin protein ligase
L – Lysine residues

The Ub system is actually constitutively active in the cell but IκB is only degraded after phosphorylation. Beauparlant et al (1996) suggested that the C-terminus of IκBα protects it from degradation by a proteasome via its interaction with p65. Scherer et al (1995) showed that E3 has substrate specificity and its interaction with serine 32 and 36 causes Ub to attach to lysine 21 and 22 because of the spatial arrangement of the N-terminus of IκBα. Therefore it is thought that serine 32 and 26 regulate IκBα-E3 ligase interaction during ubiquitination.

2.9 IκB degradation and NF-κB translocation

IκB degradation takes place via the 26S proteasome, which is ATP dependent. Chen et al (1995) showed that pre-treatment of cells with a peptide aldehyde inhibitor, MG132, prevented IκB degradation and this led to the accumulation of phosphorylated and ubiquitinated IκBα still associated with NF-κB. After IκB degradation, NF-κB is free to translocate to the nucleus and bind to the κB site of an appropriate gene promoter via the RHD, causing altered gene transcription (Baldwin, 1996). Transducing activation signals from cytoplasm to nucleus is an example of NF-κB behaving as a second messenger (Ghosh & Baltimore, 1990).

NF-κB nuclear import occurs via the importin-α family of proteins which recognise the NLS. NLS-importin-α in the cytoplasm associates with importin-β which guides the complex into the nucleus via nuclear pores.

NF-κB-dependent gene transcription provides its own negative feedback mechanism as NF-κB also activates IκBα gene transcription. Newly synthesised IκBα moves from the cytoplasm to the nucleus, inhibits NF-κB-DNA binding and therefore results in the cessation of NF-κB dependent transcription (Arenzana-Seisdedos et al, 1995). The newly formed NF-κB-IκBα complex is then exported back to the cytoplasm. The process involves a nuclear export sequence (NES) found in the C-terminus of IκBα. The NES is recognised by a family of proteins known as exportins which allow the NF-κB-IκBα complex to leave the nucleus (Arenzana-Seisdedos et al, 1997). NF-κB and IκBα are mutual regulators where levels of one control levels of the other, thereby regulating NF-κB dependent gene transcription.

2.10 IκB Kinases (IKK)

NF-κB inducers are believed to act via several different pathways that intersect at some point, probably in close proximity to the NF-κB-IκB complex. Phosphorylation of IκB required the presence of a kinase and early suggestions for this included PKA, Raf-1 and double stranded RNA-dependent kinase (PKR). None of these, however, were shown to

phosphorylate the essential serine residues 32 and 36 (May & Ghosh, 1998).

In the search for a suitable kinase candidate which (a) phosphorylated serine 32 and 36 on IκBα and (b) depended upon Ub for its activity, a 700kDa kinase complex was identified (Woronicz et al, 1997, Mercurio et al, 1997). This 700kDa complex was further investigated and found to contain two catalytic kinase components. These were named IKKα/IKK1 and IKKβ/IKK2 and have molecular weights of 85 and 87kDa respectively. Using cloned IKKα and IKKβ, exposure to NF-κB inducers led to rapid induction of kinase activity (Mercurio et al, 1997).

IKKα and β contain common structural motifs – an N-terminal serine/threonine kinase domain, a leucine zipper (LZ) and a C-terminal helix-loop-helix (HLH) (Fig. 2.5). The LZ induces dimerisation of IKKα and IKKβ. IKKα and IKKβ form either homo- or heterodimers (May & Ghosh, 1998). In some cells, different dimers can elicit different responses to the same stimuli. For example in HeLa cells the heterodimer produces a more potent response to TNFα stimulation than the IKKβ homodimer, showing that IKKα is essential for full activation of NF-κB (Mercurio et al, 1999). IKK's ability to form different dimers is important in enabling differential NF-κB regulation in different cell lines by a variety of mechanisms.

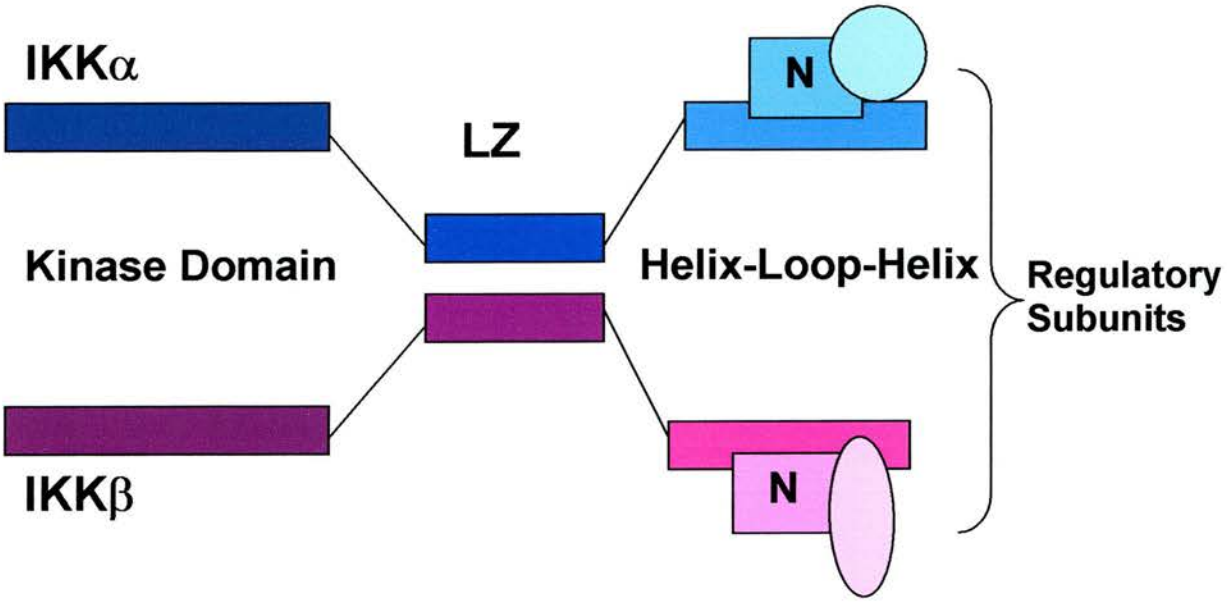

Figure 2.5. Schematic diagram of the structure of IKKα and IKKβ

LZ – Leucine zipper
N - NFκB essential modulating factor (NEMO)

A regulatory subunit, necessary for formation of the IKK complex, exists and is known as IKKγ or NF-κB essential modulating factor (NEMO). It is a glutamine rich 419 amino acid protein which has a LZ and several coiled protein motifs. It interacts preferentially with IKKβ and is an essential component for NF-κB activation (Yamaoka et al, 1998). Rothwarf et al (1998) used truncated NEMO to show that the IKK complex could still bind to IκB but its action was inhibited. This suggests that NEMO plays an essential role in IKK activation and it may link the IKK complex to activators upstream of IKK.

Research by Mercurio et al (1999) into the IKK complex revealed a protein common to all IKK dimers in HeLa cells. Subsequent purification and cloning of this protein, known as IκB kinase associated protein 1 (IKAP-1) showed that *in vitro* it binds with IKKβ (but not IKKα) and required specific N-terminus residues to achieve this. Mutation of these residues disrupted NF-κB transduction, suggesting IKAP-1 must play an essential but unclear role in NF-κB activation, as it does not contain an enzymatic motif. IKAP-1 purification reveals it to be the human homologue of murine NEMO and this is thought to provide a scaffold for IKKβ complexes to localise with upstream components of the NF-κB activation pathway (Mercurio et al, 1999; Yamaoka et al, 1998).

Cohen et al (1998) identified another IKK complex protein known as IK complex associated protein (IKAP). It is able to assemble IKKα, IKKβ,

NF-κB inducing kinase (NIK) and NF-κB-IκB into a complex. Krappmann et al (2000), however, showed that IKAP is not associated with IKKα or IKKβ and does not play a specific role in NF-κB activation induced by cytokines.

2.11 IKK Regulation

Research has yet to reveal exactly how IKKs are stimulated by upstream molecules. Activation of IKK is serine specific and responds to a number of NF-κB activators such as TNFα (Ghosh et al, 1995). TNFα responses are mediated by two surface receptors known as TNFR1 and TNFR2 (Smith et al, 1994). TNFRs activate a family of signal transduction molecules known as TNF receptor associated factors (TRAFs) (Rothe et al, 1995; Hsu et al, 1997). TRAFs can also be activated by the Il-1 receptor (IL-1R). TNFR and IL-1R have been shown to associate TRAFs 2 and 6 respectively, which subsequently activate kinases and continue transmitting the stimulus.

Mercurio & Manning (1999) suggest that phosphorylation of IKKα and IKKβ occurs at serines 176 & 180 and 177 & 181 respectively. This phosphorylation may be mediated by an upstream kinase which is likely to be a member of the protein kinase family known as mitogen-activated protein kinase-kinase kinase (MAP3K, MAPKKK or MEKK). NF-κB inducing kinase (NIK) is a member of this family and interacts with TRAF-2 and also associates with IKKα and IKKβ (Woronicz et al, 1997).

Use of an inactive mutant of NIK by Malinin et al (1997) resulted in NF-κB activation being inhibited following TNFα or IL-1 exposure. This demonstrates that NIK is an integral part of both pathways. Nakano et al (1998) showed that over-expression of NIK caused IKKα and IKKβ activation and that it phosphorylates IKKα preferentially on serine 176, leading to its activation.

Further research, however, has questioned the physiological significance of NIK. Woronicz et al (1997) showed NIK to be present when the IKK complex was biochemically purified. Over-expression of NIK showed its interaction with IKKα, but under physiological conditions no such interaction was observed. Furthermore, Hu et al (1999) showed that IKK activation is dependent on the IKKβ subunit, but NIK preferentially targets the IKKα subunit.

Another MAPKKK, identified as MEKK-1, phosphorylates serines in the activation loop of IKKβ. Use of an inactive mutant of IKKβ resulted in inhibition of NF-κB activation via MEKK-1, suggesting that it acts through IKKβ alone (Nakano et al, 1998). Co-expression of NIK and MEKK-1 enhanced the ability of IKK to phosphorylate IκB, however IKKα and IKKβ, and subsequently NF-κB, appear to be activated by independent mechanisms (Mercurio & Manning, 2000).

2.12 Fluid shear stress mediated activation of NF-κB

Much work has been carried out which shows that haemodynamic forces alter the structure, function and gene expression of the endothelium (Davies, 1995; Braddock et al, 1998; Papadaki & Eskin, 1997; Chien et al, 1998). A cis-acting element in the platelet derived growth factor-B (PDGF-B) gene which is involved in FSS responses was identified by Resnick et al (1993). This shear stress response element (SSRE) contains a core binding sequence of six base pairs GAGACC) which binds transduction factors in bovine aortic endothelial cell (BAEC) nuclear extracts. Further studies showed that inserting the SSRE into reporter genes made them inducible by shear, proving the effectiveness of the SSRE (Resnick & Gimbrone, 1995). However, the pathway through which the haemodynamic force is sensed and transduced to the level of gene expression is still not clear.

Lan et al (1994) showed that NFκB is activated in BAEC subjected to FSS of 12 dynes.cm^{-2}. NF-κB stimulation was observed within 30 minutes and was maximal after 60 minutes of FSS. NF-κB (p50/p65) was later identified to bind specifically to the SSRE of PDGF-B in BAEC which had been subjected to FSS of 10 dynes.cm^{-2} (Khachigian et al, 1995). However, FSS activated translocation of NF-κB was not sufficient to modulate all genes that are known to contain recognition sequences for NF-κB. Suggestions why this may be the case include NF-κB sites in individual genes containing slight differences, alteration of

the structure of NF-κB by FSS or even the interaction of other transcription factors (Khachigian et al, 1995; Papadaki & Eskin, 1997).

2.13 Scope of the present study

Very little is known about the upstream signalling pathway involved in NF-κB activation by flow in human endothelial cells. The implication of NF-κB in the pathogenesis of atherosclerosis (Collins et al, 1993; Brand et al, 1996; Hajra et al, 2000) now makes this matter of particular interest. The work here utilised HUVEC in electrophoretic mobility shift assay (EMSA), kinase assays, luciferase assays and immunofluorescence to investigate the roles, if any, of IκBs, IKKs, NIK, TPL-2 and PKC in the signalling pathway initiated by FSS and resulting in NF-κB dependent gene transcription.

CHAPTER 3

NF-κB MATERIALS AND METHODS

Suppliers of reagents and details of apparatus are given in Appendix 1.

3.1 – Cell Culture

All experiments were carried out using human umbilical vein endothelial cells (HUVEC) prior to passage 10, which were cultured under sterile conditions in a class II flow hood.

3.1.1 – Maintenance of HUVEC

HUVEC were maintained in EBM-2 medium supplemented with 5% Foetal Bovine Serum (FBS), human epidermal growth factor (hEGF), human fibroblast growth factor (hFGF), vascular endothelial growth factor (VEGF), ascorbic acid, hydrocortisone, long R3-IGF-1, heparin, gentamicin and amphotericin. The growth medium was changed on alternate days and cells were cultured in a humidified incubator at 37°C with 5% CO_2 / 95% Air.

Cells (approx. $1x10^6$) were rederived from liquid nitrogen and seeded into a $75cm^2$ flask with 20ml medium as required. They were maintained until confluence before being trypsinised and seeded appropriately (see 3.1.2) for experimental use.

3.1.2 – Trypsinisation and seeding of HUVEC

Upon reaching confluence, the medium was removed and the flask rinsed with 4ml hepes buffered saline solution (HBSS). 3ml 0.01%

trypsin/EDTA was added and the flask incubated at 37°C for 2 minutes or until the cells had rounded up. 4ml of culture medium was added to stop trypsinisation and the suspension transferred to a universal tube. The HUVEC were counted using a Coulter counter® Z1™ Series particle counter. They were then seeded on either sterile 22 x 22mm borosilicate glass coverslips or 26 x 76mm plain, low iron glass slides at a density of $2x10^4$ cells.cm^{-2}.

Coverslips and slides were maintained as in 3.1.1 for varying periods of time and used, as appropriate, for experimentation.

3.1.3 - DNA Plasmid and Transient Transfection of NIK, IKK1 and IKK2

HUVEC were cultured on coverslips until they reached 80% confluence. Using Lipofectamine™ transfection technology, 5ug of pCDNA3 empty vector, pcDNA expression plasmids containing cDNAs for NIK, IKK1 or IKK2 or the corresponding catalytically inactive mutant NIKmut (Malinin et al, 1997), IKK1mut or IKK2mut (Regnier et al, 1997) were ectopically expressed in these cells. Cells were incubated for 4 hours at 37°C with the lipofectamine and DNA constructs, and then rinsed once with EBM-2 medium and maintained in culture until the cells reached confluence. For effective transfection, the fluid shear stress (FSS) experiments and static controls were used within 36 hours.

HUVEC on both coverslips and slides were exposed to FSS at 15 dynes.cm^{-2}. The apparatus is described in 3.3. Controls were prepared

and analysed in the same way, using cells which had not been exposed to FSS.

3.2 Drug treatment of HUVEC

HUVEC were incubated for 30 minutes prior to FSS with either the proteasome inhibitor MG132 (20μM) or leptomycin B (20nM), an inhibitor of IκBα nuclear export. Drug treated static controls were also prepared. To determine if Protein Kinase C (PKC) was essential for the cellular response to flow, cells were exposed to combinations of 25ng.ml^{-1} phorbol 12-myristate 13-acetate (PMA) and 1μg.ml^{-1} ionomycin with or without 100nM bisindolylmaleimide (bisin) for 30 minutes prior to exposure to FSS or fixing for immunofluorescence (in the case of static controls). With PMA, ionomycin and bisin combination treatment, cells were pre-treated with bisin for 30 minutes and the culture medium was changed before the addition of PMA and ionomycin. HUVEC cultured in 6 well plates and on slides were treated with 30ng.ml^{-1} TNF for 0, 5, 10, 20, 30, 60, 120 and 240 minutes. These cells were used for immunoblotting and kinase assay experiments for comparison with the effects of flow.

3.3 – Flow apparatus

One of two parallel plate flow chambers, similar to that described by Viggers et al (1986), were used to subject cells to uniform laminar shear stress (Fig. 3.1). One chamber was used for cells grown on coverslips

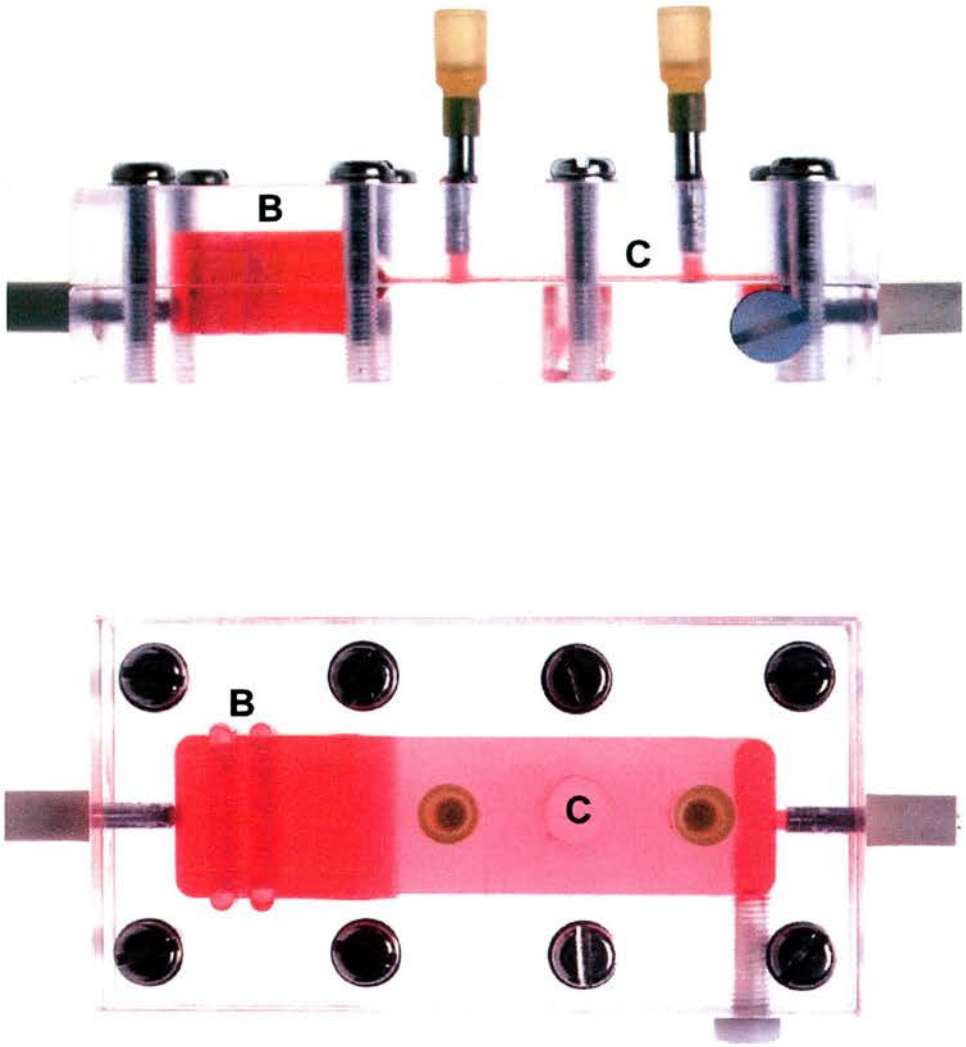

Figure 3.1 Illustration of side-on and aerial views of a flow chamber.

Medium enters from the left and passes through the baffles (B) to ensure uniform flow velocity. The medium then passes over the cells on either coverslips (C) or microscope slides.

for structural and morphological studies. The second was used for cells grown on microscope slides and used to provide material for biochemical analysis.

The flow chamber was connected, using gas impermeable Masterflex™ tubing, into a closed loop perfusion system containing two flasks with culture medium, driven by a peristaltic pump (Fig. 3.2). The culture medium was gassed with 5%CO_2 / 95% air and the whole apparatus set-up was contained in a class II flow hood within a 37°C hot-room.

It was determined that the chambers produced two dimensional uniform laminar flow by measuring the shear stress generated at different pump flow rates and comparing these with theoretical calculations. These calculations are detailed in Appendix 1.3. In all experiments, the flow rate through each chamber was set to generate 15 dynes.cm^{-2} shear stress which is within the physiological range of medium sized arteries (Shyy et al, 1994).

3.4 – Immunofluorescence and fluorescence microscopy

3.4.1 Paraformaldehyde fixation method and immunofluorescence

The nuclear translocation of NF-κB in response to FSS and drug treatment was investigated using immunofluorescence. Cells were rinsed with PBSc before fixing in 3% paraformaldehyde/PBS. Three rinses in PBSa and then two washes in 0.1M Glycine/PBSc, to quench the paraformaldehyde, followed. Two washes in PBSa were followed by

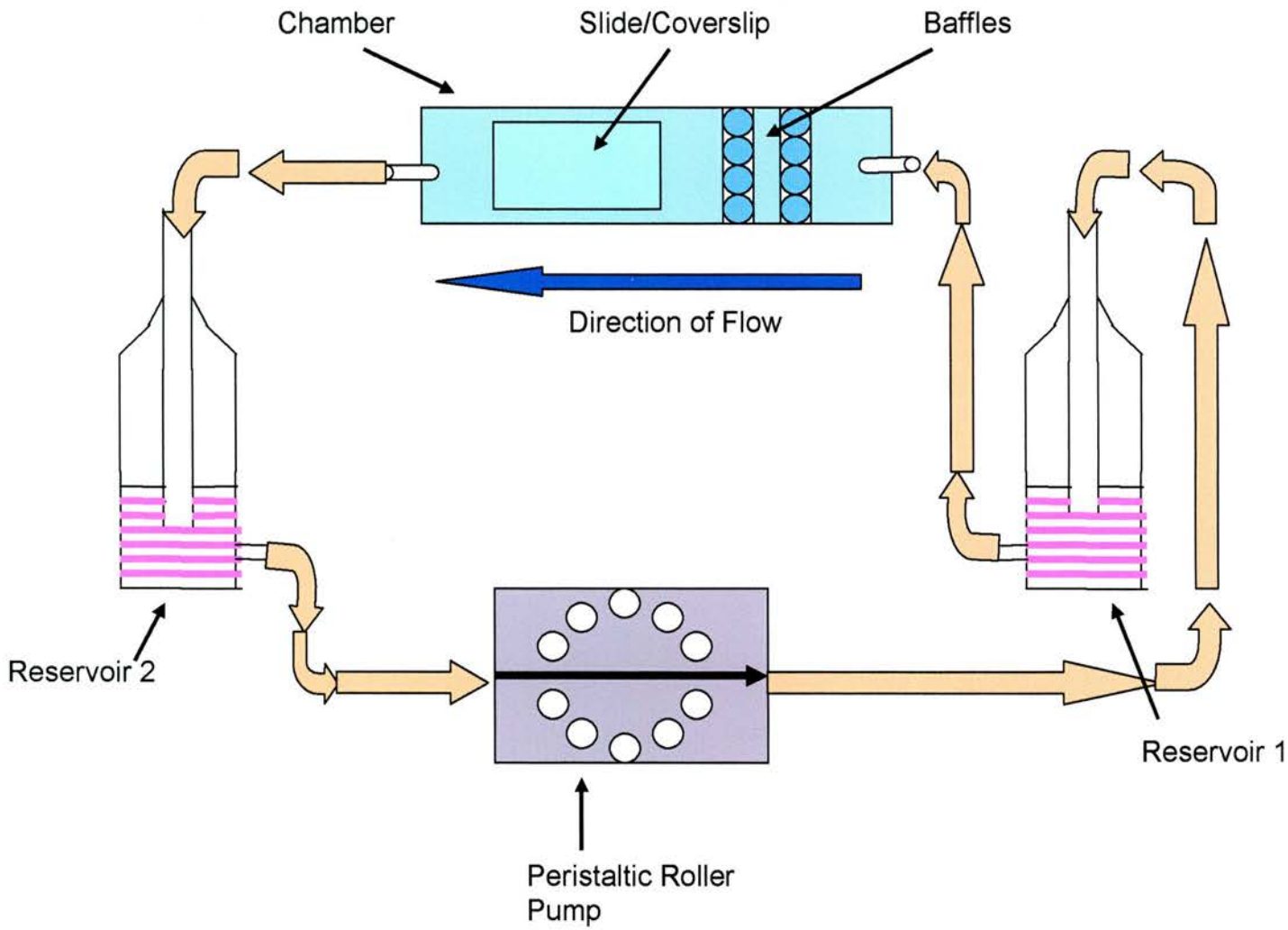

Figure 3.2 Schematic of closed loop perfusion chamber for fluid shear stress experiments.

permeabilisation in 0.2% Triton-X100/PBS. After rinsing again in PBSa, the cells were blocked in 0.2% BSA/PBS before addition of the primary antibody solution and incubation at room temperature in the dark. Monoclonal primary antibodies to hnRNP A1 and p-65 were used at concentrations of 1:200 and 1:100 respectively. Rabbit polyclonal antibodies to NIK, IKK1, IKK2, and p65 were all used at a concentration of 1:100. Following three rinses in 0.2% BSA, goat anti-mouse FITC (GAMF) and goat anti-rabbit Texas Red (GART) secondary antibodies were used at a concentration of 1:200 and incubated as for the primary antibodies. After further rinses in BSA and PBS, the preparations were mounted using Hydromount, a non-fluorescing mountant.

3.4.2 – Microscopy

A Zeiss Axioplan Universal fluorescence microscope with x40, x60 (oil) and x100 (oil) objectives was used for initial viewing of images.

For recording images, a Nikon Microphot fluorescence microscope which includes a digital camera, was used at x100 magnification. The camera images were viewed using NIH image software and recorded as TIFF files before being stored on Zip disks or CD-ROM and transferred to Adobe Photoshop 6.0 for size and resolution amendments.

All images in Chapter 4 were collected using this technique.

3.5 – Western Blotting

Degradation of the NF-κB inhibitor proteins IκBα and IκBβ was studied by Western blotting. Cells were sheared as described in 3.3 and lysates were made according to the method detailed in 3.5.1. Rabbit polyclonal primary antibodies to IκBα and IκBβ and sheep polyclonal affinity purified antibodies to p105 and p50 were used to detect the appropriate proteins. All primary antibodies were used at a concentration of 1:1000. The secondary antibodies used were anti-sheep HRP and goat anti-rabbit HRP, at concentrations of 1:10,000.

3.5.1. – Cell Extract Preparation

Cells grown on microscope slides and subjected to flow were extracted using a hot lysis method. Excess medium was drained from the slide and the cells were rinsed with warm PBSa. 750μl of boiling Laemmli buffer was pipetted onto the slide surface. A cell scraper was then used to remove the cells from the slide. The resulting viscous solution was removed to an Eppendorf tube and syringed through a 25G needle before being boiled for 5 minutes in a water bath. The lysate was then centrifuged for 5 minutes at 12,000 RPM, transferred to a clean tube and stored at -20°C.

3.5.2. – Protein Estimation

The protein content of the cell extracts was measured using a protein estimation kit which was compatible with the lysis buffer used to prepare

the extracts. Standard concentrations of BSA were prepared, along with blanks and cell extract samples, as per instructions provided with the kit. All samples were read in a dual beam spectrophotometer set at a wavelength of 720nm. A standard calibration curve was constructed and the protein concentrations of the cell extracts calculated from this.

The cell extracts could then be diluted to relevant dilutions using Laemmli buffer. 1μl of bromophenol blue dye and 3μl of β-mercaptoethanol was added per 100μl of extract. The extracts were boiled for 5 minutes in a fume hood and stored at -20°C.

3.5.3. – Gel Electrophoresis and Western Blotting

Protein separation was carried out using sodium dodecyl sulphate-polyacrylamide gel electrophoresis (SDS-PAGE) and the proteins were transferred from the gel using the semi-dry method onto nitrocellulose membrane for immunoblotting. Membranes were blocked and then probed with primary antibodies followed by secondary antibodies with horseradish peroxidase tags. The antibody solutions were made up in 15% Marvel/PBS-T. The proteins were then detected using the enhanced chemiluminescence technique (ECL™).

Immunoblots were scanned for densitometric and quantitative analysis using the data inspector function of the SoftWorx 2.5 programme. A 10x2 pixel box was used on each band and intensities recorded.

In the case of 4.2.2; intensity values were normalised in respect to the corresponding reprobed blot for actin, which was used to check for

uniformity of loading on the gel as its' levels are shown not to change when subjected to FSS (Beers, 2002). Actin blot intensities were measured and averaged. The difference between the average value and the individual actin band values was calculated. The resulting differences were used to adjust the corresponding IκBα, IκBβ, p105 and p50 values. This intensity data was then expressed as a percentage of the control (0 minute FSS) value (Appendix 1.8) and displayed graphically (Fig 4.2.2). In the case of 4.3, 3 readings were taken from 3 separate experiments (n1, n2 and n3). All control (0 min FSS) values (9 in total) were averaged. This value was set as 1 in order to calculate fold activation values.

Every value for all other test conditions was converted to an arbitrary value relative to the mean control value. Mean fold activation values for each experiment (n1, n2 and n3) were calculated (Appendix 1; 2.0.2). The average value for each test condition was displayed graphically (Fig 4.3).

3.6 – Electrophoretic mobility shift assay (EMSA)

Extracts of sheared cells (3.5.1) were analysed in a gel electrophoresis DNA binding assay. A ^{32}P labelled double stranded oligonucleotide (5' GTCCTCA**GAGACC**CCCTAAGC 3') containing a 6 base pair shear stress response element (SSRE, in bold) which binds DNA (Khachigian et al, 1996) was added to the nuclear extract and separated by gel electrophoresis. Free DNA and DNA/protein complexes have different

electrophoretic mobilities, allowing separation in a poly-acrylamide gel. Radioactivity was detected using a phosphorimager. A molecular weight marker was also run on the gel, to determine molecular weights of the resulting sample bands. The marker was not radioactively labelled and the marker bands were measured before the remainder of the gel was subjected to radioactivity detection. 15 minutes pre-incubation with antibodies against p50 and p65 or 1μl pre-immune serum prior to addition of the radiolabelled oligonucleotide was used to identify the DNA-binding complexes. Pre-incubation in the ame manner with 10ng of recombinant p50/p65 heterodimer was used as a positive control. A competition assay was carried out using a 20-fold molar excess of unlabelled oligonucleotide.

3.7 - Luciferase assay

HUVEC grown on microscope slides were transfected with 10μg of 3enh Con A Luc plasmid which contains 3 binding sites for NF-κB. Other HUVEC were transfected with Con A Luc plasmid which lacks the NF-κB binding sites, as a negative control. Upon reaching confluence, the cells were exposed to FSS for 12 hours and then maintained in culture for an additional 24 hours. The cells were lysed and the cell extracts were standardised by performing a protein estimation via the Lowry method before luciferase activity was assayed. Luciferase activity, expressed in relative light units (RLU), was measured using a MicroLumat plate reader.

3.8 - IKK Immunocomplex kinase activity assay

HUVEC were exposed to flow (15 dynes.cm^{-2}) or treated with TNFα (30ng.ml) for the noted times and subsequently lysed in 1ml of lysis buffer. The lysate was cleared by high-speed centrifugation at 80,000 RPM at 4^{o}C for 30 minutes. The supernatant was then incubated for 2 hours at 4^{o}C with 10μl of protein A beads conjugated to an antibody raised in sheep and affinity purified against the C-terminus of IKK1 (residues 734-745). The immunoprecipitated material was washed twice with lysis buffer, twice with pulldown buffer and once with kinase assay buffer. The immunocomplex was then resuspended in 20μl kinase assay buffer containing 3μCi of [γ-^{32}P] ATP, 10 μM ATP and 1μg of either wild type GST-N Terminal IκBα (amino acids 1-70) or the GST-N Terminal IκBα 32 S/E and 36 S/E mutant, giving a total volume of 30μl. The reaction was terminated by adding 3x SDS sample after 1 hour at 30°C. The samples were boiled for 5 minutes and then separated on a 12.5% SDS polyacrylamide gel. On completion of gel-electrophoresis, the radioactive species was detected using a phosphorimager.

Transfection of cells, luciferase assays and the IKK immunocomplex kinase activity assays were performed in the BMS department, University of St Andrews by Dr David Hay and Dr Lesley Thomson respectively.

CHAPTER 4

NF-κB RESULTS

4.1 NF-κB dependent gene transcription is stimulated by FSS

The aim of the experiment was to reveal whether DNA binding of a known shear stress response element (SSRE) oligonucleotide would occur in nuclear extracts of cells which had been subjected to fluid shear stress (FSS) and whether this bound oligonucleotide would show any association with p65. A luciferase assay was then used to confirm whether FSS caused NF-κB-dependent gene transcription.

Uniform FSS (15 dynes.cm^{-2}) was applied to HUVEC for periods of 5-240 min. Nuclear extracts were prepared and an electrophoretic mobility shift assay (EMSA) carried out using a ^{32}P labelled shear stress response element (SSRE) -containing oligonucleotide which includes a NFκB-binding 6 base pair sequence (GAGACC) (Fig. 4.1a). A transient increase in DNA binding was observed, peaking at ~30min (approximately 3x control levels) and decreasing to ~50% of its maximal value in cells sheared for 60-240min. (Fig. 4.1b). Nuclear extracts were pre-treated with p65 and p50 antibodies and sheared for 30 minutes – the timepoint showing maximal DNA binding. This revealed a supershift where the antibody binds to the protein but does not inhibit DNA (Fig 4.1a). This indicates that activation of flow causes the p50/p65 heterodimer to bind to the SSRE. Extracts pre-treated with pre-immune serum (PIS) and sheared under the same conditions had no effect on DNA binding (Fig 4.1a). Binding of the recombinant p50/p65 by the oligonucleotide is shown as a positive control (P.C., Fig 4.1a). This

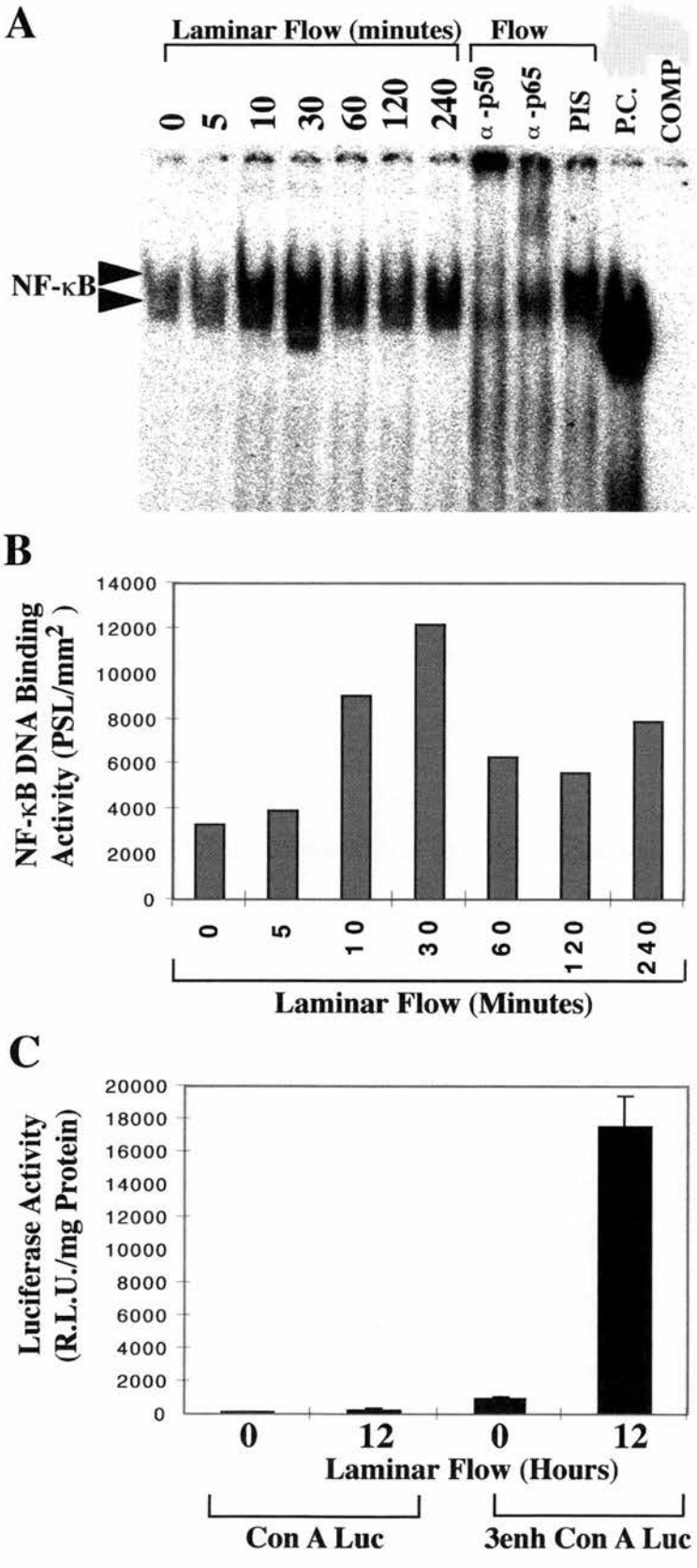
A
Laminar Flow (minutes)
Flow
0
5
10
30
60
120
240
α -p50
α -p65
PIS
P.C.
COMP
NF-κB
B
NF-κB DNA Binding Activity (PSL/mm2)
14000
12000
10000
8000
6000
4000
2000
0
0
5
10
30
60
120
240
Laminar Flow (Minutes)
C
Luciferase Activity (R.L.U./mg Protein)
20000
18000
16000
14000
12000
10000
8000
6000
4000
2000
0
0
12
0
12
Laminar Flow (Hours)
Con A Luc
3enh Con A Luc

Figure 4.1

C shows a gene reporter assay using an NF-κB dependent luciferase reporter (3enh Con-A-Luc) containing 3 κB binding sites. Cells exposed to flow for 12 hours showed a x19 increase in activity of the luciferase reporter in comparison to cells in static culture. A luciferase reporter lacking the κB binding sites (Con-A-Luc) was used as a control and revealed only a x2.6 increase in activity in response to FSS. Results are mean ± standard error (S.E.) of 3 experiments.

binding was prevented in a competition experiment where excess unlabelled SSRE oligonucleotide (x20) was used. No ^{32}P labelled material was observed on the gel (COMP; Fig 4.1a). All radioactivity was detected using a phosphorimager.

The NF-κB dependent luciferase reporter (3enh Con A-Luc) was transfected into HUVEC to measure NF-κB dependent gene transcription. A negative control using a luciferase reporter which lacks the NF-κB concensus binding sites (Con A-Luc) was also prepared. Confluent HUVEC monolayers were exposed to FSS (15 dynes.cm^{-2}) for 12 hours and then left in culture for 24 hours. Nuclear extracts were prepared and their luciferase activity was measured (Fig. 4.1c). 3enh Con A-Luc reporter cells showed a ~19 fold increase in luciferase activity. The NF-κB independent reporter cells (Con A-Luc) showed only a ~2.6 fold increase. This reveals that FSS enhances NF-κB –dependent gene transcription.

4.2 IκBα and IκBβ degradation, but not p105, is stimulated by FSS and TNFα

The aim of the experiment was to determine, using western immunoblotting, whether IκBα, IκBβ and p105 are degraded when HUVEC were stimulated by FSS or TNFα. HUVEC were subjected to FSS (15 dynes.cm^{-2}) or TNFα (30ng.ml) for periods of time ranging from 5-240 min (Fig. 4.2.1, 4.2.2). Whole cell lysates were prepared and analysed via Western blotting and ECL, using rabbit polyclonal

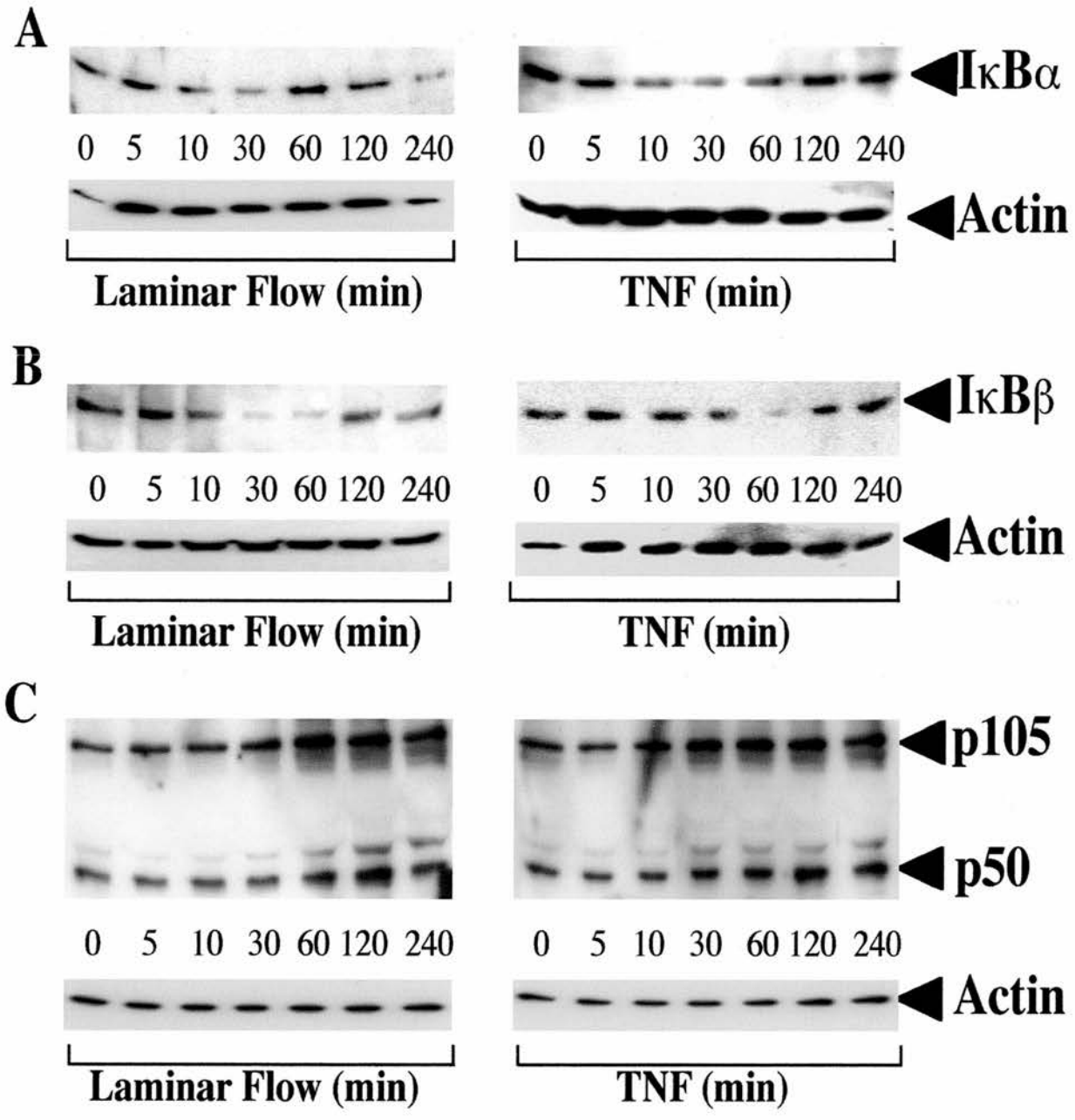
A
IκBα
0 5 10 30 60 120 240
0 5 10 30 60 120 240
Actin
Laminar Flow (min)
TNF (min)
B
IκBβ
0 5 10 30 60 120 240
0 5 10 30 60 120 240
Actin
Laminar Flow (min)
TNF (min)
C
p105
p50
0 5 10 30 60 120 240
0 5 10 30 60 120 240
Actin
Laminar Flow (min)
TNF (min)

Figure 4.2.1

A

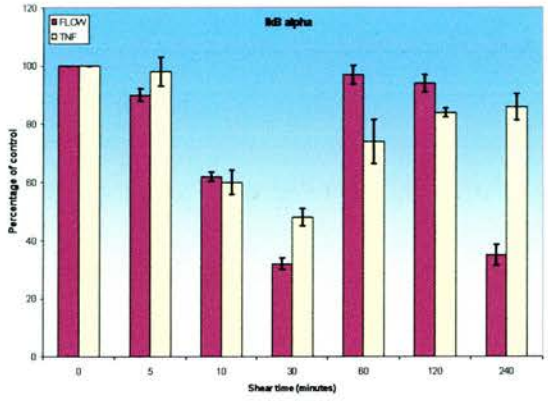

C

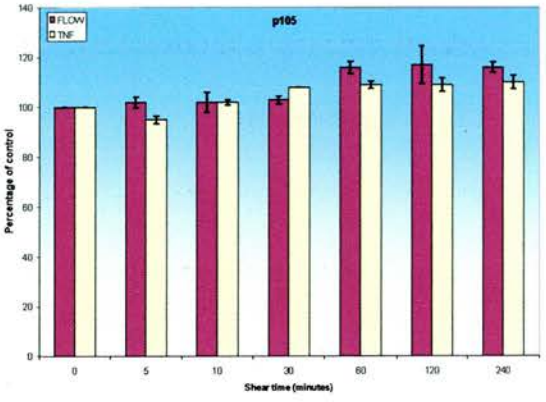

B

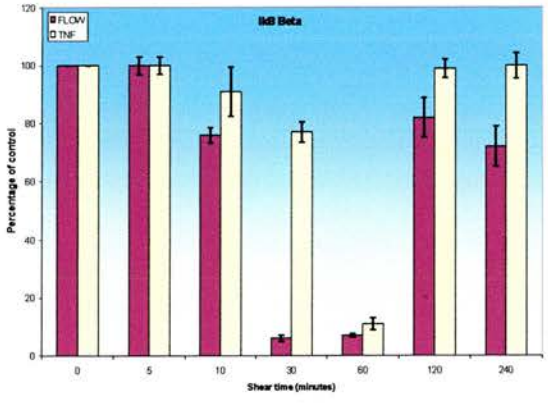

D

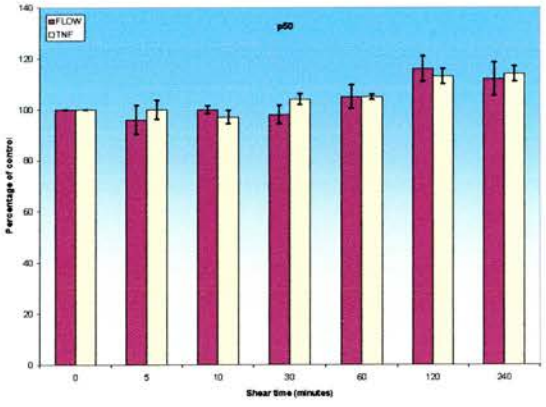

Figure 4.2.2

antibodies to IκBα, IκBβ$_1$ and affinity purified sheep polyclonal antibody to p105/p50 (Fig. 4.2.1). Gel densitometry was used to quantify the levels of protein and normalised with respect to actin. Quantitative data is derived from the mean of 3 separate experiments under each condition (Fig. 4.2.2, Appendix 1.8).

FSS caused a transient decrease of IκBα to ~32% of the level seen in static culture after 30 min. Levels were fully recovered after 60 and 120 min. (Fig. 4.2.2a). After 240 min, IκBα levels had decreased again to ~35% of the static culture level, suggesting a pattern of degradation which is biphasic. FSS also caused a transient decrease of IκBβ$_1$, to 6-7% of the level of unsheared control cells, after 30-60 min (Fig. 4.2.2b). Complete recovery of IκBβ$_1$ levels was seen after 120-240 min FSS.

TNFα (30ng.ml) stimulation caused maximal IκBα degradation to ~48% of unstimulated control after 30 min treatment (Fig. 4.2.2a). Slight recovery was observed after 120 and 240 min TNFα treatment. IκBβ$_1$ levels were maximally degraded to ~11% of unstimulated controls after 60 min TNFα treatment and were fully recovered after 120 min treatment (4.2.2b).

Neither FSS nor TNFα caused a decrease in the levels of p105 and instead a small increase was observed after 60, 120 and 240 min (Fig. 4.2.2c).

4.3 Endogenous IKK is activated by FSS and TNFα

To establish whether shear stress induced degradation of IκB isomers was dependent on IKK1 and IKK2, levels of endogenous IKK activity was measured in HUVEC extracts using a kinase assay. HUVEC were subjected to FSS (15 dynes.cm^{-2}) or TNFα (30ng.ml) for periods of 5-240 min. before performing a kinase assay (Chapter 3.8). Cell extracts were prepared and the IKK complex was immunoprecipitated with a sheep polyclonal antibody raised against the IKK1 C-terminus. This antibody also recognises IKK2.

Kinase activity was measured by monitoring the incorporation of ^{32}P into a glutathione-S-transferase (GST) -IκBα 1-70 wild type (WT) fusion protein. A negative control experiment was carried out by using a mutant form of this substrate (GST-IκBα 1-70 S32E/S36/E (S/E) where the critical phosphoacceptor serine (S) residues 32 and 36 were replaced with glutamic acid (E) residues.

FSS caused endogenous IKK to be rapidly activated, peaking after 5 min and again after 120 min exposure to FSS (Fig. 4.3A,B). In contrast, TNFα stimulation caused cells to exhibit peak kinase activity after 10 min TNFα treatment, after which kinase activity decreased to control (0 min) levels between 30 and 240min (Fig. 4.3C,D). The mutant substrate (GST-IκBα 1-70 S32E/S36E (S/E) showed no sign of phosphorylation

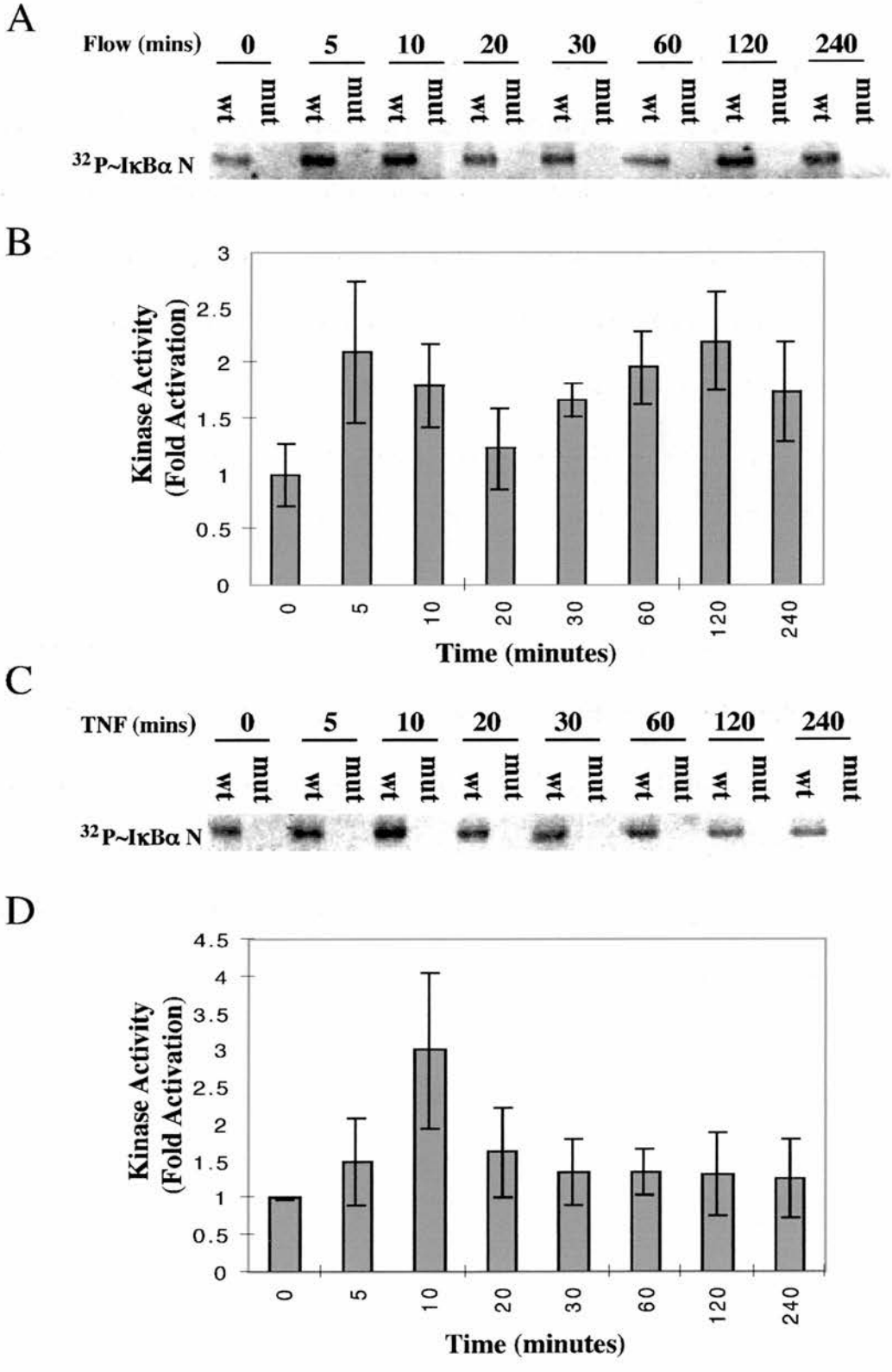
A
Flow (mins)
0
5
10
20
30
60
120
240
wt
mut
32P~IκBα N
B
Kinase Activity (Fold Activation)
Time (minutes)
C
TNF (mins)
D

Figure 4.3

when exposed to either FSS or TNFα which confirmed the specificity of the kinase assay (Fig. 4.3A,C).

The levels of IKK recovered after immunoprecipitation following exposure to FSS or TNFα were detected via immunoblotting (Fig. 4.3A,C) and were found to remain constant.

4.4 Single cell observations of NF- κB activation by FSS

Nuclear translocation of the p65 subunit of NF-κB under flow was observed using immunofluorescence. Control HUVEC (Fig. 4.4a,b) and HUVEC transfected with an empty vector, pcDNA3, as a vehicle control (Fig. 4.4c,d) were subjected to 30 or 120 min FSS (15 dynes.cm^{-2}). Random areas of the coverslip were photographically enlarged and cells showing p65 nuclear staining were expressed as a percentage of the total number of cells examined in each particular area for a given condition (n=100-150 cells).

After 30 min FSS, NF-κB nuclear translocation was maximal. The percentage of activated cells under control and pcDNA3 transfected conditions was 42 +/- 12% and 45 +/- 3% respectively (Fig. 4.4 b,d). These results correlate with EMSA and Western blotting data which show DNA binding and degradation of IκBα and IκBβ$_1$ to be maximal after 30 min FSS (Fig. 4.2). p65 nuclear staining after 120 min (not

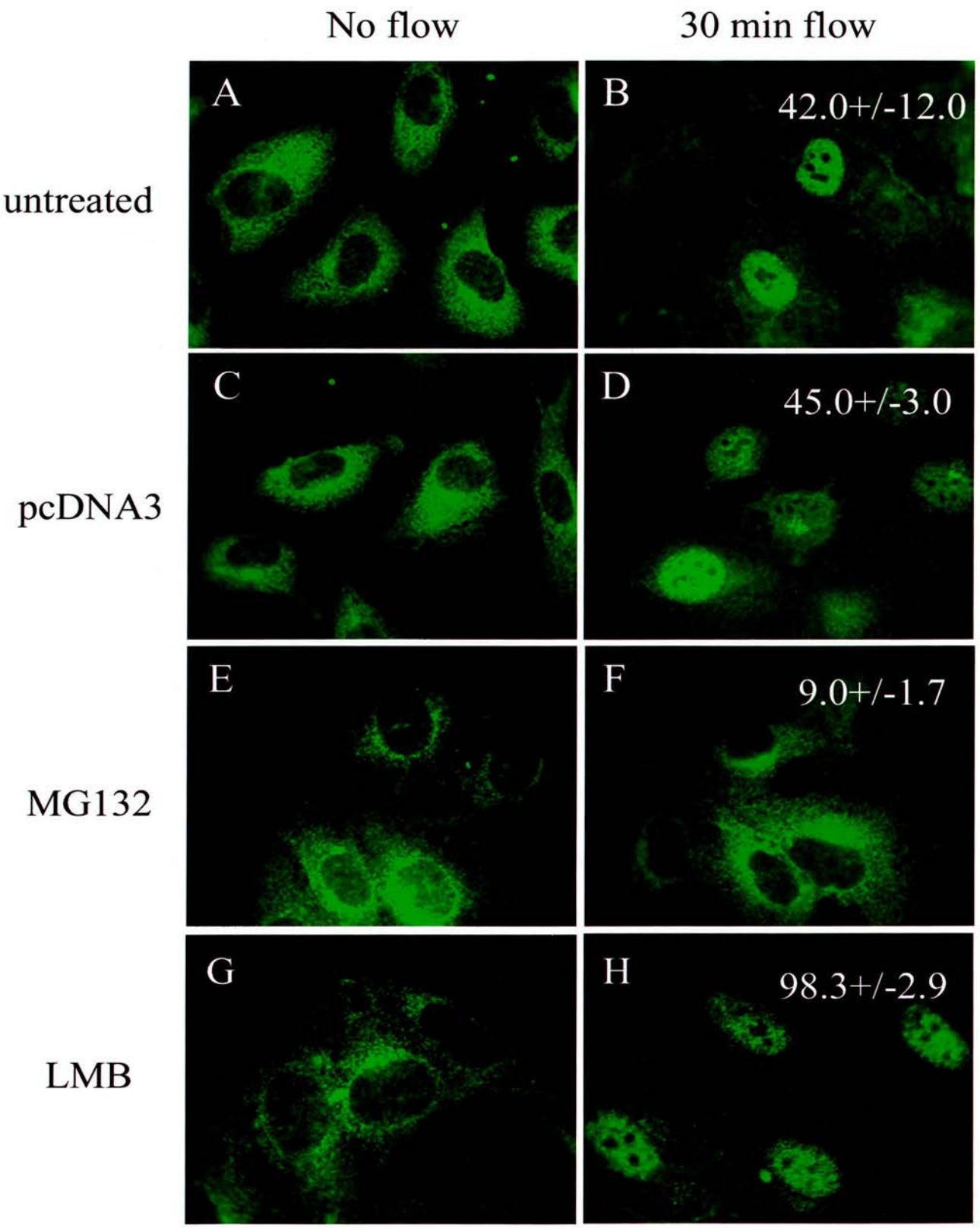
No flow
30 min flow
untreated
pcDNA3
MG132
LMB
A
B
42.0+/-12.0
C
D
45.0+/-3.0
E
F
9.0+/-1.7
G
H
98.3+/-2.9

Figure 4.4

shown) in control and pcDNA3 transfected cells was decreased to 33 +/- 5.5% and 39 +/- 7.8% respectively.

Nuclear p65 staining was also observed in cells which were treated with either MG132 or leptomycin B (LMB) for 30 min prior to FSS. MG132 is a specific inhibitor of proteosome-mediated degradation of IκB proteins (Alkalay et al, 1995). This prevents nuclear translocation of NF-κB. LMB is a target for exportin-1 and prevents NF-κB complexed with newly synthesised IκBα from leaving the nucleus (Fornerod et al, 1997). MG132 pre-treatment prevented p65 nuclear translocation when stimulated by FSS. Only 9 +/- 1.9% of the MG132 treated cells were observed to have nuclear p65 staining after 30 min FSS (Fig. 4.4e,f) and only 6 +/- 2% after 120 min FSS (not shown). After LMB pre-treatment, almost all cells showed nuclear p65 staining. After 30 min FSS 97 +/- 1% (Fig. 4.4g,h) and after 120 min FSS 98 +/- 2% of cells showed nuclear staining (not shown).

Distribution of the shuttling protein hnRNPA1, a pre-mRNA protein which shuttles between the nucleus and cytoplasm (Pinol-Roma & Dreyfuss, 1992) was unaffected by FSS (data not shown), confirming that FSS selectively affects NF-κB nuclear translocation.

4.5 Nuclear translocation of p65 by flow is blocked by catalytically inactive mutants of IKK1 and IKK2.

The aim of the experiment was to show, via immunofluorescence, whether IKK1 and IKK2 have a role in flow-activated p65 nuclear translocation. Plasmids containing wild type IKK1 and IKK2 (w/t IKK1 and w/t IKK2) or the corresponding kinase inactive mutants (K44A) were transfected into HUVEC. These cells were then exposed to FSS (15 dynes.cm^{-2}) to determine whether FSS activation of NF-κB is reliant upon the presence of IKK1 and/or IKK2 (Fig. 4.5). Double indirect immunofluorescence with a mouse monoclonal p65 antibody and a rabbit polyclonal antibody to IKK1 or IKK2 was used to monitor nuclear translocation of p65.

In the experimental conditions, the levels of endogenous IKK1 and IKK2 were below the threshold of detection by immunofluorescence. Therefore, only cells in which w/t or mutant kinases were over-expressed were stained. Percentages of cells containing p65 nuclear staining were measured as described in 4.4.

After 30 min FSS, p65 was observed in the nuclei of cells (45.0±5.0% and 39.0±4.6%, respectively) which were over-expressing w/t IKK1 (Fig. 4.5b) and w/t IKK2 (Fig. 4.5f). However, very little nuclear staining was seen in cells which had been transfected with the mutant IKK1 (Fig. 4.5d) or mutant IKK2 (Fig. 4.5h) (19.0±2.0% and 21.0±1.0%

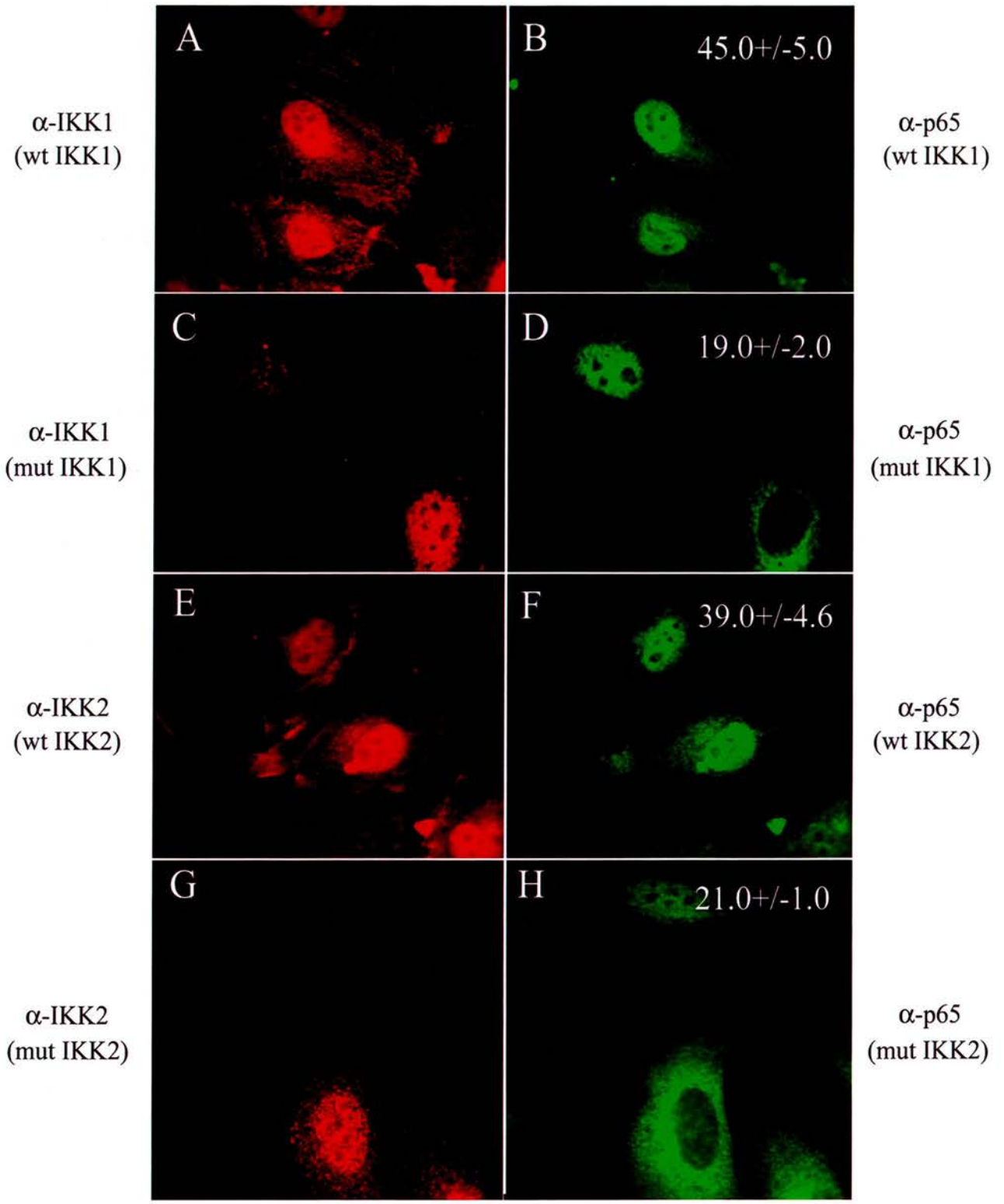
A
B
45.0+/-5.0
α-IKK1
(wt IKK1)
α-p65
(wt IKK1)
C
D
19.0+/-2.0
α-IKK1
(mut IKK1)
α-p65
(mut IKK1)
E
F
39.0+/-4.6
α-IKK2
(wt IKK2)
α-p65
(wt IKK2)
G
H
21.0+/-1.0
α-IKK2
(mut IKK2)
α-p65
(mut IKK2)

Figure 4.5

respectively). These results demonstrate the need for the presence of IKK1 and IKK2 in NF-κB activation by FSS.

4.6 Nuclear translocation of p65 is blocked by a catalytically inactive mutant of NIK, but not TPL2.

The aim of the experiment was to show, via immunofluorescence, whether NF-κB inducing kinase (NIK) or tumour progression locus 2 (TPL2) are essential in the signalling pathway of flow-activated p65 nuclear translocation. Plasmids encoding wild type NIK (w/t NIK) or the corresponding catalytically inactive mutant (KK429-430AA) were transfected into HUVEC. These cells were then subjected to FSS (15 dynes.cm^{-2}). Double indirect immunofluorescence with a mouse monoclonal p65 antibody and a rabbit polyclonal NIK antibody was the method used to observe NF-κB nuclear translocation.

Endogenous levels of NIK were below the level of detection, meaning only those over-expressing w/t or NIK are stained. Percentages of cells containing p65 nuclear staining were measured as described in 4.4.

FSS induced NF-κB nuclear translocation in cells expressing wild type NIK (52.0±7.0%) (Fig. 4.6 a,b), but not in cells expressing mutant NIK (12.0±2.7%) (Fig. 4.6 c,d). This data reveals NIK to be an essential component of the upstream signalling pathway which is activated by FSS and results in NF-κB activation.

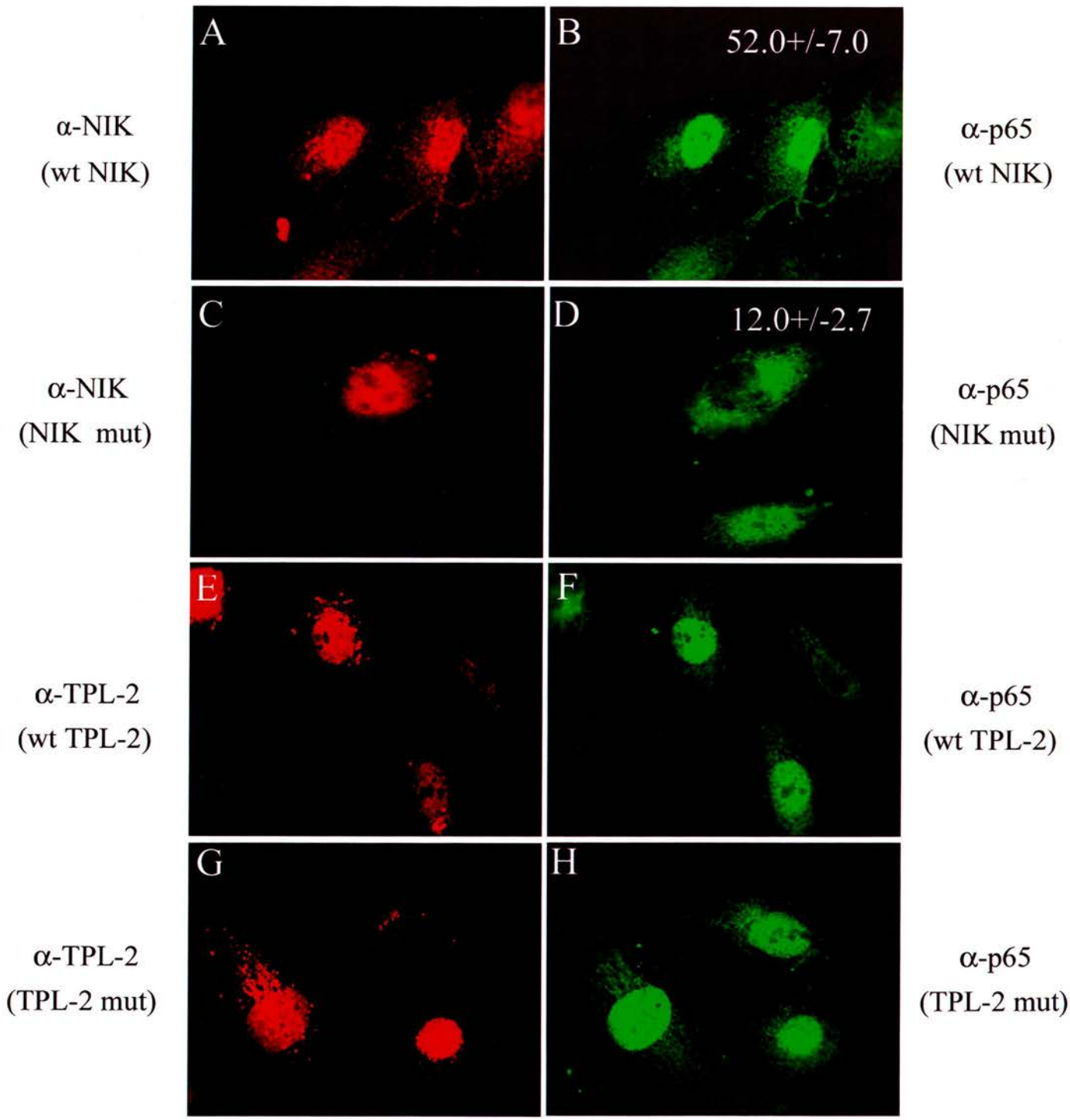
A
B
52.0+/-7.0
α-NIK
(wt NIK)
α-p65
(wt NIK)
C
D
12.0+/-2.7
α-NIK
(NIK mut)
α-p65
(NIK mut)
E
F
α-TPL-2
(wt TPL-2)
α-p65
(wt TPL-2)
G
H
α-TPL-2
(TPL-2 mut)
α-p65
(TPL-2 mut)

Figure 4.6

Plasmids encoding wild type TPL2 protein (w/t TPL2) or the corresponding catalytically inactive mutant (TPL2 mut, A270) were transfected into HUVEC. These cells were then exposed to FSS (15 dynes.cm^{-2}) for 30 min. Double indirect immunofluorescence using a mouse monoclonal p65 antibody and a rabbit polyclonal TPL2 antibody was used to monitor p65 nuclear translocation. Again, endogenous TPL2 levels were below the level of detection. FSS-induced p65 nuclear translocation in cells expressing wild type TPL2 (Fig 4.6 e,f) and in those expressing mutant TPL2 (Fig. 4.6 g,h) revealing that TPL2 is not a necessary component in the upstream signalling pathway activated by FSS and resulting in NF-κB activation.

4.7 FSS activation of NF-κB is not dependent on protein kinase C (PKC)

The aim of the experiment is to show, via immunofluorescence, whether protein kinase C (PKC) is a necessary component in the FSS-induced signalling pathway which results in NF-κB activation. HUVEC were treated with phorbol 12-myristyl 13-acetate (PMA) which activates PKC and the calcium ionophore, ionomycin, which mimics inducers of NF-κB signalling by increasing the intracellular calcium concentration. These agonists cause activation of NF-κB and induce nuclear translocation of p65 (Fig. 4.7c). Treating cells with bisindoylmaleimide-1 (bisin; 100nM), which selectively inhibits PKC isoforms, for 30 min before addition of PMA and ionomycin prevented nuclear translocation of p65.

Figure 4.7

Bisindolymaleimide 1 (bisin) blocks agonist, but not flow-induced p65 nuclear translocation.

Bisin selectively inhibits isoforms of PKC and does not affect p65 distribution in static cultures (A,B). PMA and Ionomycin treatment, which cause agonist-induced p65 nuclear translocation (C), was blocked by bisin (30 min, 100nM, D), revealing a role for PKC in agonist induced p65 nuclear translocation. However, bisin did not block flow-dependent nuclear translocation (E,F) showing that PKC is not necessary in the flow-induced signalling pathway which results in NF-κB activation.

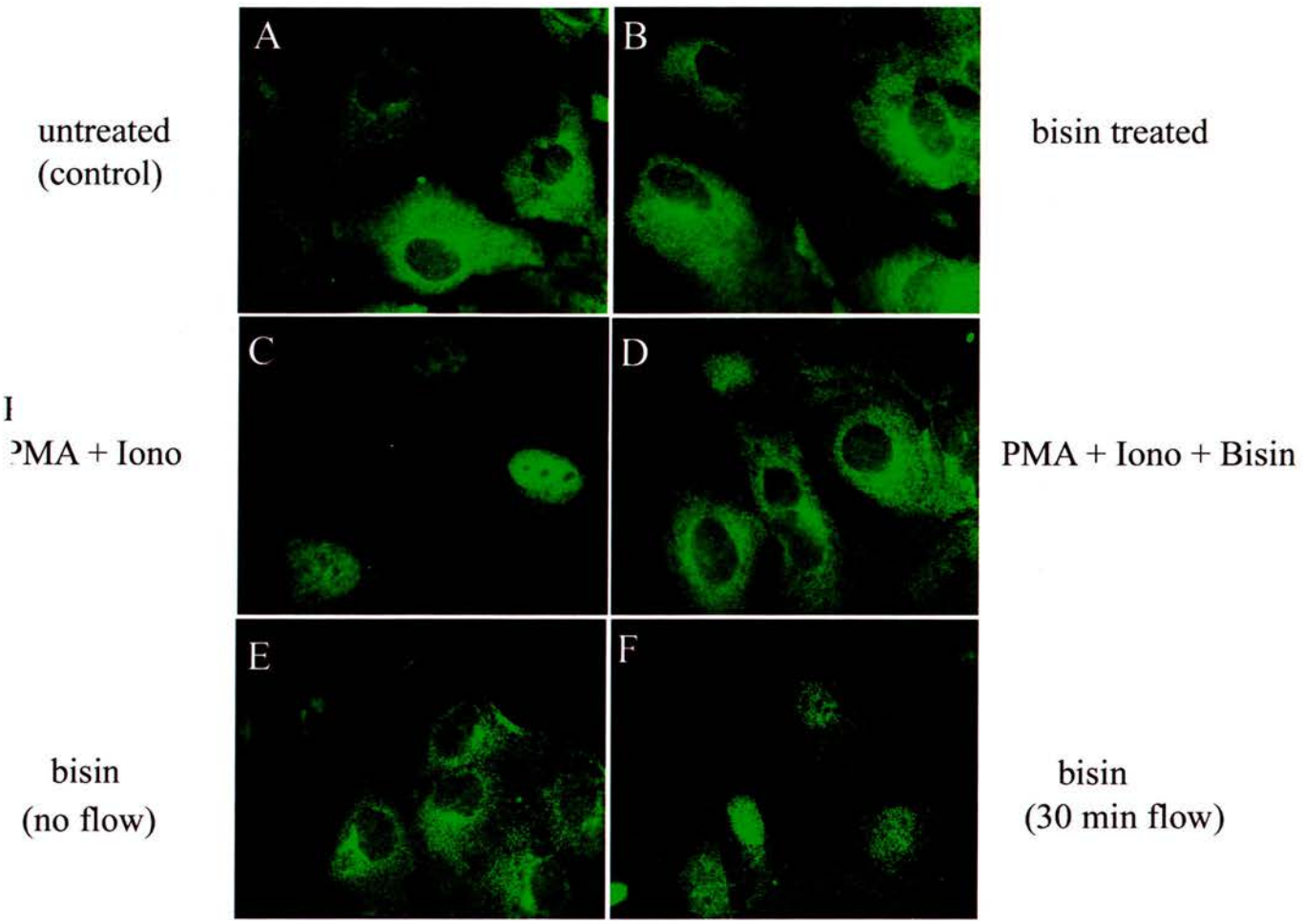
A
B
C
D
E
F
untreated
(control)
bisin treated
I
PMA + Iono
PMA + Iono + Bisin
bisin
(no flow)
bisin
(30 min flow)

Figure 4.7

Treatment with bisin in resting cells as a control had no effect on nuclear p65 staining (Fig. 4.7b) compared with untreated resting cells (Fig. 4.7a). Pre-treating cells with bisin before exposure to FSS failed to block p65 nuclear translocation. These results reveal that the PKC isoforms found in HUVEC (PKC α, ε and ζ) are necessary for agonist-induced NF-κB activation but are not part of the FSS induced activation of NF-κB.

CHAPTER 5

NF-κB DISCUSSION

There exist a number of pieces of evidence to suggest that NF-κB – dependent gene regulation is linked in some way to atherogenesis (de Martin et al, 2000). Advanced atherosclerotic lesions have been shown to contain activated NF-κB (Collins, 1993). Brand et al (1996) showed that a number of the genes expressed in atherosclerotic lesions are known to be NF-κB –regulated.

Areas of the endothelial vasculature which are at increased risk of exhibiting atherosclerotic lesions in the future, such as bifurcations, have been shown to contain several up-regulated components of the signalling pathway of NF-κB, such as IκBα, IκBβ, Rel A. The suggestion is that the endothelium may be primed by local haemodynamic forces to respond to systemic risk factors should they arise in the future (Hajra et al, 2000).

The cells in the experiments described here were subjected to uniform and unidirectional laminar flow, creating a 15 dynes.cm^{-2} shear stress. This shear stress was applied for anything from 5 minutes to 4 hours. After 5-10 minutes of exposure to FSS, both IκBα and IκBβ levels were decreased. This decrease was maximal after ~ 30-60 minutes. After ~ 60-120 minutes of FSS, the levels of IκBα and IκBβ, respectively, were seen to be restored fully.

In accordance with these results, p50/p65 heterodimer binding to the SSRE was maximal after 30-60 minutes and reduced binding was

observed between 60-120 minutes of exposure to FSS, as shown by EMSA. Furthermore, p65 nuclear translocation was maximal after 30-60 minutes, where the cytoplasmic levels of p65 were correspondingly decreased. This was shown using immunofluorescence microscopy.

Recovery of IκBα levels is expected as its gene is activated by NF-κB (Auphan et al, 1995; de Martin et al, 1993). Newly-synthesised IκBα moves from the cytoplasm to the nucleus and binds to NF-κB. This causes NF-κB to dissociate from DNA, causing gene transcription to be terminated (Arenzana-Seisdedos et al, 1995). The nuclear NF-κB-IκBα complex is then exported to the cytoplasm, but this process can be blocked by LMB (Rodriguez et al, 1999). The experiments presented here showed that p65 export to the cytoplasm under flow could also be blocked by LMB. This reveals that NF-κB gene transcription autoregulation also occurs when NF-κB is induced by flow.

These experiments also showed that flow-induced p65 nuclear translocation in cells transfected with kinase inactive mutants of NIK, IKK1 and IKK2 was prevented. However, in cells over-expressing a dominant negative form of TPL2 kinase nuclear translocation was normal. It has been shown that TPL2 has a role in p105 post-translational modification (Belich et al, 1999). Flow does not reduce p105 levels, correlating with TPL2s lack of involvement in the activation process. IKK-mediated phosphorylation of serines 927 and 932 on p105

leads to β-TRCP –mediated ubiquitination. This triggers the subsequent destruction of p105 by the proteasome pathway (Lang et al, 2003). The experiments presented here showed no degradation of p105, suggesting that IKK-dependent phosphorylation of p105 is not activated by flow. Furthermore, bisin, a PKC inhibitor, fully blocked activation of NF-κB induced by PMA and ionomycin, but it did not prevent p65 nuclear translocation induced by flow. Reviewing these findings leads to the conclusion that NIK, IKK1 and IKK2 are required for shear stress activation of NF-κB, but PKC and TPL2 are not involved. In addition, the ability of MG132 to block p65 nuclear translocation reveals that flow-activated NF-κB requires IκB proteolysis via that proteasome pathway.

The experiments here show activation of IKK1/2 to be the earliest event detected. IKKs were also shown to be activated by flow by Bhullar et al (1998) although the time course was different to that seen here. In the Bhullar study, IKK activity was shown to be monophasic and required ~ 30 minutes to reach a maximum value of ~ 3.5x control levels. IKK activity then dropped back to control levels after 2 hours. The experiments here show IKK activation to be far more rapid with a maximum of ~ 2x control levels reached after only 5 minutes. IKK activity then dropped to near control levels after 20 minutes, only to once again increase after 120 minutes to reach a second peak. This is suggestive of a pattern of IKK activation which is biphasic. Further studies on cells exposed to flow for periods greater than 120 minutes

would help to decide whether this is so. What is of interest here, however, is that flow –induced activation of the AP-1 transcription factor has been reported to be biphasic (Lan et al, 1994). The difference between the kinase assays presented here and those of Bhullar et al could perhaps be attributed to methodological differences. Bhullar used bovine endothelial cells that over-expressed IKK1 and IKK2, but the results here were obtained by measuring *endogenous* IKK in human endothelial cells.

Use of the luciferase reporter assay showed that flow-induced NF-κB – dependent transcription was maximal after ~ 30 minutes. However, nuclear staining for p65 showed fewer than 50% of the cells were activated at this time. This study used flow chambers which were carefully tested to ensure that steady two-dimensional flow was generated. This testing procedure, however, involved measuring the shear forces exerted on the uniform flat surface of a glass coverslip and failed to account for the surface topography of a real cell monolayer. Atomic force microscopy studies on endothelial monolayers was carried out by Barbee et al (1994). Their measurements were used to estimate shear stress spatial gradients as a result of surface undulations on the cell monolayer. They revealed that cells vary in height over a ~ 6μm range and have a mean slope of 11°. In a subsequent study, Barbee et al (1995) calculated that for a nominal FSS of 12 dynes.cm^{-2} the actual FSS on the steepest part of the cell would change at the rate of

+/- 4 dynes.cm^{-2}.sec^{-1}. For example, if the steep region of a cell was only 2μm long, the shear stress experienced could reach as much as 20 dynes.cm^{-2} on the upstream surface and as little as 4 dynes.cm^{-2} on the downstream surface. The heterogeneous responses of cells to flow might therefore be attributed to in part by this variability.

In summary, the results presented here reveal that NF-κB –dependent gene regulation in human endothelial cells can be induced by flow. The mechanism of action involves NIK, IKK1/2 signalling and degradation of NF-κB inhibitor proteins (IκBs) by the 26S proteasome pathway. The results also show that neither TPL2 kinase or PKC are involved in this process. The NF-κB induced by flow in these experiments is transcriptionally active, as revealed by enhanced expression of the luciferase reporter.

CHAPTER 6

MICROTUBULE INTRODUCTION

6.1 The role of microtubules in the cell

Microtubules (MT), together with actin microfilaments (MF) and intermediate filaments (IF), are one of three key components of the cytoskeleton. The cytoskeleton acts as an internal scaffold that helps determine the overall shape of the cell. It also serves to distribute organelles, as MT provide tracks along which mitochondria and vesicles can travel to the cell periphery and back again (Cleveland, 1993). They are the main component of the mitotic spindle where they attach and translocate chromosomes to spindle poles before cell division (Cleveland, 1993; Wade & Hyman, 1997).

MT are also very dynamic structures. Rapid assembly and disassembly of MT helps to mediate cellular responses to a large number of mechanical and chemical stimuli (Drubin & Hirokawa, 1998).

6.2 Structure of microtubules

MT are polymers of tubulin which are assembled from the α- and β-heterodimeric tubulin subunits (Cleveland, 1993; Downing & Nogales, 1998; Jordan & Wilson, 1998; Joshi, 1998; Wade & Hyman, 1997). α- and β-tubulin are highly homologous proteins, each around 450 amino acids in length (Downing & Nogales, 1998). Both subunits bind a guanine nucleotide, on the N-site (non-exchangeable) in α- tubulin and

the E-site (exchangeable) in β- tubulin. E-site guanine nucleotide binding is exchangeable and GTP binding here is essential for the assembly of MT. The bound GTP is hydrolysed to GDP following assembly (Cleveland, 1993). Linear arrangements of αβ tubulin dimers are termed protofilaments and 13 of these form a MT (Wade & Hyman, 1997).

Cryo-electron microscopy studies of MT have revealed a great deal about their structure, not least about the arrangement of tubulin subunits. It has been shown that tubulin protofilaments form what is termed a β-lattice, where lateral contacts are homodimeric (α-α, β-β). Once this lattice of 13 protofilaments is formed it closes into a cylinder with heterodimeric contacts that form a "seam" along the length of the MT (Fig. 6.1; Wade & Hyman, 1997).

6.3 Dynamic properties of microtubules

MT assembly is a dynamic process and even when it reaches what is apparently a steady state, each MT remains very dynamic. This characteristic is known as dynamic instability (Cleveland, 1993; Jordan & Wilson, 1998). Stability of MT has been shown to depend upon a cap of tubulin-GTP at the ends of protofilaments. The loss of this cap means it is then possible for the MT to depolymerise (Downing & Nogales, 1998).

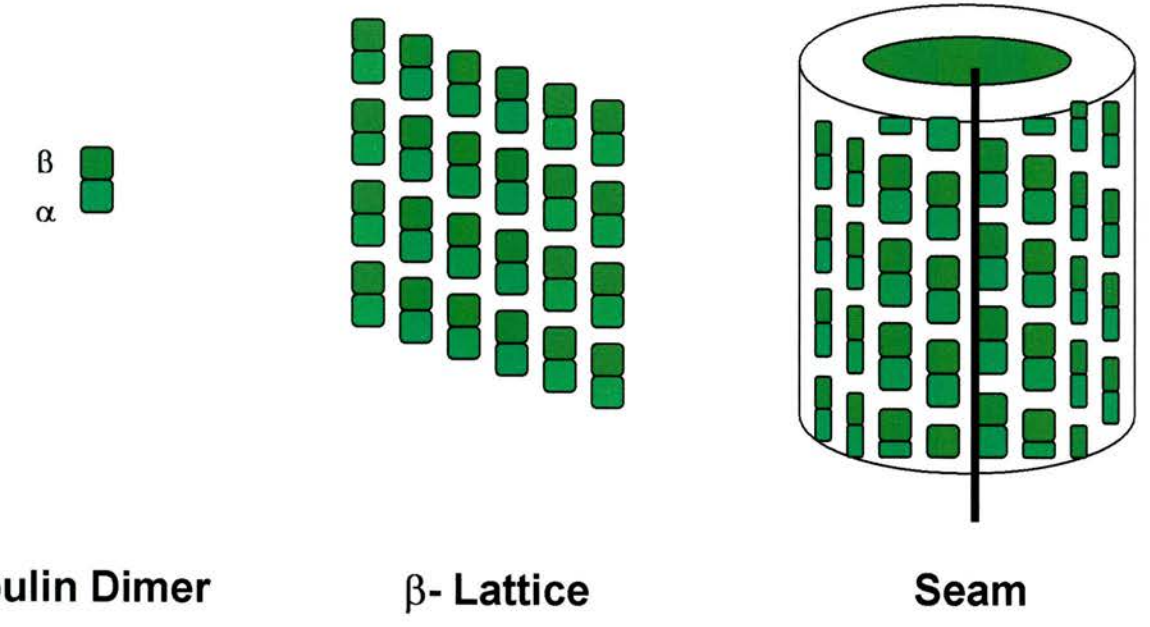

Figure 6.1 Schematic diagram of the assembly of tubulin dimers, lattices and microtubules.

MT are polar structures, with the two ends being different both in the rate of tublin subunit addition and loss. The faster growing end is termed the plus (+) end and the slower growing end is termed the minus end (-). Normally, MT are arranged in such a way that the + ends point towards the periphery of the cell (Cleveland, 1993; Joshi, 1998).

In vivo, MT nucleate within the MT organising centre (MTOC). The - end remains attached here and the + end grows out towards the edge of the cell (Wade & Hyman, 1997). However, *in vitro*, MT go through self-nucleation and both ends extend, albeit with the + end growing quicker as would be expected (Wade & Hyman, 1997). For a number of years the understanding of the mechanism behind the anchorage of MT to the MTOC was not clear. It has now been shown that it involves a third type of tubulin subunit, known as γ-tubulin (Cleveland,1993; Joshi, 1998; Wade & Hyman, 1997). γ-tubulin exists in very small amounts, ~ 5% of the level of β tubulin, and is localised exclusively within the MTOC. γ-tubulin disruption has been shown to vastly decrease the numbers of MT (Cleveland, 1993). Immunoelectron microscopy, combined with tomography to reconstruct a three-dimensional image, has shown that γ-tubulin-containing rings in the centrosomes of *Drosophila* are responsible for nucleating MT. Similar γ-tubulin ring formations have been shown to encourage MT assembly in *Xenopus* egg extracts (Wade & Hyman, 1997). Results such as these show that γ-tubulin-containing structures are essential for nucleation of MT and for determining polarity.

Strome et al (2001) used green fluorescent protein (GFP) to further elucidate the role of γ-tubulin. They generated GFP-γ-tubulin transgenic *Caenorhabditis elegans* worms and then used small interfering RNA (siRNA) to deplete *C. elegans* embryos of γ-tubulin. These embryos failed to carry out chromosome segregation but did show extensive MT arrays. These results disagree with others, suggesting that γ-tubulin is not absolutely necessary for MT nucleation but does play a big role in organisation of kinetochore and interpolar MT which function in chromosome segregation.

GFP tagged proteins have recently played an important role in the dynamic analysis of the cytoskeleton. However this technique is not without its limitations as GFP is added to the C or N terminus of the desired target protein and this could interfere with its function, making it important to demonstrate that the protein retains its normal characteristics (Rusan et al, 2001). It is possible, however, to establish permanent GFP tagged cell lines as Rusan et al (2001) showed. They established a GFP-α-tubulin LLPCK-1 cell line, named LLPCK-1α. They showed that growth and morphology of interphase and mitotic cells were not significantly different in the GFP cell line compared to the parent line and the morphology of the MT networks were indistinguishable. 17% of tubulin was GFP tagged in LLPCK-1α cells and untagged tubulin was 82% of the levels in parent cells, showing that GFP does not interfere

with the autoregulation of α-tubulin. Rusan et al (2001) also studied differences in MT dynamics in interphase and during mitosis in their GFP-tagged cell line. They showed that rates of elongation and shortening remained the same but catastrophic incidents, defined as a switch from growth towards shortening of MT, increased two-fold and rescue incidents, defined as a switch from shortening towards growth, increased nearly four-fold in mitosis compared with interphase. Static MT reduced dramatically from 73.5% to 11.4% in mitosis compared with interphase.

6.4 Tubulin – drug interactions

There are three main classes of tubulin binding drugs. These are the colchicine analogues, vincas (including vinblastine) and the taxanes (including taxol). All three of these types of agents bind to tubulin at a different site and their mechanism of action is different (Downing, 2000).

Colchicine, at high enough concentrations, causes depolymerisation of MT. It had been shown to bind to β-tubulin at a region near the α-β interface of the tubulin dimer, on the side of the filament facing the interior of the MT (Fig. 6.2). This binding site is not well defined and the exact mechanism of action is unclear. However, it is thought to induce a change in conformation of tubulin. Colchicine binding in the cleft between α and β-tubulin may actually pull the subunits closer together,

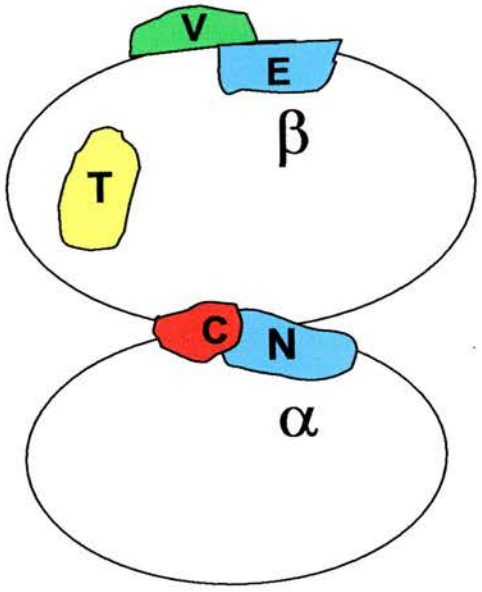

Figure 6.2. Schematic diagram of the tubulin dimer and its sites of drug interaction.

V – Vinca binding site
E – Exchangeable GTP binding site
T – Taxol binding site
C – Colchicine binding site
N – Non-exchangeable GTP binding site

explaining an observation that a region on the opposite side of the dimer becomes disordered and more sensitive to proteases (Downing, 2000). The vinca binding site is also found on β-tubulin, but at the surface which is exposed at the MT + end (Fig. 6.2). It is thought that vinblastine binding here prevents growth of the MT by causing a re-orientation of the new dimer, resulting in a kink. A build up of these kinks would lead to curved protofilaments, which is indeed what is observed in vitro (Downing, 2000).

The taxol and related taxanes bind in a pocket situated on the interior of the MT, approximately in the middle of the β monomer (Fig. 6.2). Taxol actually stabilises MT, rather than causing depolymerisation, and prevents protofilaments separating, suggesting that it strengthens lateral protofilament interactions (Downing 2000). However, Amos & Lowe (1999) suggested that taxol works by inhibiting the tendency of protofilaments to curl and therefore relieves stress that may cause dissociation of MT. The actual effect may be a combination of the two but taxol appears to stabilise the MT conformation rather than acting as an adhesive between protofilaments (Downing 2000).

6.5 Cell responses to microtubule binding agents

MT binding drugs induce many cellular responses including shape changes and biochemical changes. One of the main clinical uses of MT

binding drugs is as an anti-cancer treatment, because of their anti-mitotic action. Taxol, at low concentrations, stabilises the MT spindle during mitosis and therefore blocks mitosis, inhibits cell proliferation and induces apoptosis (Yeung et al, 1999). Taxol is used clinically in the treatment of breast cancer, prostate cancer and leukaemia as it stabilises the MT in the G2-M phase. Cells blocked at this stage eventually die via apoptosis (Yeung et al).

Another, more novel, potential anti-cancer agent is combretastatin which is structurally similar to colchicine and has a higher affinity for the colchicine binding site on tubulin (Dark et al 1997). Other colchicine-like agents had been shown to cause vascular damage within tumours but only at very near toxic doses. Combretastatin, however, which is isolated from the South African *Combretum caffrum* tree, causes vascular shutdown in tumours at only one tenth of the maximum tolerated dose. Dark et al (1997) showed that combretastatin decreased breast tumour functional vascular volume by 93% at 6 hours post administration. Also, it was shown to only affect proliferating endothelial cells and not those that were quiescent before and during combretastatin exposure.

Other effects of disrupting MT networks include the following. Treatment of rat liver epithelial cultures with colchicine or vinblastine cause the cells

to display disorganised MT and delayed spreading before adopting their normal flattened discoid formation, suggesting that an intact MT network contributes to stabilisation and spreading of the cells (Domnina et al, 1985). Disruption of MT also impairs cell migration and integrity of endothelial cells. Wounding of the endothelium stimulates migration and proliferation of cells. Migration involves re-orientation of the MTOC, but this is prevented by administration of colcemid. MTOC re-orientation relies upon an intact MT network. Disruption of actin MF with cytochalasin B does not inhibit MTOC re-orientation and does not inhibit cell migration (Gotlieb et al, 1983).

MT depolymerisation by colchicine or vinblastine does not affect proliferation in the wounded endothelium (Selden et al, 1981; Lee & Gotlieb, 2002). However, proliferation is stimulated by colchicine and vinblastine in fully confluent monolayers. These were the first agents found to elicit this effect in saturated density endothelial cells (Selden et al, 1981). The mechanism involves a transient retraction of cells from each other resulting in disturbed intercellular contacts. EC which undergo migration as a result of wounding also exhibit disturbed contacts between cells leading to the suggestion that colchicine or vinblastine use the same mechanism to stimulate proliferation and migration (Selden et al, 1981).

Loss of endothelial integrity as a result of wounding can initiate atherosclerosis *in vivo*. Disruption of MT impairs wound healing, as does MF disruption (Lee & Gotlieb, 2002). This suggests that interactions between intact MT and MF are important in maintaining endothelial integrity, especially in relation to atherosclerotic plaque formation.

Biochemical consequences of MT depolymerisation include changes in cytokine release and induction of apoptosis (Allen et al, 1991; Domnina et al, 2002). Colchicine causes an increase in the secretion of lipopolysaccharide (LPS)-induced interleukin-1β (IL-1β) but a decrease in LPS-induced TNFα release in both human blood monocytes and alveolar macrophages (Allen et al, 1991). These observations suggest that MT are important for regulating endotoxin-stimulated release of cytokines but that their precise role differs between TNFα and IL-1β.

TNFα administration in HeLa cells in the presence of colchicine or the MT-stabilising agent taxol both cause increased nuclear blebbing, over and above that due to TNFα alone (Domnina et al, 2002). TNFα and MT alteration, via depolymerisation or stabilisation, induce mitochondria to move towards the perinuclear area (Domnina et al, 2002) suggesting that this movement may induce destructive nuclear changes.

6.6 Effect of microtubule disruption on flow-induced responses of endothelial cells

Fluid shear stress (FSS) induces a number of effects upon the endothelium, as detailed in Chapter 2. Many of these responses are influenced by disruption of MT or MF, showing that the cytoskeleton is important in mediating the effects of FSS. For example, nocodazole, a synthetic chemical which disrupts MT and competes with colchicine (Paterson & Mitchison, 2002) increases cell loss during flow, but the effect is not as great as that seen with cytochalasin B, a MF disrupter (Wechezak et al, 1989). This implies that intact MF are more important than intact MT for the adaptative responses of endothelial cells to FSS. Both nocodazole and colchicine attenuate flow-induced vasodilation of rat gracilil arterioles (Sun et al, 2001). This suggests that an intact MT network is required for FSS-mediated release of nitric oxide (NO), an important vasodilator which is synthesised in and released from endothelial cells in response to flow. However, Knudsen & Frangos (1997) showed that neither disrupting MT nor MF eliminated flow-induced NO production in the endothelium, implying that an intact MT network is not necessary. Malek & Izumo (1996) studied the effects of a number of agents on the characteristic shape-change induced by flow and on remodeling of the actin cytoskeleton. They experimented with agents which blocked tyrosine kinases, protein kinase C (PKC), altered

vimentin structure, depolymerised MT or chelated intracellular calcium. They concluded that intact MT, intracellular calcium and intact tyrosine kinase all have a role in mediating the effects of flow, but that neither vimentin IF or PKC are involved.

6.7 Effect of microtubule depolymerising agents on the activation of NFκB nuclear transcription factor

There is evidence to show that MT may be important in agonist-induced activation of NF-κB, though their exact role remains controversial. The effect of depolymerising MT on NFκB activation differs considerably between cell types (see Fig 6.3). Immunofluorescence studies by Fuseler et al (2000) showed that antibody to the p65 sub-unit of NF-κB co-localised with MT in unstimulated HUVEC. Activation of NF-κB by TNFα caused the fraction of anti-p65 associated with MT to decrease significantly, from around 85% to 15%. This was due to translocation of a large fraction of cytoplasmic p65 into the nucleus. After MT were disrupted with colchicine, nuclear translocation of p65 on stimulation with TNFα was blocked. This result showed that HUVEC require an intact MT network for TNFα-activated p65 nuclear translocation. Ivanova *et al* (2001) showed a similar reliance on intact MT for the activation of NFκB by phorbol esters in CHO-K1 cells.

Cell Type	NFκB activation?	MT disrupting agent used	Reference
HUVEC	Decreased	Colchicine	Fuseler et al
CHO-K1	Decreased	Nocodazole	Ivanova et al
HeLa-S3	Increased	Nocodazole, colchicine, vinblastine, podophyllotoxin	Rosette & Karin
HBL-100	Increased	Vinblastine	Bourgarel-Rey et al
HeLa	No change	Nocodazole	Ivanova et al
2B4	No change	Nocodazole	Ivanova et al
HT29-D4	No change	Vinblastine	Bourgarel-Rey et al

Figure 6.3 - Table of action of MT depolymerising agents on p65 in different cell types.

HUVEC – Human Endothelial umbilical vein
CHO-K1 – Chinese Hamster Ovary
HeLa-S3 – Human Cervical Adenocarcinoma
HBL100 – Human Epithelial Mammary
HeLa - Human Cervical Adenocarcinoma
2B4 – T-Cell Hybridoma
HT29-D4 – Human Colon Adenocarcinoma

Other workers have reported opposing results on NFκB activation by MT disrupting agents. Rosette & Karin (1995) and Bourgarel-Rey et al (2001) showed that MT disruption induced IκBα degradation and resulted in NFκB activation. The effect of nocodazole on HeLa-S3 cells was reversible within 15 minutes, which correlated with the appearance of newly-synthesised IκBα (Rosette & Karin, 1995). These authors showed that cold shock, a well-known means of depolymerising MT, also activated NFκB. However, it was necessary to warm the cells to 37°C before nuclear translocation of p65 could be detected, showing that activation of NFκB by this means involves more than one step. This hypothesis is supported by the fact that NFκB activation by nocodazole is not maximal until 30-60 minutes, although the MT network is completely destroyed after only 15 minutes. Rosette & Karin (1995) also showed NFκB activation by nocodazole was prevented by administration of the general protein kinase inhibitor staurosporine, a result that clearly implies a role for protein kinases in the activation of NFκB by MT depolymerisation.

6.8 Immunofluorescent studies linking MT to other cellular components

Crepieux et al (1997) used immunofluorescence as an effective tool to link MT with the activation of NFκB. They showed that IκBα, an NFκB inhibitory factor, interacted with dynein light chain protein (Dlc-1).

Dynein is a motor protein associated with the – end of MT. Immunofluorescence showed co-localisation between Dlc-1, IκBα and the MTOC and co-localisation of IκBα and tubulin. This implies a link between MT and gene regulation.

Another immunofluorescence study linking dynein with MT was carried out by Helfand et al (2002). Evidence was already in place linking kinesin, a + end directed MT motor, with vimentin IF (Prahlad et al, 1998). Helfand et al (2002) used overexpression of dynamitin to discover whether the – end directed MT motor protein dynein was also linked to vimentin IF. Dynamitin is a subunit of dynactin, which is a dynein associated complex required for dynein mediated activities. Overexpression of dynamitin causes dynactin dissociation and disrupts dynein without disturbing the function of kinesin. This overexpression also causes movement of vimentin IF towards the periphery of the cell and is most likely the result of the remaining + end directed motor protein, kinesin, causing IF to move towards the + ends of MT. Immunofluorescence and electron microscopy showed an association between dynein, MT and vimentin IF, proving that both dynein and kinesin have an effect on the maintenance of networks of vimentin IF (Helfand et al, 2002).

MT have also been shown to co-localise with the ubiquitin-activating enzyme, E1. E1 was found in three distinct pools in the cytoplasm. These pools showed E1 colocalisation with actin, tubulin and IF (Trausch et al, 1993). Tubulin itself does not undergo ubiquitination but a MT associated protein, termed MAP30, does. Also, MT are tightly associated with the endoplasmic reticulum (ER) where excess or damaged proteins are actively degraded and such degradation is likely to be ubiquitin mediated (Trausch et al, 1993). These immunofluorescent studies show a wide range of cellular processes in which MT are directly or indirectly involved.

6.9 Scope of the present study

Nothing is currently known about the role of MT in the activation of NFκB in endothelial cells by flow. However, there are several studies which deal with flow-dependent activation of NFκB and its regulators including those of Davies (1995), Lan et al (1994) and Bhullar et al (1998). As discussed above, many studies have implicated MT in NFκB-dependent gene regulation in other cell types, so investigation of their role in flow dependent NFκB activation in endothelial cells was desirable in order to fill in the gap between these findings. TNFα stimulated NFκB activation was employed as a means of comparison between a purely mechanical stimulus and an agonist-receptor induced stimulus.

Immunofluorescence, and quantitative statistical analysis were performed to show any effect of MT depolymerisation on flow and TNFα-induced NFκB activation and determine whether MT are a necessary part in the p65 nuclear translocation signalling pathway.

CHAPTER 7

MICROTUBULE MATERIALS AND METHODS

7.1 – Cell Culture

See 3.1 for details.

7.1.1 – Maintenance of HUVEC

See 3.1.1 for details

7.1.2 – Trypsinisation and seeding of HUVEC

See 3.1.2 for details

7.2 – Drug Treatment of HUVEC

To elicit breakdown of MT, HUVEC were incubated with 1μM colchicine for 1 hour prior to FSS, TNFα incubation or glutaraldehyde fixation.

Agonist mediated activation of p65 in HUVEC, as a comparison for FSS mediated activation, was achieved via incubation of cells for 30 min. at 37°C with 30ng.ml^{-1} TNFα.

7.3 - FSS Apparatus

See 3.3 for details

7.4 – Immunofluorescence and Microscopy

7.4.1 – Glutaraldehyde Fixation and Immunofluorescence

Cells were rinsed twice for 5 minutes in 0.1M PIPES at pH 6.9, followed by fixation in 0.5% glutaraldehyde in PIPES for 10 minutes.
The cells were then rinsed twice for 5 minutes each in PBSc followed by three 5 minute permeabilisation rinses in 0.5% TRITON X-100. Two further 5 minutes rinses in PBSc were followed by three 10 minute rinses

in 2.5mg/ml sodium borohydride in 50% ethanol to block free aldehyde groups.

Two 5 minute PBSc rinses preceded a 30 minute blocking step in 10% goat serum.

Primary antibodies, made up in 10% goat serum, were applied and the cells incubated for 30 minutes at 37°C. The cells were then rinsed three times for 10 minutes in 0.1% Tween 20 in PBSc. Secondary antibodies, made up in 10% goat serum, were applied and incubated for 30 minutes at 37°C. Three further rinses in 0.1% Tween 20, followed by one 5 minute dH_2O rinse were carried out. The cells were then mounted on slides using a non-fluorescent mounting medium.

7.4.2 – Deconvolution Microscopy

Slides were viewed using a Deltavision deconvolution microscope with x100 (oil) objective. The images recorded are transferred to Deltavision's softWoRx 2.5 programme which deconvolves the images and can perform quantitative analysis and resolution amendments. Images were stored on CD-ROM and transferred to Adobe Photoshop 6.0 for size adjustments.

Deconvolution is a software-based process in which out of focus images can be "re-focussed" using mathematical algorithms. It allows a Z-series of images (with the same X and Y co-ordinates but varying vertical, Z-axis, focus) to be taken through the sample and these images may be scrolled through to see all of the cellular information in sequence and select the best image for the purpose.

Deconvolution has an advantage over confocal microscopy as it takes away the need to reset the focus between each "Z-slice". The images produced are often out of focus but the deconvolution software reallocates light to the correct pixels, using mathematical algorithms, which cleans up the images.

All images in Chapter 8 were collected using this technique.

7.5 – Quantitative Analysis

p65 nuclear:cytoplasmic (N:C) intensity ratios were calculated by measuring the pixel intensities of cells which had undergone immunofluorescent staining with a p65 antibody and a green fluorescing secondary antibody.

Using the Data Inspector function of the softWoRx 2.5 programme, a 10x10 pixel box was selected on the green channel (528nm). A random area of each slide was selected and 4-10, 10x10 pixel boxes were selected on both the nucleus and cytoplasm of each cell. The mean pixel intensity for each box is displayed and recorded. The same process is repeated for the background of the slide, so that measurements could be adjusted accordingly.

For each cell, the recorded pixel intensities for both the nucleus and cytoplasm were averaged. The mean background intensity was then subtracted from each value. The resulting adjusted nuclear and cytoplasmic values were used to calculate a p65 N:C intensity ratio for each cell. The number of cells measured for each condition was between 2 and 13.

These ratios were used to calculate mean and standard error values for each treatment condition (Appendix 2.6) and were displayed as a histogram (Fig. 8.3). The intensity ratios for each set of treatments (colchicine or colchicine + TNFα) were used to perform statistical tests for normality of distribution, homogeneity of variance and analysis of variance (ANOVA) in the Minitab statistical software programme (version 14).

With thanks to Dr J. Graves for advice on appropriate statistical tests and Miss S. Spring for tutoring in the use of the Minitab programme.

CHAPTER 8

MICROTUBULE RESULTS

8.1.1 and 8.1.2 Colchicine depolymerises MT in a concentration dependent manner without affecting p65 distribution

The aim of the experiment was to show, using immunofluorescent techniques, the effect of colchicine on MT and p65 distribution in HUVEC.

Varying concentrations of colchicine (150nM - 100μM) were applied to HUVEC for a period of 1 hour. Cells were then fixed and stained for tubulin (Fig. 8.1.1) and p65 (Fig. 8.1.2). Treatment with 150nM and 500nM colchicine (Fig 8.1.1 B,C) showed depolymerisation of MT, but with some remaining intact, while use of 1, 10 or 100μM colchicine (Fig. 8.1.1 D,F) showed complete depolymerisation of MT. 10 and 100μM colchicine show the beginnings of changes in distribution of tubulin from depolymerised MT towards the nucleus. (Fig. 8.1.1 E,F). Corresponding p65 staining for the colchicine treated cells (Fig. 8.1.2) shows distribution of p65 as would be observed in resting cells, with the majority in the cytoplasm. This reveals that colchicine treatment alone does not affect p65, even at concentrations greater than that required to depolymerise all MT.

Subsequent experiments were carried out using 1μM colchicine as this was the minimum concentration which caused complete depolymerisation of MT.

Figure 8.1.1 and 8.1.2

Effect of increasing concentrations of colchicine on MT and p65

Figure 8.1.1 shows a sequence of images depicting changes in MT depolymerisation with increasing colchicine concentrations (A-F). Panel A represents MT under static conditions. Panels B+C show a combination of depolymerised and intact MT after exposure to 150 and 500nM colchicine, respectively. Panel D shows all MT to be depolymerised after treatment with 1μM colchicine. Note areas of membrane ruffling here. Panels E+F show the effect of 10 and 100μM colchicine on MT. Some membrane ruffling can still be seen in E, although the tubulin from the depolymerised MT appears to be retreating towards the nucleus. Panel F shows tubulin to have pooled around the nucleus and membrane ruffling is now less apparent.

Figure 8.1.2 shows the p65 staining which corresponds to Figure 8.1.1. In all panels, p65 is seen to reside mainly in the cytoplasm, as would be expected in resting, non-activated cells. This pattern of staining reveals that p65 distribution is not affected by colchicine treatment (150nM, 500nM; B&C) or the depolymerisation of MT (1μM; D), even at concentrations exceeding that needed to cause complete depolymerisation of MT (10μM, 100μM; E&F).

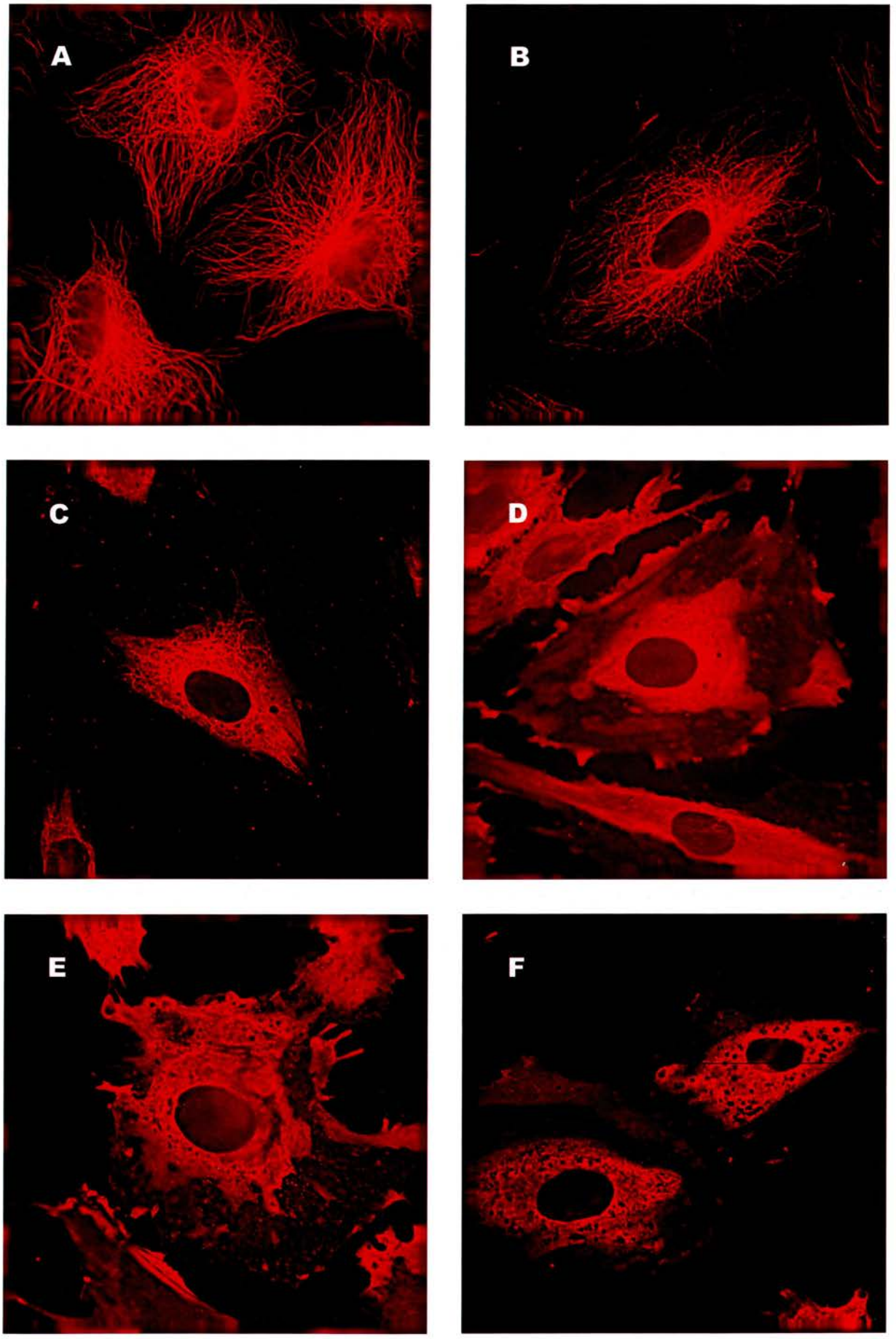

Figure 8.1.1

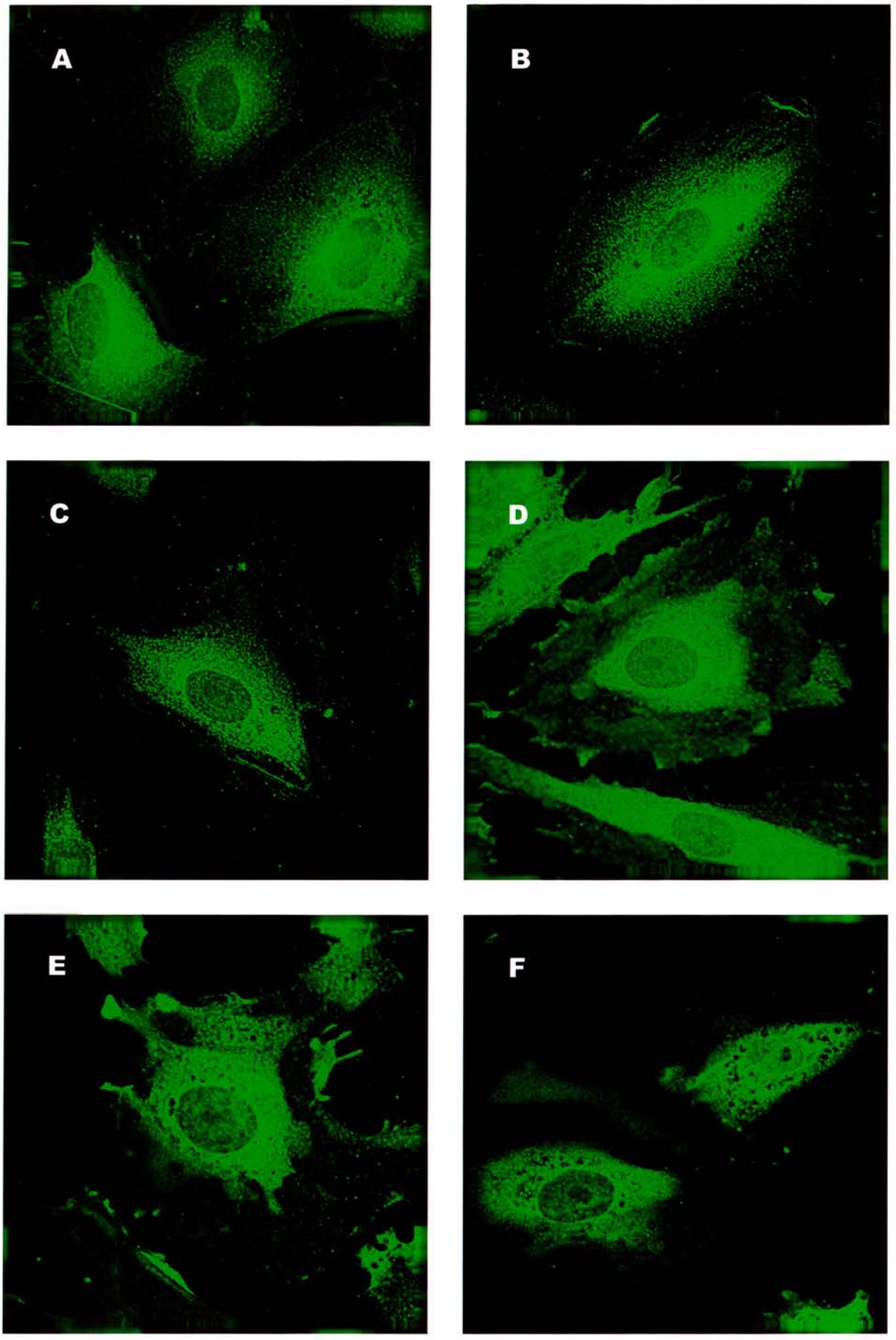

Figure 8.1.2

8.2 Colchicine treatment does not prevent TNFα-induced nuclear translocation of p65 from observations of immunofluorescent images.

The aim of the experiment was to show, using immunofluorescence, the effect of colchicine on p65 nuclear translocation in HUVEC stimulated with TNFα.

Concentrations of colchicine in the range 500nM, 1μM or 10μM were administered for 1 hour. The cells were subsequently exposed to 30ng.ml TNFα for 20 minutes, which is known to cause p65 translocation to the nucleus (Baldwin, 1996; Papadaki & Eskin, 1997) and then fixed and stained for both tubulin and p65. Control cells which had not been treated with colchicine showed intact MT and obvious p65 translocation (Fig. 8.2 A,B,C) compared with resting cells (Fig. 8.1.2 A). Use of 500nM and 1μM colchicine showed increasing levels of MT depolymerisation (Fig. 8.2 D,G). The corresponding p65 images (Fig. 8.2 D,H) showed no apparent decrease or inhibition of nuclear translocation. Even the highest concentration of colchicine (10μM), which not only caused complete MT depolymerisation but also visible cell damage (Fig. 8.2 J), did not apparently decrease the levels of p65 nuclear translocation observed (Fig. 8.2 K). This would suggest that an intact MT network is not necessary for TNFα-stimulated p65 translocation. However, quantitative data presented in Figure 8.5 reveals that increasing colchicine concentration does have an effect on the level of p65 nuclear staining.

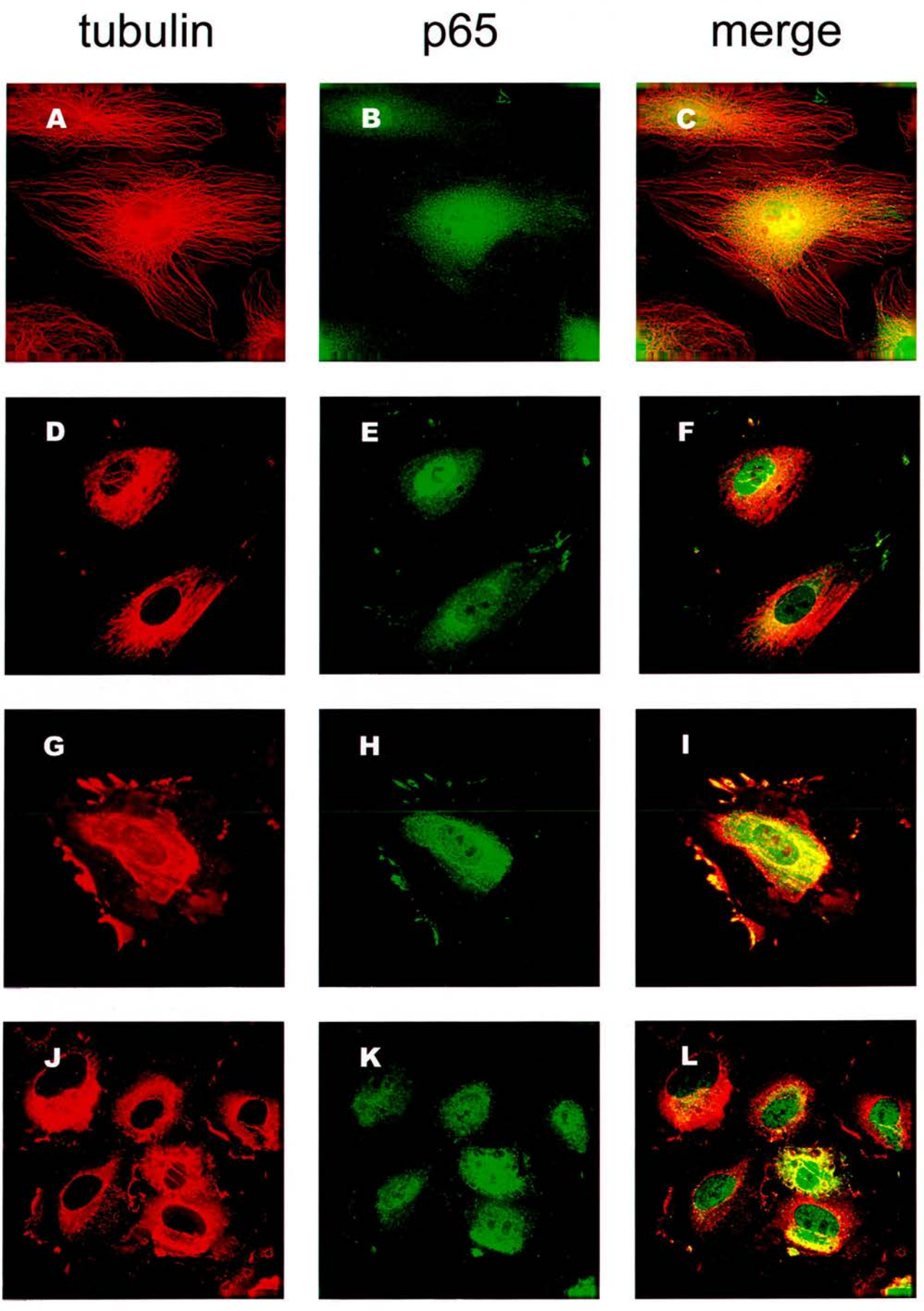

Figure 8.2

Merged pictures of the tubulin and p65 staining reveal many yellow/brown areas, indicating co-localisation of the two proteins (Fig. 8.2 C,F,I,L). Interestingly, co-localisation was seen not only around the nucleus, but also towards the cell periphery, corresponding with regions of membrane ruffling. This is clearly seen in Fig 8.2 I.

8.3 Quantitative analysis reveals that increasing colchicine concentration does not significantly affect nuclear p65 translocation in the presence of TNFα.

The aim of the experiment was to reveal whether quantitative analysis confirmed observations in 8.2 that increasing dosages of colchicine, and therefore MT depolymerisation had no effect the ability of TNFα (30ng.ml^{-1}) to induce nuclear translocation of p65.

Pixel intensity measurements for p65 staining were recorded from the cytoplasm and nucleus of immunofluorescent images of cells treated with increasing concentration of colchicine (75nM-10μM) with or without TNFα stimulation. A random area of each p65 stained slide was selected and pixel intensity of p65 staining was measured in 4-10 areas each of both the nucleus and the cytoplasm in every cell. For each cell, these measurements were averaged and adjusted by subtracting the average background intensity (from 8 areas). The resulting nuclear and cytoplasmic intensity values were used to construct a p65 nuclear:cytoplasmic (N:C) intensity ratio. Depending on the cell

A.

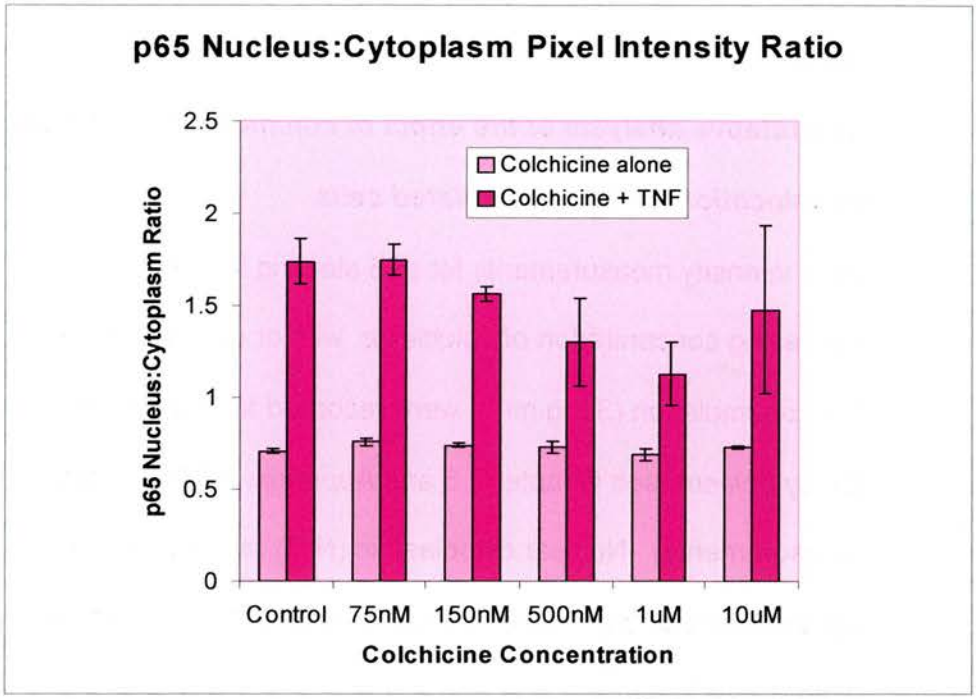

B.

Cell Treatment	Mean N:C Pixel Ratio	Standard Error	Normality p value
Control	0.71	0.012	0.236
75nM Colc.	0.76	0.019	0.474
150nM Colc.	0.74	0.012	0.308
500nM Colc.	0.73	0.029	0.104
1uM Colc.	0.69	0.029	0.079
10uM Colc.	0.73	0.008	0.963

Homogeneity of variance: p=0.420
ANOVA (1 way): p=0.249

C.

Cell Treatment	Mean N:C Pixel Ratio	Standard Error	Normality p value
Control	1.74	0.123	0.652
75nM Colc.+TNF	1.75	0.085	0.588
150nM Colc.+TNF	1.56	0.04	0.227
500nM Colc. +TNF	1.3	0.24	0.227
1uM Colc.+TNF	1.13	0.171	0.227
10uM Colc. +TNF	1.48	0.455	0.23

Homogeneity of variance: p=0.197
ANOVA (1 way): p=0.441

Figure 8.3

Figure 8.3

Quantitative analysis of the effect of colchicine on p65 nuclear translocation in TNFα-stimulated cells.

Pixel intensity measurements for p65 staining in HUVEC treated with increasing concentration of colchicine, with or without the presence of TNFα-stimulation (30ng.ml^{-1}), were recorded for both the nucleus and the cytoplasm (see Chapter 7.5 and Appendix 2.6 for details of these measurements). Nuclear:cytoplasmic (N:C) ratios of p65 staining were constructed and the mean ± standard error (S.E.) of these ratios (B,C) is plotted as a histogram (A).

An Anderson Darling test for normal distribution of the data sets was carried out. The null hypothesis is that the distribution of the data does not vary significantly from a normal distribution. With 95% confidence limits, the p values for p65 N:C ratios in cells with colchicine alone and colchicine with TNFα are all >0.05 (B,C), meaning the null hypothesis cannot be rejected and the data sets are normally distributed.

Bartlett's test for homogeneity of variance of the data was then carried out. The null hypothesis is that the variance of the data is equal. With 95% confidence limits, the p values for p65 N:C ratios in cells with colchicine and colchicine with TNFα are >0.05 (B,C), meaning that the null hypothesis cannot be rejected and the variance of the data is equal.

With normally distributed data, analysis of variance (ANOVA) can be performed, with the null hypothesis that all samples are equal. With 95% confidence limits, the p values for p65 N:C ratios in cells treated with

colchicine alone and colchicine with TNFα are both >0.05 (B,C), showing there is no significant difference within the data.

This analysis confirms the observations in 8.1.2 and 8.2 that p65 nuclear translocation is not affected by increasing colchicine concentration in unstimulated cells or by cells stimulated with TNFα.

treatment, the number of cells counted ranged from 2-13 (Chapter 7.5, Appendix 2.6).

The means of the resulting p65 N:C ratios for each cell condition were plotted as a histogram, with error bars (Fig. 8.3 A). As expected, cells treated with colchicine alone revealed a p65 N:C ratio less than 1, as the majority of p65 in unstimulated cells resides in the cytoplasm (Fig. 8.3 B). In the presence of TNFα, this ratio is more than 1, as p65 nuclear translocation is stimulated (Fig. 8.3 C).

A number of statistical tests were carried out in order to determine whether the effect of colchicine on the p65 N:C ratio is significant. Firstly, an Anderson-Darling test, was carried out, which determines whether the data are normally distributed. The null hypothesis for this test (with 95% confidence limits) is that the distribution of the data does not differ significantly from a normal distribution. If $p>0.05$, then the distribution of the data is not significantly different to that of a normal distribution. For both treatment with colchicine alone and in the presence of TNFα, the resulting p values are >0.05, showing normal distribution of the data (Fig. 8.3 B,C).

Next, Bartlett's test was carried out to test the homogeneity of variance of the data. The null hypothesis (with 95% confidence limits) is that the variances are equal. If $p>0.05$, then the variances are not significantly different. For both treatment with colchicine alone and in the presence

of TNFα, the resulting p values are >0.05, showing equal variances (Fig. 8.3 B,C).

Having confirmed that the data are normally distributed, a one way analysis of variance (ANOVA) was carried out to test whether the samples are equal. The null hypothesis (with 95% confidence limits) is that all samples are equal. If p>0.05, the samples are not significantly different. Again, for both treatment with colchicine alone and colchicine with TNFα, the resulting p values are >0.05, revealing that there is no significant difference within the data (Fig 8.3 B,C).

These statistical tests confirm that there is no significant change in the p65 N:C ratio in the presence of increasing concentrations of colchicine in resting cells or those stimulated with TNFα. This confirms the observations in 8.2 that an intact MT network is not necessary for p65 nuclear translocation stimulated by TNFα. It also confirms the observations in 8.1.1 and 8.1.2 that MT depolymerisation has no effect on the distribution of p65 in unstimulated cells.

8.4 Colchicine treatment does not prevent flow-induced nuclear translocation of p65.

The aim of the experiment was to show, using immunofluorescence, the effect of colchicine on p65 nuclear translocation in HUVEC stimulated with FSS.

Figure 8.4

Effect of FSS and colchicine on p65 nuclear translocation.

Panels A-C show MT, p65 and a merged image, respectively, under control conditions with 30 min. FSS only. FSS causes nuclear translocation of p65 (B), which in non-stimulated cells is mostly confined within the cytoplasm (Fig. 8.1.2 A). Note the small amount of co-localisation of tubulin and p65 visible in panel C, indicated by yellow/brown staining. Panels D-F show MT, p65 and a merged image, respectively of cells treated with 1μM colchicine and stimulated with 30 min. FSS. MT are completely depolymerised (D), but this has no effect on the nuclear translocation of p65 stimulated by flow (E), suggesting that an intact MT network is not necessary for flow-induced p65 nuclear translocation. Panel F reveals a high level of co-localisation between p65 and tubulin from depolymerised MT, denoted by yellow/brown staining.

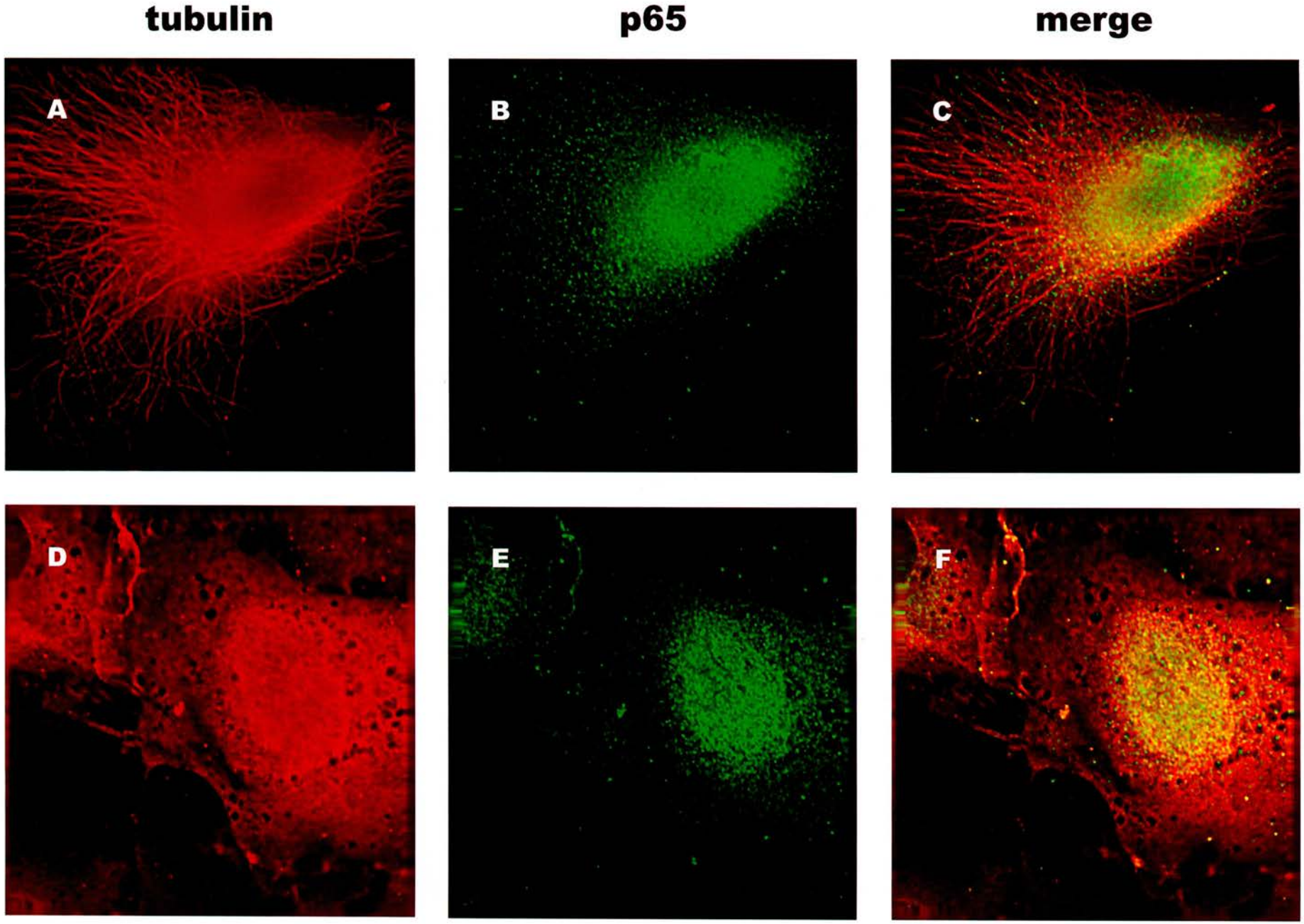

Figure 8.4

HUVEC were subjected to 1μM colchicine for 1 hour, followed by 30 minutes flow at 15 dynes.cm^{-2}. The cells were then fixed and stained for tubulin and p65 (Fig. 8.4). Fig. 8.4 A-C show control conditions with flow only where nuclear translocation of p65 is observable (as seen earlier in Chapter 4, Fig. 4.4) and visibly increased compared to p65 levels in resting cells, which is mainly cytoplasmic (Fig. 8.1.2 A). Treatment with 1μM colchicine, which depolymerises all MT (Fig. 8.4 D) did not inhibit the flow-induced nuclear translocation of p65 (Fig.8.4 E) suggesting that an intact MT network is not necessary for the stimulation of p65 nuclear translocation by flow. In the merged pictures, some co-localisation was seen between p65 and tubulin (Fig. 8.4 C,F), as was also observed in TNFα induced cells (Fig. 8.2 C,F,I,L).

8.5 Colchicine does not interfere with autoregulation of NF-κB gene transcription.

The aim of the experiment was to show, using immunofluorescence, the effect of colchicine, FSS or both on p65 nuclear translocation in the presence of leptomycin B (LMB), which blocks nuclear export of p65.

Cells were activated with 120 min. FSS (15 dynes.cm^{-2}) and stained for p65 and tubulin (Figure 8.5 A-C). The amount of p65 observed in the nucleus after 120 min. FSS (Fig. 8.5 B) is visibly reduced in comparison to cells subjected to 30 min. FSS (Fig. 8.4 B). This is due to an autoregulatory feedback mechanism where p50/p65 held in a complex with newly-synthesized IκB, is exported from the nucleus in a CRM-1-

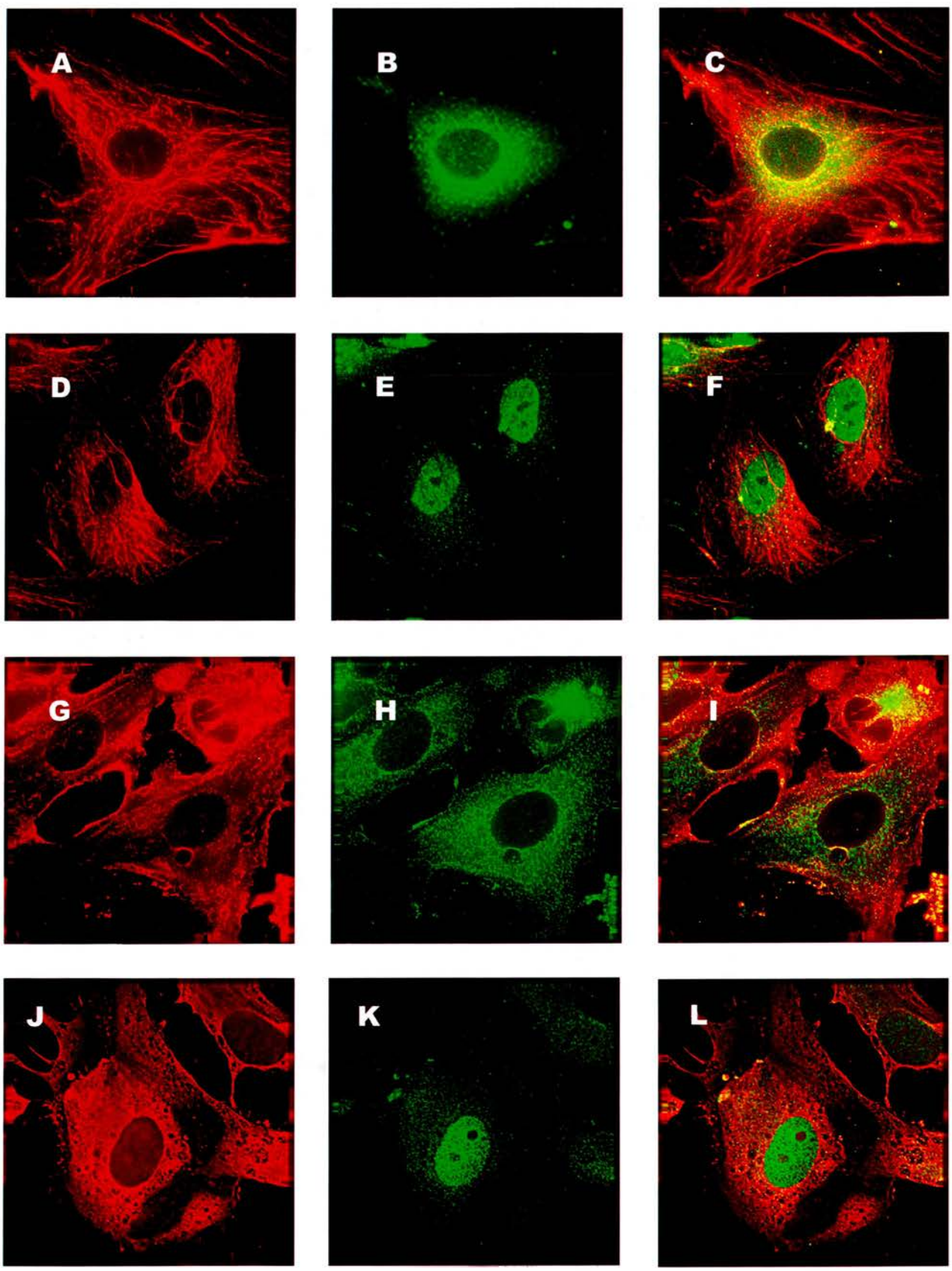

Figure 8.5

dependent process (Arenzana-Seisdedos et al, 1995)). Use of leptomycin B (LMB), which blocks nuclear export of p65 (Fornerod et al, 1997), with 120 min. FSS (Fig. 8.5 D-F) shows p65 nuclear staining (Fig. 8.5 E) and shows that LMB is effective in cells subjected to flow-induced nuclear translocation. 1μM colchicine has no effect on p65 autoregulation after 120 min. FSS (Fig. 8.5 G-I), revealing that an intact MT network is not required for p65 export from the nucleus. The use of 1μM colchicine and LMB, along with 120 min. FSS stimulation (Fig. 8.5 J-L) shows p65 is held in the nucleus by the effect of LMB (Fig. 8.5 K), as also seen in Fig. 8.5 E. This reveals that colchicine has no effect on the mechanism of action of LMB and that an intact MT network is not required for LMB to prevent p65 from being exported from the nucleus. The merged pictures (Fig. 8.5 C,F,I,L) show a small amount of co-localisation of tubulin and p65, but less that that seen in Figures 8.2 and 8.4.

CHAPTER 9

MICROTUBULE DISCUSSION

Loss of endothelial integrity is critically important in the initiation and progression of atherosclerosis (Lee & Gotlieb, 2002). Regulation of endothelial cell integrity is known to involve the cytoskeleton, including MT (Selden et al, 1981; Hu et al, 2002; Lee & Gotlieb, 2002). It is well established that FSS and NF-κB are involved in atherogenesis (see Chapters 2 & 5). The experiments described here were undertaken to determine whether or not MT are involved in mediating the effects of flow on NF-κB activation. This was done by studying the effects of disrupting MT with differing concentrations of colchicine on nuclear translocation of p65. The effects of colchicine on activation of NF-κB by TNFα were also studied for comparison.

HUVEC were exposed to different concentrations (150nm - 1μM) of colchicine for a period of 1 hour. Colchicine depolymerised MT in a concentration-dependent manner, with 1μM being the minimum concentration required for complete depolymerisation. Colchicine-treated cells (75nM-10μM) were then stimulated with TNFα. This is known to cause proteolysis of IκBα and result in nuclear translocation of activated NF-κB (Arenzana-Seisdedos et al, 1995).

MT depolymerisation does not cause NF-κB activation

The experiments showed that MT depolymerisation *per se* did not activate NF-κB as judged by immunofluorescence using an antibody to

p65. The nuclear:cytoplasmic ratio of p65 staining intensities was unaffected by colchicine (Figure 8.3). This is in contrast to results obtained by others. For example, Rosette & Karin (1995) showed that MT depolymerisation, using either colchicine, nocodazole, vinblastine or podophyllotoxin, resulted in activation of NF-κB as shown using EMSA. Activation was not seen when an inactive analogue of colchicine (β-lumicolchicine) was used instead; furthermore, it could be prevented by pre-treating cells with taxol, a MT-stabilising drug. Interestingly, these experiments were not performed on endothelial cells, but on HeLa-S3 cells. There is other evidence that the response to MT depolymerisation could be cell-type dependent. Ivanova et al (2001) showed that NF-κB in HeLa cells was not activated by nocodazole, nor in 2B4 cells. However, results obtained with HeLa-S3 cells did cause NF-κB activation and were similar to those of Rosette & Karin (1995). Experiments with CHO-K1 cells further complicate the picture since 30 min treatment with nocodazole prevented p65 nuclear translocation altogether, whereas nuclear translocation was normal when cells were treated for a further 30 min. Finally, Jung et al (2003) showed that MT-depolymerising agents activated NF-κB gene transcription in a lung tumour cell line (A549).

Nuclear translocation of NF-κB in response to TNFα is unaffected by colchicine

MT depolymerisation did not affect nuclear translocation of NF-κB in response to TNFα in observations of cells immunostained using antibody to p65. Quantitative measurements of the relative intensity of nuclear versus cytoplasmic staining, using the softWoRx programme, confirmed these observations. Analysis of variance (ANOVA) testing revealed that there was no significant difference within the data where increasing concentrations of colchicine were applied to TNFα-stimulated cells. These results show that MT integrity is not necessary for NF-κB activation by TNFα.

These same experiments revealed extensive co-localisation of depolymerised tubulin and p65 in the region of cytoplasm surrounding the nucleus. Fuseler et al (2000) showed that p65 co-localises with intact MT in untreated cells. They demonstrated that extent of the co-localisation was reduced in TNFα-activated cells due to movement of p65 into the nucleus. After pre-treating cells with colchicine (100nM) TNFα stimulation no longer resulted in a reduction in the degree of co-localisation: thus, MT depolymerisation inhibited nuclear import of p65, showing that intact MT are required for this process. This result contrasts with the findings here which show quantitatively that depolymerisation of MT has no effect on TNFα-stimulated p65 nuclear translocation.

Co-localisation of tubulin and p65 immunoreactivity was not confined to the region immediately surrounding the nucleus, but was also seen near the cell periphery, in regions of membrane ruffling (Fig 8.2), and sporadically in the form of isolated dot-like staining in other regions of the cytoplasm too. Thus, p65 immunoreactivity is always found in close association with depolymerised tubulin. This suggests that p65 may be bound to intact MT in untreated cells. Work by Crepieux et al (1997) showed that IκBα also co-localises with α-tubulin in COS-1 cells, using immunofluorescence. This is of interest, since p65 is held in the cytoplasm by IκBα. Crepieux et al (1997) also revealed via immunoprecipitation that IκBα interacts with Dlc-1 in HeLa cells. This is of further interest since Dlc-1 is part of the dynein –end MT motor and work by Helfand et al (2002) showed that disrupting dynein caused movement of vimentin towards the cell periphery. These results suggest that there are links between the cytoskeleton and proteins involved in gene regulation, but that a breakdown of cytoskeletal elements, such as MT, does not always result in increased or impaired activation of genes.

Intact MT are not required for flow-induced activation of NF-κB

Almost nothing is known about the effect of MT depolymerisation on flow-induced NF-κB activation. However, work by Chen et al (2003) showed that disrupting MT with nocodazole had no effect on NF-κB translocation by flow in the MC3T3-E1 murine preosteoblastic cell line.

The results presented here are in agreement with those of Chen et al (2003), as treatment with 1μM colchicine for 1 hour previous to flow did not inhibit nuclear translocation of p65. Merged images of tubulin and p65 staining revealed co-localisation between the two proteins, as seen in cells induced by TNFα.

Intact MT are not required for flow induced auto-regulation of NF-κB

Export of NF-κB from the nucleus by newly-synthesised IκBα, activated by FSS, is an auto-regulatory mechanism (Arenzana-Seisdedos et al, 1995). This nuclear export can be blocked by the use of leptomycin B (LMB) (Rodriguez et al, 1998). The experiments presented here show that the action of colchicine has no effect on and is not affected by LMB. Furthermore, LMB plus colchicine does not inhibit the translocation of p65 to the nucleus in FSS stimulated cells, confirming that colchicine does not inhibit the NF-κB gene transcription auto-regulation mechanism. Tubulin/p65 merged immunofluorescence images reveal only a small amount of co-localisation.

Summary

The results presented here reveal that colchicine depolymerises MT in a concentration dependent manner in human endothelial cells and that lack of an intact MT network does not affect p65 nuclear translocation, induced by flow or by TNFα. Furthermore, MT depolymerisation has no effect on the NF-κB autoregulatory mechanism. These experiments also

reveal extensive levels of co-localisation between p65 and tubulin in both TNFα and FSS stimulated cells with depolymerised MT.

CHAPTER 10

OVERALL DISCUSSION AND SCOPE FOR FURTHER STUDY

10.1 Physiological relevance of the present study

Dysfunction of the endothelium underlies many disorders of the cardiovascular system, including atherosclerosis. Atherosclerosis is a chronic inflammatory condition that can ultimately lead to MI, stroke, aneurysm and peripheral vascular disease. Haemodynamic forces appear to play a very important part in atherogenesis, as *in vivo* observations show that atheroma appear most often at arterial bifurcations or sharply curved segments where disturbed blood flow patterns predominate. Disturbed flow has shown to be pre-atherogenic by causing an increased uptake of lipoproteins and the appearance of leukocyte adhesion molecules on the endothelial cells. Smooth muscle cells proliferate and synthesise a connective tissue matrix and accumulation of lipids and cholesterol follows (Topper et al, 1996; Traub & Berk, 1998; Nagel et al, 1999).

Atheroma are only very rarely observed in straight arterial sections where laminar flow occurs (Caro et al, 1969; Davies et al, 2001). *In vitro* studies involving the subjection of cultured endothelial monolayers to measurable levels of laminar flow showed that endothelial integrity and wound healing were favoured under these conditions and coagulation, smooth muscle growth, leukocyte and monocyte migration and lipoprotein uptake were all regulated (Traub & Berk, 1998), revealing a possible atheroprotective role for laminar flow.

FSS is a tractive force associated with flow and endothelial cells are uniquely responsive to this. Therefore, a more thorough understanding of the mechanisms involved in the response of these cells to flow would be considerably relevant in the clinical sense.

10.2 Signalling pathway intermediates involved in FSS-induced NF-κB gene transcription

Shear stress activates signalling cascades whose downstream targets include several nuclear transcription factors which modify gene expression in endothelial cells with NF-κB being one of these (Shyy et al, 1995; Khachigian et al, 1995, Lan et al 1994).

NF-κB regulates more than 50 genes, encoding for such things as cytokines, growth factors, adhesion molecules, viruses and immunoregulating proteins (May & Ghosh, 1998).

NF-κB is active in advanced atherosclerotic lesions (Brand et al, 1996) where many of the expressed genes are NF-κB-dependent (Collins, 1993). NF-κB is not active in areas of the vasculature which are considered high risk but are currently free of atherosclerotic lesions. However, the resting levels of some NF-κB signalling elements are much increased in disease prone but currently disease free areas (Hajra et al, 2000). These authors found 5-18 fold increases from control levels of p65, IκBα and IκBβ in high-risk areas of the vasculature of mice. However, little NF-κB was activated, leading to the suggestion that the signal transduction pathway triggered by NF-κB activation may be

"primed" in these areas in order to respond subsequently to systemic risk factors. An understanding of the NF-κB signalling pathway activated by FSS would be of obvious and considerable clinical interest

The results presented here and published (Hay et al, 2003) attempted to identify some of the upstream intermediates involved in flow-induced activation of NF-κB in human endothelial cells. It is shown that IKK1/2 are rapidly activated (~3-5 min.) by moderate shear stress, followed by degradation of IκBα and β, nuclear translocation of p65 (a sub-unit of NF-κB) and enhanced 3κB luciferase reporter expression. Transfection of cells with catalytically inactive mutants of IKK1 and 2 or a mutant of NIK blocked flow-induced p65 nuclear translocation, revealing a role for all three enzymes in the flow-activated pathway. Treatment with an inhibitor of proteasome-mediated IκB degradation (MG132) also blocked this translocation, revealing a role for the proteasome pathway in flow-induced activation of NF-κB. Transfection with a catalytically inactive mutant of TPL2 or treatment with a protein kinase C inhibitor (bisin) did not block flow-induced NF-κB nuclear translocation, revealing that neither TPL2 kinase or PKC isoforms are part of this signalling pathway.

10.3 Involvement of the cytoskeleton in the mechanotransduction of FSS

The sensitivity of endothelial cells to flow is very well established, but how they sense and respond to altered flow from a mechanical viewpoint is much less clearly understood. Davies (1995) put forward a

decentralised model of mechanotransduction whereby flow activates primary cell surface mechanosensors and these sensors transmit the signal to other cell sites via an intracellular force transmission pathway which involves the cytoskeleton.

The first cytoskeletal element shown to change under flow was actin (Levesque & Nerem, 1985; Masuda & Fujiwara, 1993; Girard & Nerem, 1995; Fujiwara et al, 1998). Vimentin intermediate filaments have also been shown to undergo rapid displacement in endothelial cells subjected to flow (Helmke et al, 2000; 2001). MT were shown to re-orientate and align in fibroblasts in response to flow (Oakley & Brunette, 1993). Malek & Izumo (1996) found that the absence of an intact MT network blocked the formation of actin stress fibres and re-alignment in endothelial cells. It became apparent that FSS has an effect on the cytoskeleton, but it was not known whether these changes were significant in the response of the endothelium to altered flow, or more specifically to NF-κB activation.

10.4 Role of MT in FSS-induced NF-κB activation

MT have been implicated in the mechanism of activation of NF-κB, although the exact nature of this involvement is controversial. Rosette & Karin (1995) showed that the use of the MT depolymerising agents colchicine and nocodazole activated NF-κB-dependent gene transcription in HeLa cells suggesting that destabilising MT favours the

activation of NF-κB. Conversely, Fuseler et al (2000) showed that increasing concentrations of colchicine caused a decrease in nuclear translocation of NF-κB in endothelial cells, suggesting that an intact MT network is required for this activation. Both of these studies relied upon agonist-induced NF-κB activation of cells. MT are also implicated in the mechanotransduction of shear stress by endothelial cells, but the nature of the results is again controversial. Knudsen & Frangos (1997) showed that MT depolymerising agents increased flow-induced NO output. However, Sun et al (2001) reported that these agents prevented flow-induced vasodilatation. In considering these findings, MT integrity affects flow-mediated responses and there is an implication that NF-κB gene transcription is sensitive to these changes. Work consistent with this idea includes Crepieux et al (1997) who describe a physical interaction between IκBα and Dlc-1, a component of the minus-end MT motor dynein. Chen et al (2003) showed that nocodazole-mediated depolymerisation of MT did not affect flow-induced NF-κB nuclear translocation in murine preosteoblastic cells (MC3T3-E1).

Results presented here revealed that MT are depolymerised by colchicine in a concentration dependent manner and TNFα-induced NF-κB nuclear translocation was not affected by increasing concentrations of colchicine, contrasting with the results presented by Fuseler et al (2000). Colchicine did not have an effect upon flow-induced nuclear translocation of NF-κB, in agreement with Chen et al (2003).

Furthermore, the use of LMB to prevent nuclear export of NF-κB by newly synthesised IκBα was not affected by MT depolymerisation, revealing that an intact MT network is not required for this auto-regulatory mechanism to occur. Immunofluorescent observations revealed a high level of co-localisation between tubulin and p65, especially around the edge of the cell in so-called membrane ruffles.

10.5 Further experiments

There are many ways in which to expand upon the work presented here. It would be of interest to transfect HUVEC with a 3κB luciferase reporter and perform a luciferase assay after colchicine treatment and induction by flow, in order to assess whether the translocated NF-κB is transcriptionally active. Use of a small interfering RNA (siRNA) for tubulin, which binds to an RNA-induced silencing complex (RISC) that targets and degrades a homologous transcript, thereby suppressing gene expression, would be useful to further explore any role tubulin may have in the activation of NF-κB by flow. Western blotting and immunofluorescence would be used assess the efficacy of gene silencing. Immunoprecipitation would be a beneficial tool to determine any association between p65 and tubulin, as seems to be suggested here by co-localisation observed in immunofluorescent images. The present studies were undertaken using fixed material to compare different cell populations before and after treatment with colchicine

and/or induction by flow. Many of the uncertainties of this approach could be avoided by the use of living cells expressing tubulin tagged with fluorescent protein markers (e.g. GFP). This would allow for increased spatio-temporal resolution of any structural changes induced by flow. Furthermore, nuclear translocation of fluorescent protein-tagged p65 could also be used as an indicator of NF-κB activation.

Similar sets of experiments involving the other main cytoskeletal elements, actin and vimentin, would help to further elucidate the role of the cytoskeleton in the response of endothelial cells to flow.

10.6 Scope for extended study

The cytoskeleton also has a role in its interaction with focal adhesions (FA). FA typically anchor actin stress fibres to components of the extracellular matrix such as fibronectin, vitronectin and laminin. This connection is indirect and is mediated via transmembrane proteins called integrins. Standard actin FA were described by Davies (1995), but an unusual type of FA which anchors both actin and vimentin and is termed a vimentin-associated matrix adhesion (VMA) was reported by Flitney et al (2001) and Gonzales et al (2001). Flitney et al (2001) also showed that a vimentin-associated protein called plectin is present at VMAs and co-localises with vimentin, $\alpha v\beta_3$ integrin, vinculin, paxillin and the tips of actin stress fibres and that this co-localisation is observed most prominently on the cytoplasmic face of VMAs. They postulated that

plectin functions to connect vimentin to actin and/or $\alpha v\beta_3$ integrin at VMAs.

Experimental studies on vimentin in response to flow reveal that vimentin bundles near the endothelial cell surface undergo rapid displacement (Helmke et al, 2000; 2001) and are involved in flow-mediated vasodilatation (Smiesko & Johnson, 1993) which is attenuated in transgenic animals lacking vimentin (Henrion et al, 1997). Importantly, form the point of view of this study, the activation of IKK1/2 in response to flow can be inhibited by use of a blocking antibody to the $\alpha v\beta_3$ integrin (Bhullar et al, 1998). The same integrin lies in the centre of the VMA and furthermore MEKK1, an upstream activator of IKK1/2 is found at FA in several types of cell (Christerson et al, 1999).

It has been shown that there are too many links between NF-κB activation and the cytoskeleton in response to flow to overlook the importance of these elements in the mechanotransduction pathway. However, there remains a great deal of research in this field to elucidate exactly which of these cytoskeletal proteins are involved and how they contribute to the conversion of the physical endothelial cell response to flow into a chemical signalling pathway which ultimately affects gene transcription of NF-κB and possible protection/progression of atherosclerosis.

Adams, M.D., Dubnick, M., Kervelage A.R., Moreno, R., Kelley, J.M., Utterback, T.R., Nagle, J.W., Fields, C., Venter, J.C. (1992) Sequence identification of 2,375 human brain genes. *Nature 355: 632-634.*

Allen, J.N., Herzyk, D.J., Wewers, M.D. (1991) Colchicine has opposite effects on interleukin-1β and tumour necrosis factor-α production. *Am. J. Physiol. 261 (Lung Cell. Mol. Physiol. 5): L315-L321.*

Amos, L.A., Lowe, J. (1999) How Taxol stabilises microtubule structure. *Chemistry & Biology 6 (3): R65-R69.*

Arenzana-Seisdedos, F., Thompson, J., Rodriguez, M.S., Bachelerie, F., Thomas, D., Hay, R.T. (1995) Inducible nuclear expression of newly synthesized IκBα negatively regulates DNA-binding and transcriptional activities of NF-κB. *Mol. Cell. Biol. 15 (5): 2689-2696.*

Arenzana-Seisdedos, F., Turpin, P., Rodriguez, M., Thomas, D., Hay, R.T., Virelizier, J-L., Dargemont, C. (1997) Nuclear localization of IκBα promotes active transport of NF-κB from the nucleus to the cytoplasm. *J. Cell Sci. 110: 369-378.*

Auphan, N., DiDonato, J.A., Rosette, C., Helmberg, A., Karin, M., (1995) Immunosuppression by glucocorticoids: inhibition of NF-κB activity through induction of IκB synthesis. *Science 270: 286-290.*

Baldwin, A.S. Jr., (1996) The NF-κB and IκB proteins: new discoveries and insights. *Annu. Rev. Immunol. 14: 649-681.*

Baeuerle, P.A., Baltimore, D., (1988) IκB: a specific inhibitor of the NF-κB transcription factor. *Science 242: 540-546.*

Barbee, K.A., Davies, P.F., Lal, R., (1994) Shear stress-induced organisation of the surface topography of living endothelial cells imaged by atomic force microscopy. *Circ. Res. 74 (1): 163-171.*

Barbee, K.A., Mundel, T., Lal, R., Davies, P.F., (1995) Subcellular distribution of shear stress at the surface of flow-aligned and non-aligned endothelial monolayers. *Am. J. Physiol. 268 (Heart Circ. Physiol. 37): H1765-H1772.*

Beauparlant, P., Lin, R., Hiscott, J., (1996) The role of the C-terminal domain of IκBα in protein degradation and stabilization. *J. Biol. Chem. 271 (18): 10690-10696.*

Beers, C. (2002) Flow-dependent restructuring of the intermediate filament cytoskeleton and activation of NF-κB in cultured endothelial cells. *University of St Andrews PhD Thesis.*

Belich, M.P., Salmeron, A., Johnston, L.H., Ley, S.C., (1999) TPL-2 kinase regulates the proteolysis of the NF-κB-inhibitory protein NF-κB1 p105. *Nature 397: 363-368.*

Bhullar, I.S., Li, Y-S., Miao,H., Zandi, E., Kim, M., Shyy, J.Y-J., Chien, S. (1998) Fluid shear stress activation of IκB kinase is integrin dependent. *J. Biol. Chem. 273 (46): 30544-30549.*

Bourgarel-Rey, V., Vallee, S., Rimet, O., Champion, S., Braguer, D., Desobry, C., Briand, C., Barra, Y. (2001) Involvement of nuclear factor κB in c-myc induction by tubulin polymerization inhibitors. *Mol. Pharmacol. 59 (5): 116501170.*

Braddock, M., Schwachtgen, J-L., Houston, P., Dickson, M.C., Lee, M.J., Campbell, C.J. (1998) Fluid shear stress modulation of gene expression in endothelial cells. *News Physiol. Sci. 13: 241-246.*

Brand, K., Page, S., Rogier, G., Armin, B., Brandt, R., Knuchuel, R., Page, M., Kaltschmidt, C., Baeuerle, P.A., Neumeler, D. (1996) Activated transcription factor nuclear factor-kappa B is present in the atherosclerotic lesion. *J. Clin. Invest. 97 (7): 1715-1722.*

Caro, C.G., Fitz-Gerald, J.M., Schroter, R.C. (1969) Arterial wall shear and distribution of early atheroma in man. *Nature 223 (211): 1159-1160.*

Chen, N.X., Geist, G.J., Genetos, D.C., Pavalko, F.M., Duncan, R.L. (2003) Fluid shear-induced NF-κB translocation in osteoblasts is mediated by intracellular calcium release. *Bone 33 (3): 399-410.*

Chen, Z., Hagler, J., Palombella, V.J., Melandri, F., Scherer, D., Ballard, D., Maniatis, T. (1995) Signal-induced site-specific phosphorylation targets I kappa B alpha to the ubiquitin-proteasome pathway. *Gen. Dev. 9: 1586-1597.*

Chien, S., Li, S., Shyy, J.Y-J. (1998) Effects of mechanical forces on signal transduction and gene expression in endothelial cells. *Hypertension 31 (2): 162-169.*

Christerson, L.B., Vanderbilt, C.A., Cobb, M.H. (1999) MEKK-1 interacts with alpha-actinin and localises to stress fibres and focal adhesion. *Cell Motil. Cytoskeleton 43 (3): 186-198.*

Cleveland, D.W., (1994) Tubulin and associated proteins. *Guidebook to the cytoskeletal and motor proteins: 101-105. Kreis, T., Vale, R., Ed. Oxford University Press, Oxford.*

Collins, T. (1993) Endothelial nuclear factor-kappa B and the initiation of the atherosclerotic lesion. *Lab. Invest. 68 (5): 499-508.*

Crepieux, P., Kwon, H., Leclerc, N., Spencer, W., Richard, S., Lin, R., Hiscott, J. (1997) IκBα physically interacts with a cytoskeleton-associated protein through its signal response domain. *Mol. Cell. Biol. 17 (12): 7375-7385.*

Dark, G.G., Hill, S.A., Prise, V.E., Tozer, G.M., Pettit, G.R., Chaplin D.J. (1997) Combretastatin A-4, an agent that displays potent and selective toxicity toward tumor vasculature. *Cancer Res. 57: 1829-1834.*

Davies, P.F., Remuzzi, A., Gordon, E.J., Dewey, C.F.Jr., Gimbrone, M.A.Jr. (1986) Turbulent fluid shear stress induces vascular endothelial cell turnover *in vitro. Proc. Natl. Acad. Sci. USA. 83: 2114-2117.*

Davies, P.F. (1989) How do vascular endothelial cells respond to flow? *News in Physiolog. Sci. 4: 22-25.*

Davies, P.F. (1995) Flow-mediated endothelial mechanotransduction. *Physiol. Rev. 75: 519-560.*

Davies, P.F., Shi, C., Depaola, N., Helmke, B.P., Polacek, D.C. (2001) Hemodynamics and the focal origin of atherosclerosis: a spatial approach to endothelial structure, gene expression and function. *Ann. N.Y. Acad. Sci. 947: 7-17.*

de Martin, R., Vanhove, B., Cheng, Q., Hofer, E., Csizmadia, V., Winkler, H., Bach, F.H. (1993) Cytokine-inducible expression in endothelial cells of an IκBα-like gene is regulated by NFκB. *EMBO J. 12 (7): 2773-2779.*

de Martin, R., Hoeth, M., Hofer-Warbinek, R., Schmid, J.A. (2000) The transcription factor NF-κB and the regulation of vascular cell function. *Arterioscler. Thromb. Vasc. Biol. 20: e83-e88.*

Dewey, C.F., Bussolari, S.R., Gimbrone, M.A.Jr., Davies, P.F. (1981) The dynamic response of vascular endothelial cells to fluid shear stress. *J. Biomech. Eng. 103: 177-185.*

DiDonato, J., Mercurio, F., Rosett, C., Wu-Li, J., Suyang, H., Ghosh, S., Karin, M. (1996) Mapping of inducible IκB phosphorylation sites that signal its ubiquitination and degradation. Mol. Cell. Biol. 16 (4): 1295-1304.

DiDonato, J.A., Hayakawa, M., Rothwarf, D.M., Zandi, E., Karin, M. (1997) A cytokine-responsive IκB kinase that activates the transcription factor NF-κB. *Nature 388: 548-554.*

Dimmeler, S., Assmus, B., Hermann, C., Haendeler, J., Zeiher, A.M. (1998) Fluid shear stress stimulates phosphorylation of Akt in human endothelial cells. Involvement in suppression of apoptosis. *Circ. Res. 83: 334-341.*

Domnina, L.V., Rovensky, J.A., Vasiliev, J.M., Gelfand, I.M. (1985) Effect of microtubule-destroying drugs on the spreading and shape of cultured epithelial cells. *J.Cell. Sci. 74: 267-282.*

Domnina, L.V., Yu, O., Ivanova, B., Cherniek, B.V., Skulachev, P., Vasiliev, J.M. (2002) Effects of the inhibitors of dynamics of cytoskeletal structures on the development of apoptosis induced by the tumour necrosis factor. *Biochemistry (Mosc.) 67 (7): 737-746.*

Downing, K.H., Nogales, E. (1998) Tubulin and microtubule structure. *Curr. Opin. Cell Biol. 10: 16-22.*

Downing, K.H. (2002) Structural basis for the interaction of tubulin with proteins and drugs that affect microtubule dynamics. *Annu. Rev. Cell Dev. Biol. 16: 89-111.*

Drubin, D., Hirokawa, N. (1998) Cytoskeleton. *Curr. Opin. Cell Biol. 10: 13-15.*

Ernst, M.K., Dunn, L.L., Rice, N.R. (1995) The PEST-like sequence of IκBα is responsible for inhibition of DNA binding but not for cytoplasmic retention of c-rel or RelA homodimers. *Mol. Cell Biol. 15 (2): 872-882.*

Flitney, F.W., Beers, C., Cameron, V., Jones, J., Khuon, S., Goldman, R.D. (2001) Fluid shear stress-dependent remodelling of the intermediate filament (IF) cytoskeleton in cultured endothelial cells. *Vasc. Endo.- Source & Target of inflammatory mediators 1 (330): 356-357. J. Catravas et al Ed.*

Fujiwara, K., Masuda, M., Osawa, M., Katoh, K., Kano, Y., Harada, N., Lopes R.B. (1998) Response of vascular endothelial cells to fluid flow. *Biol. Bull. 194: 384-386.*

Fuseler, J.W., Merrill, D.M., Wolf, R.E. (2000) Translocation of nuclear factor kappa B (NF-κB) in tumour necrosis factor (TNF) activated human endothelial cells (HUVECs) is dependent on cytoplasmic microtubules. *Mol. Biol. Cell 11:359a.*

Ghosh, G., Van Duyne G., Ghosh, S., Sigler, P.B. (1995) Structure of NF-κB p50 homodimer bound to a κB site. *Nature 373: 303-310.*

Ghosh, S., Baltimore, D. (1990) Activation *in vitro* of NF-κB by phosphorylation of its inhibitor IκB. *Nature 344: 678-682.*

Gimbrone, M.A.Jr., Nagel, T., Topper, J.N. (1997) Biochemical activation: an emerging paradigm in endothelial adhesion biology. *J. Clin. Invest. 99 (8): 1809-1813.*

Girard, P.R., Nerem, R.M. (1995) Shear stress modulates endothelial cell morphology and F-actin organization through the regulation of focal adhesion-associated proteins. *J. Cell. Physiol. 163: 179-193.*

Gonzales, M., Weksler, B., Tsuruta, D., Goldman, R.D., Yoon, K.J., Hopkinson, S.B., Flitney, F.W., Jones, J.C.R. (2001) Structure and function of a vimentin-associated matrix adhesion in endothelial cells. *Mol. Biol. Cell 12: 85-100.*

Gotlieb, A.I., Subrahmanyan, L., Kalnins, V.I. (1983) Microtubule-organizing centers and cell migration: effect of inhibition of migration and microtubule disruption in endothelial cells. *J. Cell. Biol. 96: 1266-1272.*

Hajra, L., Evans, A.I., Chen, M., Hydik, S.J., Collins, T., Cybulsky, M.I. (2000) The NF-κB signal transduction pathway in aortic endothelial cells is primed for activation in regions predisposed to atherosclerotic lesion formation. *PNAS 97 (16): 9052-9057.*

Hay, D.C., Beers, C., Cameron, V., Thomson, L., Flitney, F.W., Hay, R.T. (2003) Activation of NF-κB nuclear transcription factor by flow in human endothelial cells. *Biochim. Biophys. Acta 1642: 33-44.*

Helfand, B.T., Mikami, A., Vallee, R.B., Goldman, R.D. (2002) A requirement for cytoplasmic dynein and dynactin in intermediate filament network assembly and organization. *J. Cell Biol. 157 (5): 795-806.*

Helmke, B.P., Goldman, R.D., Davies, P.F. (2000) Rapid displacement of vimentin intermediate filaments in living endothelial cells exposed to flow. *Circ. Res. 86: 745-752.*

Helmke, B.P., Thakker, D.B., Goldman, R.D., Davies, P.F. (2001) Spatiotemporal analysis of flow-induced intermediate filaments in living endothelial cells exposed to flow. *Circ. Res. 86:745-752.*

Henrion, D., Terzi, F., Matrougui, K., Duriez, M., Boulanger, C., Colucci-Guyon, E., Babinet, C., Brinad, P., Friendlander, G., Polyerin, P., Levy, B.I. (1997) Impaired flow-induced dilation in mesenteric resistance arteries from mice lacking vimentin. *J. Clin. Invest. 100 (11): 2909-2914.*

Hsu, H., Solovyev, I., Colombero, A., Elliott, R., Kelley, M., Boyle, W.J. (1997) ATAR, a novel tumor necrosis factor receptor family member, signals through TRAF2 and TRAF5. *J. Biol. Chem. 272 (21): 13471-13474.*

Hu, Y-L., Li. S., Miao, H., Tsou, T-C., del Pozo, M.A., Chien, S. (2002) Roles of microtubule dynamics and small GTPase Rac in endothelial cells migration and lamellipodium formation under flow. *J.Vasc. Res. 39: 465-476.*

Hu, Y., Baud, V., Delhase, M., Zhang, P., Deerinck, T., Ellisman, M., Johnson, R., Karin, M. (1999) Abnormal morphogenesis but intact IKK activation in mice lacking the IKKα subunit of IκB kinase. *Science 284: 316-320.*

Ivanova, T.V., Ivanov, V.N., Nadezhdina, E.S. (2001) Transcription factors NF-κB and AP-1/c-fos in cell response to nocodazole. *Membr. Cell Biol. 14 (6): 727-741.*

Jaffray, E., Wood, K.M., Hay, R.T. (1995) Domain organization of IκBα and sites of interaction with NF-κB p65. *Mol. Cell. Biol. 15 (4): 2166-2172.*

Jordan, M.A., Wilson, L. (1998) Microtubules and actin filaments: dynamic targets for cancer chemotherapy. *Curr. Opin. Cell Biol. 10: 123-130.*

Joshi, H.C. (1998) Microtubule dynamics in living cells. *Curr. Opin. Cell Biol. 10: 35-44.*

Jung, Y-J., Isaacs, J.S., Lee, S., Trepel, J., Neckers, L. (2003) Microtubule disruption utilizes an NF-κB-dependent pathway to stabilize HIF-1α protein. *J. Biol. Chem. 278 (9): 7445-7452.*

Khachigian, L.M., Resnick, N., Gimbrone, M.A.Jr., Collins, T. (1995) Nuclear factor-κB interacts functionally with the platelet-derived growth factor B-chain shear stress response element in vascular endothelial cells exposed to fluid shear stress. *J.Clin. Invest. 96: 1169-1175.*

Kirkpatrick, C.J., Wagner, M., Hermanns, I., Kelin, C.L., Kohler, H., Otto, M., van Kooten, T.G., Bittinger, F. (1997) Physiology and cell biology of the endothelium: a dynamic interface for cell communication. *Int. J. Microcirc. 17: 231-240.*

Knudsen, H.K., Frangos, J.A. (1997) Role of cytoskeleton in shear stress-induced endothelial nitric oxide production. *Am. J. Physiol. (Heart Circ. Physiol. 42): H347-H355.*

Krappmann, D., Hatada, E.N., Tegethoff, S., Li, J., Klippel, K.G., Baeuerle, P.A., Scheidereit, C. (2000) The IκB kinase (IKK) complex is tripartite and contains IKKγ but not IKAP as a regular component. *J. Biol. Chem. 275 (38): 29779-29787.*

Lan, Q., Mercurius, K.O., Davies, P.F. (1994) Stimulation of transcription factors NF-κB and AP1 in endothelial cells subjected to shear stress. *Biochem. Biophys. Res. Commun. 201 (2): 950-956.*

Lang, V., Janzen, J., Fischer, G.Z., Soneji, Y., Beinke, S., Salmeron, A., Allen, H., Hay, R.T., Ben-Neriah, Y., Ley, S.C. (2003) βTrCP-mediated proteolysis of NF-κB1 p105 requires phosphorylation of p105 serines 927-932. *Mol. Cell. Biol. 23 (1): 402-413.*

Lee, J.S.Y., Gotlieb, A.I. (2002) Microtubule-actin interactions may regulate endothelial integrity and repair. *Cardio. Pathol. 11: 135-140.*

Levesque, M.J., Nerem, R.M. (1985) The elongation and orientation of cultured endothelial cells in response to shear stress. *J. Biomech. Eng. 107: 341-347.*

Malinin, N.L., Boldin, N.P., Kovalenko, A.V., Wallach, D. (1997) MAP3K-related kinase involved in NF-κB induction by TNF, CD95 and IL-1. *Nature 385: 540-544.*

Malek, A.M., Izumo, S. (1996) Mechanism of endothelial cell shape change and cytoskeletal remodeling in response to fluid shear stress. *J. Cell Sci. 109: 713-726.*

Masuda, M., Fujiwara, K. (1993) Morphological responses of single cell endothelial cells exposed to physiological levels of fluid shear stress. *Frontiers Med. Biol. Engng. 5 (2): 79-87.*

May, M.J., Ghosh, S. (1997) Rel/NF-κB and IκB proteins: an overview. *Sem. Cancer Biol. 8: 63-73.*

May, M.J., Ghosh, S. (1998) Signal transduction through NF-κB. *Immunol. Today 19 (2): 80-88.*

Mercurio, F., DiDonato, J.A., Rosette, C., Karin, M. (1993) p105 and p98 precursor proteins play an active role in NF-kappa B-mediated signal transduction. *Gen. Dev. 7 (4): 705-718.*

Mercurio, F., Zhu, H., Murray, B.W., Shevchenko, A., Bennett, B.L., Li, J.W., Young, D.B., Barbosa, M., Mann, M. (1997) IKK-1 and IKK02: cytokine-activated IκB kinases essential for NF-κB activation. *Science 278: 860-865.*

Mercurio, F., Manning, A.M. (1999) Multiple signals converging on NF-κB. *Curr. Opin. Cell Biol. 11: 226-232.*

Mercurio, F., Murray, B.W., Shevchenko, A., Bennett, B.L., Young, D.B., Li, J.W., Pascual, G., Motiwala, A., Zhu, H., Mann, M., Manning, A.M. (1999) IκB kinase (IKK)-associated protein 1, a common component of the heterogenous IKK complex. *Mol. Cell. Biol. 19 (2): 1526-1538.*

Muller, C.W., Rey, F.A., Sodeoka, M., Verdine, G.L., Harrison, S.C. (1995) Structure of the NF-κB p50 homodimer bound to DNA. *Nature 373: 311-317.*

Nagel, T., Resnick, N., Dewey, F., Gimbrone, M.A. (1999) Vascular endothelial cells respond to spatial gradients in fluid shear stress by enhanced activation by transcription factors. *Arterioscler. Thromb. Vasc. Biol. 19: 1825-1834.*

Nakano, H., Shindo, M., Sakon, S., Nishinako, S., Mihara, M., Yagita, H., Okumura, K. (1998) Differential regulation of IκB kinase α and β by two upstream kinases, NF-κB-inducing kinase and mitogen-activated protein kinase/ERK kinase kinase-1. *Proc. Natl. Acad. Sci. USA. 95: 3537-3542.*

Nerem, R.M., Alexander, R.W., Chappell, D.C., Medford, R.M., Varner, S.E., Taylor, W.R. (1998) The study of the influence of flow on vascular endothelial biology. *Am. J. Med. Sci. 316 (3): 169-175.*

Oakley, C., Brunette, D.M. (1993) The sequence of aligned microtubules, focal contracts and actin filaments in fibroblasts spreading on smooth and grooved titanium substrata.

Palmer, R.M.J., Ferrige, A. G., Moncada, S. (1987) Nitric oxide release accounts for the biological activity of endothelium-derived relaxing factor. *Nature 327: 524-526.*

Papadaki, M., Eskin, S.G. (1997) Effects of fluid shear stress on gene regulation of vascular cells. *Biotechnol. Prog. 13: 209-221.*

Patan, S. (2000) Vasculogenesis and angiogenesis as mechanisms of vascular formation, growth and remodelling. *J. Neuro-oncology, 50: 1-15*

Paterson, J.R.; Mitchison, T.J. (2002) Small molecules, big impact: a history of chemical inhibitors and the cytoskeleton. *Chemistry and Biology, 90: 1275-1285.*

Phelps, C.B., Sengchanthalangsy, L.L., Huxford, T., Ghosh, G. (2000) Mechanism of IκBα binding to NF-κB dimers. *J. Biol. Chem. 275 (38): 29840-29846.*

Pickart, C.M., Rose, I.A. (1985) Ubiquitin carboxyl-terminal hydrolase acts on ubiquitin carboxyl-terminal amides. *J.Biol. Chem. 260 (13): 7903-7910.*

Pinol-Roma, S., Dreyfuss, G. (1992) Shuttling of the pre-mRNA binding proteins between nucleus and cytoplasm. *Nature 355, 730-732.*

Prahlad, V., Toon, M., Moir, R.D., Vale, R.D., Goldman, R.D. (1998) Rapid movements of vimentin on microtubule tracks: kinesin-dependent assembly of intermediate filament networks. *J. Cell Biol. 143 (1): 159-170.*

Regnier, C.H.; Song, H.Y., Gao, X.; Goeddel, D.V.; Cao, Z.; Rothe, M. (1997) Identification and characterisation of an IκB kinase. *Cell 90:373-383.*

Resnick, N., Gimbrone, M.A.Jr. (1995) Hemodynamic forces are complex regulators of endothelial gene expression. *FASEB J. 9: 874-882.*

Roff, M., Thompson, J., Rodriguez, M.S., Jacque, J-M., Baleux, F., Arenzana-Seisdedos, F., Hay, R.T. (1996) Role of IκBα ubiquitination in signal-induced activation of NF-κB *in vivo. J. Biol. Chem. 271 (13): 7844-7850.*

Rosette, C., Karin, M. (1995) Cytoskeletal control of gene expression: depolymerisation of microtubules activates NF-κB. *J. Cell Biol. 128 (6): 1111-1119.*

Ross, R. (1993) The pathogenesis of atherosclerosis: a perspective for the 1990s. *Nature 362: 801-809.*

Rothe, M., Sarma, V., Dixit, V.M., Goeddel, D.V. (1995) TRAF2-mediated activation of NF-κB by TNF receptor 2 and CD40. *Science 269: 1424-1427.*

Resnick, N., Collins, T., Atkinson, W., Bonthron, D.T., Dewey, C.F. Jr., Gimbrone, M.A.Jr. (1993) Platelet derived growth factor B chain promoter contains a cis-acting fluid shear stress-responsive element. *Proc. Natl. Acad. Sci. USA 90: 4591-4595.*

Resnick, N., Gimbrone, M.A.Jr. (1995) Hemodynamic forces are complex regulators of endothelial gene expression. *FASEB J. 9 (10): 874-882.*

Rodriguez, M.S., Thompson, J., Hay, R.T., Dargemont, C. (1999) Nuclear retention of IκBα protects it from signal-induced degradation and inhibits NF-κB transcriptional activation. *J. Biol. Chem. 274 (13): 9108-9115.*

Rothwarf, D.M., Zandi, E., Natoli, G., Karin, M. (1998) IKK-γ is an essential regulatory subunit of the IκBα kinase complex. *Nature 395: 297-300.*

Rusan, N.M., Fagerstrom, C.J., Yvon, A-M.C., Wadsworth, P. (2001) Cell cycle-dependent changes in microtubule dynamics in living cells expressing green fluorescent protein-αtubulin. *Mol. Biol. Cell 12: 971-980.*

Scherer, D.C., Brockman, J.A., Chen, Z., Maniatis, T., Ballard, D.W. (1995) Signal-induced degradation of IκBα requires site-specific ubiquitination. *Proc. Natl. Acad. Sci. USA 92: 11259-11263.*

Selden, S.C.III., Rabinovitch, P.S., Schwartz, S.M. (1981) Effects of cytoskeletal disrupting agents on replication of bovine endothelium. *J. Cell. Physiol. 108: 195-211.*

Sen, R., Baltimore, D. (1986) Multiple nuclear factors interact with the immunoglobulin enhancer sequences. *Cell 46: 705-716.*

Shyy, J.Y., Li, Y.S., Lin, M.C., Chen, W., Yuan, S., Usami, S., Chien, S. (1995) Multiple cis-elements mediate shear stress-induced gene expression. *J. Biomech. Eng. 28 (12): 1451-1457.*

Smiesko, V., Johnson, P.C. (1993) The arterial lumen is controlled by flow-related shear stress. *News. Physiol. Sci. 8: 34-38.*

Smith, C.A., Farrah, T., Goodwin, R.G. (1994) The TNF receptor superfamily of cellular and viral proteins: activations, costimulation and death. *Cell 76: 959-962.*

Strome, S., Powers, J., Dunn, M., Reese, K., Malone, C.J., White, J., Seydoux, G., Saxton, W. (2001) Spindle dynamics and the role of γ-tubulin in early *Caenorhabditis elegans* embryos. *Mol. Biol. Cell 12: 1751-1764.*

Sun, D., Huang, A., Sharma, S., Koller, A., Kaley, G. (2001) Endothelial microtubule disruption blocks flow-dependent dilation of arterioles. *Am. J. Physiol. (Heart Circ. Physiol.) 280: H2087-H2093.*

Topper, J.N., Ci, J., Falb, D., Gimbrone, M.A.Jr. (1996) Identification of vascular endothelial genes differentially responsive to fluid mechanical stimuli: cyclooxygenase-2, manganese superoxide dismutase, and endothelial cell nitric oxide synthase are selectively up-regulated by steady laminar shear stress. *Proc. Natl. Acad. Sci. USA 93 (19): 10417-10422.*

Topper, J.N., Gimbrone, M.A.Jr. (1999) Blood flow and vascular gene expression: fluid shear stress as a modulator of endothelial phenotype. *Mol. Med. Today 5 (1): 40-46.*

Traub, O., Berk, B.C. (1998) Laminar shear stress: mechanisms by which endothelial cells transduce an atheroprotective force. *Arterioscler. Thromb. Vasc. Biol. 18: 677-685.*

Trausch, J.S., Grenfell, S.J., Handley-Gearhart, P.M., Ciechanover, A., Schwartz, A.L. (1993) Immunofluorescent localization of the ubiquitin-activating enzyme, E1, to the nucleus and cytoskeleton. *Am. J. Physiol. 264 (Cell Physiol. 33): C93-C102.*

Viggers, R.F., Wechezak, A.R., Sauvage, L.R. (1986) An apparatus to study the response of cultured endothelium to shear stress. *J. Biomech. Eng. 108: 332-337.*

Wade, R.H., Hyman, A.A. (1997) Microtubule structure and dynamics. *Curr. Opin. Cell Biol. 9: 12-17.*

Wang, D., Westerheide, S.D., Hanson, J.L., Baldwin, A.S.Jr. (2000) Tumor necrosis factor α-induced phosphorylation of RelA/p65 on Ser^{529} is controlled by casein kinase II. *J. Biol. Chem. 275 (42): 33592-33597.*

Wechezak, A.R., Wight, T.N., Viggers, R.F., Sauvage, L.R. (1989) Endothelial adherence under shear stress is dependent upon microfilament reorganization. *J. Cell. Physiol. 139: 136-146.*

White, G.E., Gimbrone, M.A.Jr., Fujiwara, K. (1983) Factors influencing the expression of stress fibers in vascular endothelial cells in situ. *J. Cell Biol. 97: 416-424.*

Woronicz, J.D., Gao, X., Cao, Z., Rothe, M., Goeddel, D.V. (1997) IκB kinase-β: NF-κB activation and complex formation with IκB kinase-α and NIK. *Science 278: 866-869.*

Yeung, T.K., Germond, C., Chen, X., Wang, Z. (1999) The mode of action of taxol: apoptosis at low concentration and necrosis at high concentration. *Biochem. Biophys. Res. Commun. 263: 398-404.*

Yamaoka, S., Courtois, G., Bessia, C., Whiteside, S.T., Well, R., Agou, F., Kirk, H.E., Kay, R.J., Israel, A. (1998) Complementation cloning of NEMO, a component of the IκB kinase complex essential for NF-κB activation. *Cell 93: 1231-1240.*

Zabel, U., Baeuerle, P.A. (1990) Purified human IκB can rapidly dissociate the complex of the NF-κB transcription factor with its cognate DNA. *Cell 61: 255-265.*

APPENDIX 1

NF-κB

1.1 – Cell Culture Techniques

Human umbilical vein endothelial cells (HUVEC) –were obtained from Dr Ailsa Webster (Cell Tech. Slough).

Class II Flow Hood- Microflow Ltd. Somerset (M51424/2)

1.1.1 – Maintenance of HUVEC

Growth Medium – EBM-2 MV Bulletkit (BW3162, BioWhittaker Ltd, Berks.), containing;

- 500ml Basal EGM-2 Medium
- 25ml foetal calf serum (FCS)
- 0.5ml human recombinant epidermal growth factor (hEGF).
- 2.0ml human fibroblast growth factor-basic w. heparin (hFGF).
- 0.5ml vascular endothelial growth factor (VEGF)
- 0.5ml ascorbic acid
- 0.2ml hydrocortisone
- 0.5ml long R3-insulin-like growth factor-1 (R3-IGF-1)
- 0.5ml gentamicin/amphotericin.

1.1.2 – Trypsinisation and Seeding of HUVEC

Hepes Buffered Saline Solution (HBSS)- BW 5022. (BioWhittaker Ltd. Berks.).

Trypsin (0.025%) / EDTA (0.01%) – BW 5012. (BioWhittaker Ltd. Berks.).

Particle Counter – Coulter Counter® Z1™ Series Particle Counter, (Beckman Coulter Ltd. Bucks.).

Coverslips – 22 x 22mm (no. 1 Thickness) borosilicate glass, (406/0187/33), (BDH, Leics.).

Slides – 76 x 26mm, low iron clear glass, 1.0-1.2mm thick, 4060180/04, (BDH, Leics.).

1.1.3 DNA Plasmid and Transient Transfection of NIK, IKK1 and IKK2

LipofectAMINE - 18324-111, (Invitrogen Ltd. Paisley).

PCDNA3 empty vector - V385-20, (Invitrogen Ltd. Paisley).

IKK1, IKK1mut, IKK2 & IKK2 mut plasmids – gift from Dr John Taylor. (Pfizer Central Research, Sandwich, Kent) (Regnier et al, 1997)

NIK & NIK mut plasmids - gift from Dr David Wallach. (Weizmann Institute of Science, Israel) (Malinin et al, 1997)

1.2 Drug Treatment of HUVEC

MG132 - PI-202, (BIOMOL, Exeter). 20μM in culture medium.

Leptomycin B - L2913, (Sigma, Dorset). 20nM in culture medium.

Phorbol 12-myristate 13-acetate (PMA) - P8139, (Sigma, Dorset). 25ng.ml^{-1} in culture medium.

Ionomycin (IONO) - I0634, (Sigma, Dorset). 1μg.ml^{-1} in culture medium.

Bisindolylmaleimide (BISIN) - 203290, (Calbiochem, Nottingham). 100nM in culture medium.

TNFα - IB-1034, (Insight Biotechnology, Middlesex). 30ng/ml in culture medium.

1.3 Flow Apparatus

Peristaltic Pump – Model 7521-47 (Cole Parmer, Hertfordshire).

Gas Impermeable Tubing - Masterflex™, L/S® 16, 3.1mm internal diameter, (Pharmed®, 06485-16, Cole-Parmer, Hertfordshire).

Calculations – Shear Stress (τ) in the chamber was calculated from pressure gradients along the channel of the chamber using the following equation:

$$\tau = (\rho g a h) / l$$

ρ = medium density ($g.cm^{-3}$)
g = acceleration due to gravity ($cm.s^{-2}$)
h = difference in pressure along chamber (cm water)
a = chamber half-height (cm)
l = distance between pressure measuring points(cm)

Experimental shear stress calculations (τ) were compared to theoretical shear stress calculations (τ^*) and found to be within +/- 15% over a 100-fold range of flow rates.

$$\tau^* = 3Qv / 2a^2W$$

Q = volume flow rate ($ml.s^{-1}$)

v = medium viscosity (Poise)

a = chamber half-height (cm)

W = channel width (cm)

1.4 Immunofluorescence

1.4.1 – Paraformaldehyde Fixation Method

PBSc –

- 100ml x10 PBS Concentrate (14200, Gibco, Paisley)
- 900ml dH_2O
- 1ml 1M $CaCl_2$ (190464K, BDH, Leics.)
- 0.5ml 1M $MgCl_2$ (22093, BDH, Leics.)

3% Paraformaldehyde -

- 3ml Paraformaldehyde (P6148, Sigma, Dorset)
- 97ml PBSc

PBSa –

- 100ml x10 PBS Concentrate (14200, Gibco, Paisley)
- 900ml dH_2O

0.1M Glycine -

- 75mg Glycine (G8898, Sigma, Dorset)
- 100ml PBSc

0.2% Triton X-100 -

- 200μl Triton X-100 (X-100, Sigma, Dorset)
- 100ml PBSc

0.2% BSA –

- 200mg Bovine Serum Albumin (441555J, BDH, Leics.)
- 100ml PBSc

Primary Antibodies –

- HnRNP A1 – A gift from Dr Gideon Dreyfuss. (University of Pennsylvania).
- p65 F6, (sc-8008, Santa Cruz, California).
- NIK - H-248, (sc-7211, Santa Cruz, California).
- IKK1 - H-744, (sc-7218, Santa Cruz, California).
- IKK2 - H-470, (sc-7607, Santa Cruz, California).
- p65 C20, (sc-372, Santa Cruz, California).

Secondary Antibodies –

- GAMF - 115-096-003, (Jackson Immunoresearch, Beds.)
- GART - 4010-07, (Southern Biotech, Alabama).

Mountant - Hydromount (362452L, BDH, Leics.)

1.5 – Fluorescence Microscopy

Fluorescence Microscope for Preliminary Viewing - (Axioplan Universal, Zeiss, Germany)

Fluorescence Microscope for Computerised Image Production – (Microphot, Nikon, Japan)

Analysis Software – NIH Image for Macintosh.

1.6 – Western Blotting

1.6.1. – Cell Extract Preparation

PBSa – See 1.4.1

Laemmli Buffer –

- 1ml Glycerol (101186M, BDH, Leics.)
- 600µl 1M pH 6.8 Tris (103156X, BDH, Leics.)
- 2ml 10% SDS (Sodium Dodecyl Sulphate) (442442F, BDH, Leics.)
- 1ml Sodium Pervanadate ([Sodium Orthovanadate]S6508, Sigma, Dorset)
- 5.4ml dH_2O

1.6.2. – Protein Estimation

Protein Estimation Kit – 500-0112 (BioRad, California)

Dual Beam Spectrophotometer – (CE594, CECIL)

1% Bromophenol Blue –

- 1g Bromophenol Blue (B3269, Sigma, Dorset).
- 100ml dH_2O

β-Mercaptoethanol - (M7154, Sigma, Dorset).

1.6.3. – Gel Electrophoresis and Western Blotting

Gel Rig - (MV2-DC, Anachem, Beds.)

Power Pack - (PSU-400/200, Anachem, Beds.)

Nitrocellulose Membrane - Protran BA85, Schleicher and Schuell (MOL3008, SLS, Nottingham)

Thick filter paper - (1703958, BioRad, California)

Semi Dry Transfer Unit - (Trans-Blot SD, BioRad, California)

Transfer Power Pack - (Power-Pac 200, BioRad, California)

Detection Flim - (Hyperfilm ECL, RPN2103H, Amersham, Bucks.)

8% Running Gel –

- 8ml MQ H_2O
- 3ml 40% Acrylamide (0496-500ML-C, Anachem, Beds.)
- 3.8ml 1.5M pH 8.8 Tris
- 150μl 10% SDS
- 150μl APS (Ammonium Persulphate) (made up in MQ H_2O) (20-3001-05, Anachem, Beds.)
- 9μl TEMED (30-3000-01, Anachem, Beds.

6% Running Gel –

- 8.8ml MQ H_2O
- 2.2ml 40% Acrylamide
- 3.8ml 1.5M pH 8.8 Tris
- 150µl 10% SDS
- 150µl 10% APS
- 12µl TEMED

4% Stacking Gel –

- 3.6ml MQ H_2O
- 623µl 40% Acrylamide
- 630µl 1M pH 6.8 Tris
- 50µl 10% SDS
- 50µl 10% APS
- 5µl TEMED

n-Butanol – (BT-105, Sigma, Dorset)

x5 Tris/Glycine Running Buffer –

- 30g Tris
- 144g Glycine (G8898, Sigma, Dorset)
- 10g SDS
- 2 litres dH_2O

- Dilute 1:5 with dH_2O for use.

Semi-Dry Transfer Buffer –

- 15g Tris
- 72g Glycine
- 1 litre Methanol (29192BL, BDH, Leics.)
- 18.75ml 10% SDS

- Make up to 5 litres with dH_2O

Ponceau Red –

- 30g Trichloroacetic acid (102864Y, BDH, Leics.)
- 30g Sulphosalicylic acid (S2130, Sigma, Dorset)
- 2g Ponceau S (P3504, Sigma, Dorset)
- 100ml dH_2O

- Dilute 1:10 with dH_2O for use.

PBS-T –

- 2 PBS-T Tablets (18902-015, Gibco, Paisley)
- 1 litre dH_2O

Primary Antibodies –

- IκBα - C-21, (Santa Cruz, California).
- Iκβ - C-20, (Santa Cruz, California).
- p105 – (SAPU, Carluke).
- p50 – (SAPU, Carluke).

Secondary Antibodies –

- Anti-rabbit horseradish peroxidase (HRP) (SC-2030, Santa-Cruz, California)
- Anti-sheep HRP – (DAKO, Cambridgeshire).

ECL Reagents – (RPN 2209, Amersham, Bucks.)

Photographic Developer, - LX24 (5070933, Kodak, Paris)

Photographic Fixative – Unifix (816756, Kodak, Paris)

1.7 – Electrophoretic Mobility Shift Assay (EMSA)

Phosphorimager – Fuji Bas 1500

Molecular weight markers – Cruz Marker™, (SC2035, Santa Cruz, California).

Molecular Weight (kDa)	**Log_{10} Molecular Weight**
132,000	5.12
90,000	4.95
55,000	4.74
43,000	4.63
34,000	4.53
23,000	4.36

1.8 Gel densitometry data for response of IκBα, IκBβ, p105, p50 to flow and TNFα

IκBα	Intensity as % of control				
FSS (min)	n1	n2	n3	mean	standard error
0	100	100	100	100	0
5	89	94	87	90	2.08
10	63	64	59	62	1.53
30	31	29	36	32	2.08
60	98	102	91	97	3.21
120	97	88	97	94	3
240	28	40	37	35	3.61

IκBα	Intensity as % of control				
TNFα (min)	n1	n2	n3	mean	standard error
0	100	100	100	100	0
5	89	99	106	98	4.93
10	54	58	68	60	4.16
30	42	51	51	48	3
60	59	83	80	74	7.55
120	82	87	83	84	1.53
240	81	82	95	86	4.51

n1, 2 and 3 are the results of pixel intensity readings from bands of western blots form 3 separate experiments. Values were gathered and calculated as described in Chapter 3.5.3.

IκBβ	**Intensity as % of control**				
FSS (min)	n1	n2	n3	mean	standard error
0	100	100	100	100	0
5	102	104	94	100	3.06
10	75	81	72	76	2.65
30	4	7	7	6	1
60	6	7	8	7	0.58
120	92	69	85	82	6.81
240	86	66	64	72	7.02

IκBβ	**Intensity as % of control**				
TNFα (min)	n1	n2	n3	mean	standard error
0	100	100	100	100	0
5	103	103	94	100	3
10	100	99	74	91	8.5
30	80	81	70	77	3.51
60	7	14	12	11	2.08
120	105	94	98	99	3.21
240	92	107	101	100	4.36

p105	**Intensity as % of control**				
FSS (min)	n1	n2	n3	mean	standard error
0	100	100	100	100	0
5	103	98	105	102	2.08
10	95	102	109	102	4.04
30	106	101	102	103	1.53
60	121	113	114	116	2.52
120	111	108	132	117	7.54
240	114	120	114	116	2

p105	**Intensity as % of control**				
TNFα (min)	n1	n2	n3	mean	standard error
0	100	100	100	100	0
5	93	98	94	95	1.53
10	103	100	103	102	1
30	108	108	108	108	0
60	107	112	108	109	1.53
120	104	110	113	109	2.65
240	111	105	114	110	2.65

p50	**Intensity as % of control**				
FSS (min)	n1	n2	n3	mean	standard error
0	100	100	100	100	0
5	103	100	85	96	5.57
10	103	98	99	100	1.53
30	91	103	100	98	3.61
60	96	111	108	105	4.58
120	112	110	126	116	5.03
240	99	117	120	112	6.56

p50	**Intensity as % of control**				
TNFα (min)	n1	n2	n3	mean	standard error
0	100	100	100	100	0
5	99	107	94	100	3.79
10	98	101	92	97	2.64
30	103	101	108	104	2.08
60	103	106	106	105	1
120	119	109	111	113	3.06
240	112	110	120	114	3.06

1.9 Luciferase Assay

3Enh Con A Luc and Con A Luc plasmids - Gift from Dr. F Arenzana-Seisdedos, (Institut Pasteur, Paris).

Lysis Buffer-

- 25mM tris phosphate
- 8mM MgCl2
- 1mM DTT
- 1% Triton X-100
- 15% glycerol

Luciferase Buffer (made up in lysis buffer)-

- 25mM luciferin
- 1mM ATP
- 1% BSA

Plate Reader – Microlumat (LB96P)

2.0 – IKK Immunocomplex Kinase Activity Assay

2.0.1 – Solutions and Equipment

Lysis Buffer:

- 20mM Tris-HCL, pH 8.0
- 500mM NaCl
- 1mM EDTA
- 1mM EGTA

- 0.25% NP-40
- 1mM DTT
- 10mM β-glycerophosphate
- 300μM sodium orthovanadate
- 2SF, 2μM phenylmethylsulfonylfluoride (PMSF)
- 10mM sodium fluoride
- 1 protease inhibitor tablet (Boehringer Mannheim, E. Sussex).

Protein A beads conjugated with sheep affinity purified primary antibody to C-terminal of IKK – (Diagnostics Scotland, Edinburgh).

Pulldown Buffer:

- 40mM Tris-HCl
- pH 8.0, 500mm NaCl
- 6mM EDTA
- 6mM EGTA
- 0.1% NP-40
- 1mM DTT
- 10mM β-glycerophosphate
- 300μM sodium orthovanadate
- 2μM PMSF
- 10mM sodium fluoride
- 1 protease inhibitor tablet (Boehringer Mannheim, E. Sussex).

Kinase Assay Buffer –

- 20mM Hepes pH 7.7
- 2mM $MgCl_2$
- 1mM DTT
- 10mM β-glycerophosphate
- 300μM sodium orthovanadate
- 10mM sodium fluoride
- 1 protease inhibitor tablet (Boehringer Mannheim, E. Sussex).

Additives - 3μCi [γ-^{32}P] ATP, 1μg wildtype GST-N terminal IκBα (amino acids 1-70) or GST-N IκBα 32 S/A.

Phosphorimager – Fuji-Bas 1500

N.B. – Transfection of cells, luciferase assays and IKK Immunocomplex kinase activity assays were kindly carried out by Dr David Hay and Dr Lesley Thomson (University of St Andrews, BMS Department.)

2.0.2 – Quantitative tables of data for IKK kinase assay.

IKK	**Kinase Activity**	**(Fold Activ^{n})**			
FSS (min)	n1	n2	n3	Mean	S.E.M.
CTRL 0	1.43	1.43	0.54	1.03	0.26
5	2	3.17	1.13	2.1	0.59
10	1.94	2.35	1.14	1.81	0.36
20	1.14	1.94	0.61	1.23	0.39
30	1.9	1.92	1.48	1.7	0.14
60	1.86	2.32	1.36	1.92	0.28
120	2.2	2.89	1.33	2.14	0.45
240	1.53	2.69	1.12	1.78	0.47

IKK	**Kinase Activity**	**(Fold Activ^{n})**			
TNFα (min)	n1	n2	n3	Mean	S.E.M.
CTRL 0	0.79	1.32	1.04	1.05	0.15
5	0.81	2.72	0.97	1.5	0.61
10	1.43	5.08	2.61	3	1.07
20	0.66	2.67	1.5	1.61	0.58
30	0.82	2.25	1.1	1.39	0.44
60	0.97	1.94	1.29	1.4	0.29
120	0.7	2.45	0.99	1.38	0.54
240	0.66	2.29	1.04	1.33	0.49

n1, 2 and 3 are 3 separate experiments, each value being the average of 3 pixel intensity readings from western blot bands. The numbers are displayed as fold activation values calculated from the control (0 min) data, as described in Chapter 3.5.3.

APPENDIX 2

MICROTUBULES

2.1 - Cell Culture Techniques

See appendix 1.1 for details.

2.1.1. – Maintenance, trypsinisation and Seeding of HUVEC

See appendix 1.1.1. and 1.1.2. for details.

2.2 – Drug treatment of HUVEC

Colchicine – C9754, (Sigma, Dorset). 1μM in culture medium.

TNFα - IB-1034, (Insight Biotechnology, Middlesex). 30ng.ml^{-1} in culture medium.

2.3 – Flow Experiments

See appendix 1.3 for details.

2.4 – Immunofluorescence

2.4.1 – Glutaraldehyde Fixation Method

0.1M PIPES –

- 3.46g PIPES (P3768, Sigma, Dorset)
- 100ml dH_2O
- pH to 6.9 with HCl (H7020, Sigma, Dorset)

0.5% Glutaraldehyde –

- 500µl 25% Glutaraldehyde (R1012, Agar Scientific, Essex)
- 100ml 0.1M PIPES, pH 6.9.

PBSc – See appendix 1.4.1

0.5% Triton X-100 –

- 500µl Triton X-100 (X-100, Sigma, Dorset)
- 100ml PBSc

Sodium Borohydride 2.5mg/ml –

- 250mg Sodium Borohydride (S9125, Sigma, Dorset)
- 100ml 50% Ethanol

10% Goat Serum –

- 10ml Goat Serum (T028, Diagnostics Scotland, Lanarkshire)
- 90ml PBSc

Primary Antibodies –

- Mouse monoclonal tubulin (T5168, Sigma, Dorset)
- Rabbit polyclonal p65 –C20 (sc-372, Santa Cruz, California)

Secondary Antibodies -

- Goat anti mouse Alexa 568 ($GAMA_{568}$) (A11004, Molecular Probes, Oregon).
- Goat anti rabbit Alexa 488 ($GARA_{488}$) (A11008, Molecular Probes, Oregon).

0.1% Tween 20 –

- 100µl Tween 20 (P9416, Sigma, Dorset).
- 100ml PBSc

Mountant – See 1.4.1

2.5 – Deconvolution Microscopy

Deconvolution Microscope and softWoRx 2.5 programme – Applied Precision Instruments (Washington, U.S.A)

2.6 – Quantitative Analysis

Intensity measurement recordings – softWoRx 2.5 programme, Applied Precision Instruments (Washington, U.S.A.)

Statistical testing – Minitab, Version 14.

Tables of raw data - from which mean nuclear:cytoplasmic (N:C) p65 ratios of intensity of staining were constructed and all statistical tests were carried out.

Control	**75nM** colchicine	**150nM** colchicine	**500nM** colchicine	**1uM** colchicine	**10uM** colchicine
0.762115	0.812133	0.763158	0.766021	0.655804	0.744928
0.684211	0.765458	0.73166	0.675949	0.659472	0.717172
0.71	0.738426	0.721951	0.759124	0.745399	0.749263
0.829978	0.726845				0.698381
0.648649					0.724891
0.698376					0.702614
0.713439					0.743869
0.715517					
0.680352					
0.745358					
0.679688					
0.683805					
0.740826					

Control	**75nm Colchicine +TNF**	**150nM Colchicine +TNF**	**500nM Colchicine +TNF**	**1μM Colchicine +TNF**	**10μM Colchicine +TNF**
2.18671	1.59146	1.52254	1.53968	0.9597	0.88985
1.66588	1.76116	1.60349	1.06024	1.30149	1.16802
1.86692	1.88441				2.37338
1.27515					
1.64615					
1.80503					

With thanks to Dr J. Graves for advice on appropriate statistical tests and Miss S. Spring for tutoring in the use of the Minitab programme.